Application of Dynamic Fracture Mechanics Concepts to Composites: Annual Report 1999

by

J.J. Mason

Department of Aerospace and Mechanical Engineering
University of Notre Dame

Notre Dame, Indiana 46556
June, 1999

Structural/Solid Mechanics
Laboratory Report No. 99/4

Application of Dynamic Fracture Mechanics Concepts to Composites: Annual Report 1999

J.J. Mason [1]
Department of Aerospace and Mechanical Engineering
University of Notre Dame
Notre Dame, IN 46556

June, 1999

[1]Associate Professor, Principal Investigator

Abstract

This report summarizes the work completed in the year June 1998–May 1999 for the principal investigator's Young Investigator Program grant, the last scheduled year for this three year grant. The report is divided into five chapters covering new analytical solutions for dynamic cracks in orthotropic composites. Each chapter stands alone and has been submitted, accepted or prepared for publication in a refereed journal. First, closed form solutions for uniformly loaded semi-infinite cracks in orthotropic materials are presented. Next, solutions regarding the stress intensity factor at the tip of propagating cracks in orthotropic materials are presented. In addition, closed form, dynamic Green's functions solutions are given for semi-infinite cracks in orthotropic materials. Previously, in last year's report, numerical Green's function solutions were presented for this case the first time. These newer, closed form solutions are much easier to produce and implement in more complex solutions. The problem of having a crack in transversely isotropic material rotated with respect to the crack front is also solved with some effort. The methodology used in finding all these solutions may be used in other problems including penetration mechanics. Such applications are currently being explored. Finally, experimental investigation of the application of these solutions to dynamic crack initiation in composites under impact conditions is being completed. It is expected that a report on that work will be submitted in six months with the final report for this contract. (All funds for the grant have been expended. A six month no cost extension has been granted.)

Contents

REPORT DOCUMENTATION PAGE

Form Approved
OMB No. 0704-0188

1. AGENCY USE ONLY *(Leave blank)*	2. REPORT DATE	3. REPORT TYPE AND DATES COVERED
	23 June 99	Annual, 1 June 98 - 31 May 99

4. TITLE AND SUBTITLE

On the Application of Dynamic Fracture Mechanics to Continuous Fiber Reinforced Composite Materials

5. FUNDING NUMBERS

G ND0014-96-0774

PR 96PR05511-00

6. AUTHOR(S)

J.J. Mason

7. PERFORMING ORGANIZATION NAMES(S) AND ADDRESS(ES)

University of Notre Dame
Department of Aerospace & Mechanical Engineering
365 Fitzpatrick Hall
Notre Dame, IN 46556

8. PERFORMING ORGANIZATION REPORT NUMBER

9. SPONSORING / MONITORING AGENCY NAMES(S) AND ADDRESS(ES)

Office of Naval Research
800 N. Quincy St.
Arlington, VA 22217-5660

10. SPONSORING / MONITORING AGENCY REPORT NUMBER

11. SUPPLEMENTARY NOTES

Portions of this report have been submitted for publication in Int. J. Fracture, J. Mech. Phys. Sol., J. Composite Mat., Int. J. Solids & Structures.

a. DISTRIBUTION / AVAILABILITY STATEMENT

Approved for public release; distribution unlimited.

12. DISTRIBUTION CODE

13. ABSTRACT ***(Maximum 200 words)***

This report summarizes the work completed in the year June 1998 – May 1999 for the principal investigator's Young Investigator Program grant, the last scheduled year for this three year grant. The report is divided into five chapters covering new analytical solutions for dynamic cracks in orthotropic composites. Each chapter stands alone and has been submitted, accepted or prepared for publication in a refereed journal. First, closed form solutions for uniformly loaded semi-infinite cracks in orthotropic materials are presented. Next, solutions regarding the stress intensity factor at the tip of propagating cracks in orthotropic materials are presented. In addition, closed form, dynamic Green's functions solutions are given for semi-infinite cracks in orthotropic materials. Previously, in last year's report, numerical Green's function solutions were presented for this case the first time. These newer, closed form solutions are much easier to produce and implement in more complex solutions. The problem of having a crack in transversely isotropic material rotated with respect to the crack front is also solved with some effort. The methodology used in finding all these solutions may be used in other problems including penetration mechanics. Such applications are currently being explored. Finally, experimental investigation of the application of these solutions to dynamic crack initiation in composites under impact conditions is being completed. It is expected that a report on that work will be submitted in six months with the final report for this contract. (All funds for the grant have been expended. A six month no cost extension has been granted.)

14. SUBJECT TERMS

Stress intensity factor, dynamic fracture, orthotropic materials.

15. NUMBER OF PAGES

164

16. PRICE CODE

17. SECURITY CLASSIFICATION OF REPORT	18. SECURITY CLASSIFICATION OF THIS PAGE	19. SECURITY CLASSIFICATION OF ABSTRACT	20. LIMITATION OF ABSTRACT
Unclassified	Unclassified	Unclassified	UL

Chapter 1

A New Method for Examining Dynamically Loaded, Semi-infinite Stationary Cracks in Orthotropic Materials

Co-authored with C. Rubio-Gonzalez and accepted for publication in the Journal of Mechanics and Physics of Solids

The elastodynamic response of an infinite orthotropic material with a semi-infinite crack under impact loads is examined. Three loading modes are considered, i.e., opening, in-plane shear and antiplane shear. Solution for the stress intensity factor history around the crack tip is found. Laplace and Fourier transforms along with the Wiener-Hopf technique are employed to solve the displacement formulation of the equations of motion. The asymptotic expression for the stress near the crack tip is analyzed which lead to a closed-form solution of the dynamic stress intensity factor for each loading mode. It is found that the stress intensity factors are proportional to the square root of time as in the isotropic case. Results for orthotropic materials are shown to converge to known solutions for isotropic materials derived independently.

1.1 Introduction

Several problems have been examined in dynamic fracture mechanics for isotropic materials. In fact, there are many closed form solutions for stationary and propagating cracks in isotropic materials under dynamic loading (Freund 1990, Chen and Sih 1977). The stationary semi-infinite crack under uniform step loading in the crack faces was considered first by Maue (1954). The equivalent propagating case was studied by Baker (1962). For orthotropic materials the available solutions are fewer in number, *finite* cracks under impact loading have been analyzed by Kassir and Bandyopadhyay (1983), Shindo and Nozaki (1991), Rubio-Gonzalez and Mason (1998) using integral transform methods. These authors reduce their problems to a Fredholm integral equation in the Laplace transform domain which is solved numerically. The stress intensity factor is recovered in the time domain by numerical Laplace inversion of this solution. Although this approach can be used to solve problems with non-symmetric loads (Rubio-Gonzalez and Mason 1998) it is restricted to finite cracks and numerical solutions. With the growing use of composites in many engineering applications it is desirable to have closed form solutions for fundamental problems in cracked orthotropic materials. The semi-infinite crack is a fundamental problem because cracks under dynamic loads can usually be considered semi-infinite for a short duration of time immediately after loading. In the present work the semi-infinite crack problem under impact loads in orthotropic material is analyzed, a closed form solution for the dynamic stress intensity factor is obtained for each loading mode, i.e., opening, in-plane shear and antiplane shear. Following the example of Baker (1962), Laplace and Fourier transforms are applied to the displacement equations of motion and combined with the Wiener-Hopf technique to find expressions for the stress ahead of the crack tip and the displacements on the crack faces. Asymptotic analysis of the stress near the crack tip leads to expressions for the stress intensity factors $K_I(t)$, $K_{II}(t)$, and $K_{III}(t)$.

1.2 Governing Equations, in-plane problems

Consider the plane problem of an infinite orthotropic medium containing a semi-infinite crack, Figure 1.1. Let E_i, μ_{ij} and ν_{ij} $(i,j = 1,2,3)$ be the engineering elastic constants of the material where the indices 1, 2, and 3 correspond to Cartesian coordinates (x,y,z) chosen to coincide with the axes of material orthotropy. The crack faces are along the negative $x-$axis and the origin of the xy axes is the crack tip. Uniform tractions are applied to the crack faces in directions depending upon the problem considered.

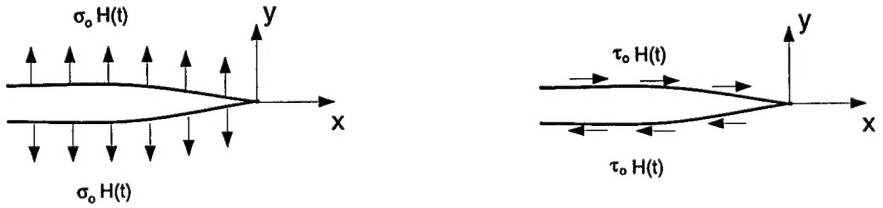

(a) (b)

Figure 1.1: Schematic of the semi-infinite crack geometry. (a) Normal loading, (b) In-plane shear loading.

Restricting the problem to two dimensions with wave propagation limited to the $x-y$ plane by setting all the derivatives with respect to z to be zero, it is readily shown that the displacement equations of motion (Nayfeh 1995) reduce to

$$c_{11}\frac{\partial^2 u}{\partial x^2} + \frac{\partial^2 u}{\partial y^2} + (1+c_{12})\frac{\partial^2 v}{\partial x \partial y} = \frac{1}{c_s^2}\frac{\partial^2 u}{\partial t^2}, \tag{1.1}$$

$$\frac{\partial^2 v}{\partial x^2} + c_{22}\frac{\partial^2 v}{\partial y^2} + (1+c_{12})\frac{\partial^2 u}{\partial x \partial y} = \frac{1}{c_s^2}\frac{\partial^2 v}{\partial t^2}, \tag{1.2}$$

where u and v are the x and y components of the displacement vector and c_{11}, c_{12} and c_{22} are non-dimensional parameters related to the elastic constants by the relations:

$$\begin{aligned} c_{11} &= \frac{E_1}{\mu_{12}[1-(E_2/E_1)\nu_{12}^2]}, \\ c_{22} &= (E_2/E_1)c_{11}, \\ c_{12} &= \nu_{12}c_{22} = \nu_{21}c_{11}, \end{aligned} \tag{1.3}$$

for generalized plane stress, and by

$$\begin{aligned} c_{11} &= \frac{E_1}{\mu_{12}\Delta}(1-\nu_{23}\nu_{32}), \\ c_{22} &= \frac{E_2}{\mu_{12}\Delta}(1-\nu_{13}\nu_{31}), \\ c_{12} &= \frac{E_1}{\mu_{12}\Delta}(\nu_{21}+\frac{E_2}{E_1}\nu_{13}\nu_{32}), \\ \Delta &= 1-\nu_{12}\nu_{21}-\nu_{23}\nu_{32}-\nu_{31}\nu_{13}-\nu_{12}\nu_{23}\nu_{31}-\nu_{13}\nu_{21}\nu_{32}, \end{aligned} \tag{1.4}$$

for plane strain. In the orthotropic solid, $c_s = \sqrt{\mu_{12}/\rho}$ represents the velocity of the in-plane shear wave propagating along the the principal material axes and ρ is the mass density. The stresses are related to the displacements by the equations:

$$\begin{aligned} \frac{\sigma_x}{\mu_{12}} &= c_{11}\frac{\partial u}{\partial x}+c_{12}\frac{\partial v}{\partial y}, \\ \frac{\sigma_y}{\mu_{12}} &= c_{12}\frac{\partial u}{\partial x}+c_{22}\frac{\partial v}{\partial y}, \\ \frac{\tau_{xy}}{\mu_{12}} &= \frac{\partial u}{\partial y}+\frac{\partial v}{\partial x}. \end{aligned} \tag{1.5}$$

1.3 Normal Impact

In the case of normal tractions to the crack faces, figure 1.1(a), a spatially uniform pressure of magnitude σ_0 is assumed to be suddenly applied at $t = 0$. Exploiting symmetry and taking only the upper half plane $y \geq 0$, the corresponding boundary conditions are

$$\begin{aligned} \sigma_y(x,0,t) &= -\sigma_0 H(t) \quad \text{for} \quad -\infty < x < 0, \\ \tau_{xy}(x,0,t) &= 0 \quad \text{for} \quad -\infty < x < \infty, \\ v(x,0,t) &= 0 \quad \text{for} \quad x > 0, \end{aligned} \tag{1.6}$$

where $H(t)$ is the Heaviside step function. In addition, the conditions of zero displacements at infinity and zero initial conditions are assumed.

The method of solution of the governing equations presented here follows that described in Freund (1990) for the isotropic case with some significant differences; displacement potentials are not used and no assumptions are made about the form of the unknown functions.

In equations (1.1) and (1.2), the time variable may be removed by application of the Laplace transform

$$f^*(p) = \int_0^\infty f(t)\, e^{-pt}\, dt, \quad f(t) = \frac{1}{2\pi i}\int_{Br} f^*(p)\, e^{pt}\, dt, \tag{1.7}$$

where Br denotes the Bromwich path of integration which is a line parallel to the imaginary axis in the p-plane. Applying relations (1.7) to equations (1.1) and (1.2) and assuming zero initial conditions for the displacements and velocities, the transformed field equations become

$$c_{11}\frac{\partial^2 u^*}{\partial x^2} + \frac{\partial^2 u^*}{\partial y^2} + (1+c_{12})\frac{\partial^2 v^*}{\partial x \partial y} - \frac{p^2}{c_s^2}u^* = 0, \tag{1.8}$$

$$\frac{\partial^2 v^*}{\partial x^2} + c_{22}\frac{\partial^2 v^*}{\partial y^2} + (1+c_{12})\frac{\partial^2 u^*}{\partial x \partial y} - \frac{p^2}{c_s^2}v^* = 0, \tag{1.9}$$

where the transformed displacement components, u^* and v^*, are now functions of the variables x, y, and p. The application of the Laplace transform to the boundary conditions (1.6) gives

$$\begin{aligned} \sigma_y^*(x,0,p) &= -\sigma_0\frac{1}{p} \quad \text{for} \quad -\infty < x < 0, \\ \tau_{xy}^*(x,0,p) &= 0 \quad \text{for} \quad -\infty < x < \infty, \\ v^*(x,0,p) &= 0 \quad \text{for} \quad x > 0. \end{aligned} \tag{1.10}$$

To obtain a solution of the differential equations (1.8) and (1.9) subject to conditions (1.10), the Fourier transform is applied in this work,

$$F(s) = \int_{-\infty}^{\infty} f(x)\, e^{isx}\, dx, \quad f(x) = \frac{1}{2\pi}\int_{-\infty}^{\infty} F(s)\, e^{-isx}\, ds, \tag{1.11}$$

rather than the double sided Laplace transform. It is assumed that the displacements in the Laplace transform domain have the form

$$u^*(x,y,p) = \frac{1}{2\pi}\int_{-\infty}^{\infty} A(s,y,p)e^{-isx}\, ds, \tag{1.12}$$

$$v^*(x,y,p) = \frac{1}{2\pi}\int_{-\infty}^{\infty} B(s,y,p)e^{-isx}\, ds, \tag{1.13}$$

where A and B are the Fourier transforms of the Laplace transform of the displacements, u^* and v^*, respectively, and are yet to be determined. Substituting these transforms into

equations (1.8) and (1.9), the functions A and B are found to satisfy the simultaneous ordinary differential equations

$$(c_{11}s^2 + p^2/c_s^2)A - \frac{d^2A}{dy^2} + (1 + c_{12})is\frac{dB}{dy} = 0, \tag{1.14}$$

$$(s^2 + p^2/c_s^2)B - c_{22}\frac{d^2B}{dy^2} + (1 + c_{12})is\frac{dA}{dy} = 0. \tag{1.15}$$

The solution of these equations which vanishes for $y \to \infty$ is

$$\begin{aligned} A(s,y,p) &= A_1(s,p)e^{-\gamma_1 y} + A_2(s,p)e^{-\gamma_2 y}, \\ B(s,y,p) &= \frac{-i\alpha_1}{s}A_1(s,p)e^{-\gamma_1 y} - \frac{i\alpha_2}{s}A_2(s,p)e^{-\gamma_2 y}, \end{aligned} \tag{1.16}$$

where A_1 and A_2 are arbitrary functions and $\alpha_j(s,p)$ stands for the functions

$$\alpha_j(s,p) = \frac{c_{11}s^2 + p^2/c_s^2 - \gamma_j^2}{(1 + c_{12})\gamma_j}, \quad j = 1,2 \tag{1.17}$$

with γ_1^2 and γ_2^2 being two distinct roots of the quadratic equation

$$c_{22}\gamma^4 + [(c_{12}^2 + 2c_{12} - c_{11}c_{22})s^2 - (1 + c_{22})p^2/c_s^2]\gamma^2 + (c_{11}s^2 + p^2/c_s^2)(s^2 + p^2/c_s^2) = 0. \tag{1.18}$$

It can be shown that for many materials the roots γ_1 and γ_2 are real and positive and the expressions for the displacements in the Laplace transform domain become:

$$u^* = \frac{1}{2\pi}\int_{-\infty}^{\infty}(A_1e^{-\gamma_1 y} + A_2e^{-\gamma_2 y})e^{-isx}\,ds, \tag{1.19}$$

$$v^* = \frac{-i}{2\pi}\int_{-\infty}^{\infty}(\alpha_1A_1e^{-\gamma_1 y} + \alpha_2A_2e^{-\gamma_2 y})\frac{e^{-isx}}{s}ds. \tag{1.20}$$

And, using (1.5) the corresponding expression for τ_{xy}^* is given by

$$\tau_{xy}^* = -\frac{\mu_{12}}{2\pi}\int_{-\infty}^{\infty}[(\alpha_1 + \gamma_1)A_1e^{-\gamma_1 y} + (\alpha_2 + \gamma_2)A_2e^{-\gamma_2 y}]e^{-isx}\,ds. \tag{1.21}$$

Applying the second condition of (1.10) to equation (1.21) yields

$$\begin{aligned} A_2(s,p) &= -\beta_1A_1(s,p), \\ \beta_1 &= \frac{\alpha_1 + \gamma_1}{\alpha_2 + \gamma_2}. \end{aligned} \tag{1.22}$$

Therefore, the expressions for the transformed components of displacement become

$$u^*(x,y,p) = \frac{1}{2\pi}\int_{-\infty}^{\infty}(e^{-\gamma_1 y} - \beta_1 e^{-\gamma_2 y})A_1(s,p)e^{-isx}\,ds, \tag{1.23}$$

$$v^*(x,y,p) = \frac{-i}{2\pi}\int_{-\infty}^{\infty}(\alpha_1 e^{-\gamma_1 y} - \beta_1\alpha_2 e^{-\gamma_2 y})\frac{A_1(s,p)}{s}e^{-isx}\,ds, \tag{1.24}$$

and the associated stress components are given by

$$\sigma_x^* = \frac{-i\mu_{12}}{2\pi}\int_{-\infty}^{\infty}[(c_{11}s^2 - \alpha_1\gamma_1 c_{12})e^{-\gamma_1 y} - (c_{11}s^2 - \alpha_2\gamma_2 c_{12})\beta_1 e^{-\gamma_2 y}]\frac{A_1(s,p)}{s}e^{-isx}ds, \tag{1.25}$$

$$\sigma_y^* = \frac{-i\mu_{12}}{2\pi}\int_{-\infty}^{\infty}[(c_{12}s^2 - \alpha_1\gamma_1 c_{22})e^{-\gamma_1 y} - (c_{12}s^2 - \alpha_2\gamma_2 c_{22})\beta_1 e^{-\gamma_2 y}]\frac{A_1(s,p)}{s}e^{-isx}ds, \tag{1.26}$$

$$\tau_{xy}^* = \frac{-\mu_{12}}{2\pi}\int_{-\infty}^{\infty}(\alpha_1 + \gamma_1)[e^{-\gamma_1 y} - e^{-\gamma_2 y}]A_1(s,p)e^{-isx}ds. \tag{1.27}$$

Introducing the functions

$$E(s,p) = \frac{1}{s}(\alpha_1 - \beta_1\alpha_2)A_1(s,p), \tag{1.28}$$

$$F(s,p) = -\frac{\sqrt{s^2 + p^2/c_d^2}}{(\alpha_1 - \beta_1\alpha_2)\xi}[c_{12}s^2 - \alpha_1\gamma_1 c_{22} - \beta_1(c_{12}s^2 - \alpha_2\gamma_2 c_{22})], \tag{1.29}$$

$$\xi = \frac{-1}{c_{11}(1+c_{12})(N_1+N_2)}\{(c_{12}^2 + c_{12} - c_{11}c_{22})(c_{12}N_1N_2 - c_{11}) - c_{22}[c_{12}N_1^2N_2^2 + c_{11}(N_1^2 + N_1N_2 + N_2^2)]\}, \tag{1.30}$$

$$N_{1,2}^2 = \frac{1}{2c_{22}}\{c_{11}c_{22} - c_{12}^2 - 2c_{12} \pm [(c_{11}c_{22} - c_{12}^2 - 2c_{12})^2 - 4c_{11}c_{22}]^{1/2}\}, \tag{1.31}$$

where the velocity $c_d = \sqrt{c_{11}}c_s$ represents the dilatational wave speed along the $x-$axis and in view of the first and third boundary conditions in (1.10), equations (1.24) and (1.26) yield the following pair of dual integral equations for the determination of the function $E(s,p)$

$$\sigma_y^*(x,0,p) = \frac{i\mu_{12}\xi}{2\pi}\int_{-\infty}^{\infty}\frac{F(s,p)}{\sqrt{s^2 + p^2/c_d^2}}E(s,p)e^{-isx}\,ds = -\frac{\sigma_0}{p} \qquad -\infty < x < 0, \tag{1.32}$$

$$v^*(x,0,p) = \frac{-i}{2\pi}\int_{-\infty}^{\infty}E(s,p)e^{-isx}\,ds = 0 \qquad 0 < x < \infty. \tag{1.33}$$

Let $v_-^*(x,p)$ be the unknown Laplace transform of the vertical displacement on the negative $x-$axis, and $\sigma_+^*(x,p)$ be the unknown Laplace transform of the normal stress on the positive $x-$axis, so that

$$v^*(x,0,p) = \begin{cases} 0 & \text{for } x > 0 \\ v_-^*(x,p) & \text{for } x < 0 \end{cases} \qquad \sigma_y^*(x,0,p) = \begin{cases} \sigma_+^*(x,p) & \text{for } x > 0 \\ -\sigma_0/p & \text{for } x < 0. \end{cases} \tag{1.34}$$

Then the Laplace transform of the normal stress and the vertical displacement on the whole boundary $y = 0$ is given by,

$$\frac{i\mu_{12}\xi}{2\pi}\int_{-\infty}^{\infty}\frac{F(s,p)}{\sqrt{s^2+p^2/c_d^2}}E(s,p)e^{-isx}\,ds = -\frac{\sigma_0}{p}H(-x)+\sigma_+^*(x,p), \tag{1.35}$$

$$\frac{-i}{2\pi}\int_{-\infty}^{\infty}E(s,p)e^{-isx}\,ds = v_-^*(x,p), \tag{1.36}$$

and, by Fourier transform inversion, these equations give

$$i\mu_{12}\xi\frac{F(s,p)}{\sqrt{s^2+p^2/c_d^2}}E(s,p) = -\frac{\sigma_0}{pis}+\Sigma_+(s), \tag{1.37}$$

$$-iE(s,p) = V_-(s), \tag{1.38}$$

where

$$\Sigma_+(s) = \int_0^{\infty}\sigma_+^*(x,p)e^{isx}dx, \tag{1.39}$$

$$V_-(s) = \int_{-\infty}^{0}v_-^*(x,p)e^{isx}dx, \tag{1.40}$$

$$\int_{-\infty}^{0}\left(\frac{-\sigma_0}{p}\right)e^{isx}dx = -\frac{\sigma_0}{ips}.$$

From the physics of the problem it is reasonable to assume that the function $\sigma_+^*(x,p)$ and $v_-^*(x,p)$ are exponentially bounded at infinity and this ensures the existence of their Fourier transform (1.39) and (1.40). In particular it is shown by Noble (1958) that

if $|\sigma_+^*(x,p)| < M_1e^{\lambda_- x}$ as $x \to +\infty$ then $\Sigma_+(s)$ is analytic in $\mathrm{Im}(s) = \lambda > \lambda_- = \lambda_1$,

and if $|v_-^*(x,p)| < M_2e^{\lambda_+ x}$ as $x \to -\infty$ then $V_-(s)$ is analytic in $\mathrm{Im}(s) = \lambda < \lambda_+ = \lambda_2$.

1.3.1 Wiener-Hopf technique

Eliminating $E(s,p)$ from (1.37) and (1.38) yields a Wiener-Hopf equation

$$\frac{\sigma_0}{ips}-\Sigma_+(s) = \mu_{12}\xi\frac{F(s,p)}{\sqrt{s^2+p^2/c_d^2}}V_-(s) \tag{1.41}$$

which contains only the two unknown functions $\Sigma_+(s)$ and $V_-(s)$, and now the Wiener-Hopf technique can be applied as follows. Suppose that the function $L(s)$ is defined and factored

as

$$L(s) = \frac{L_-(s)}{L_+(s)} = \mu_{12}\xi \frac{F(s,p)}{\sqrt{s^2 + p^2/c_d^2}} \tag{1.42}$$

then equation (1.41) becomes

$$\frac{\sigma_0}{ips} L_+(s) - \Sigma_+(s)L_+(s) = L_-(s)V_-(s). \tag{1.43}$$

Assume that the function $D(s)$ can be decomposed as

$$\frac{\sigma_0}{ips} L_+(s) = D(s) = D_+(s) + D_-(s) \tag{1.44}$$

then equation (1.43) becomes

$$D_+(s) - \Sigma_+(s)L_+(s) = L_-(s)V_-(s) - D_-(s) = W(s). \tag{1.45}$$

The first member of this equation is analytic in the upper half of the $s-$plane $\mathrm{Im}(s) = \lambda > \max(\lambda_1, \lambda_2) < 0$ and the second member is analytic in the lower half of the $s-$plane $\mathrm{Im}(s) = \lambda < 0$. Therefore, the regions of analyticity overlap. After determining $W(s)$, solutions for $\Sigma_+(s)$ and $V_-(s)$ can be found.

After algebraic manipulation it can be shown that the function $F(s,p)$ is given by

$$\begin{aligned} F(s,p) \;=\; & \frac{1}{\xi\sqrt{c_{11}}\sqrt{c_{11}s^2 + p^2/c_s^2}(\gamma_1+\gamma_2)(1+c_{12})} \Big\{ c_{22}c_{12}\gamma_1^2\gamma_2^2 - \gamma_1\gamma_2(1+c_{12})c_{12}^2 s^2 + \\ & (c_{11}s^2 + p^2/c_s^2)\left[c_{22}(\gamma_1^2+\gamma_2^2) + \gamma_1\gamma_2(1+c_{12})c_{22} + s^2(c_{12}+c_{12}^2 - c_{11}c_{22}) - c_{22}p^2/c_s^2\right]\Big\}. \end{aligned}$$

The only zeros of $F(s,p)$ are of the form $\pm ip/c_R$ where c_R is the Rayleigh wave speed. This can be seen by substituting $s = ip/v$ in $F(s,p)$, letting $F(s,p) = 0$ and dividing by the non-zero factors, then $F(ip/v, p) = 0$ reduces to

$$\sqrt{\frac{c_{22}}{c_{11}}}\left(\frac{c_{11}c_{22} - c_{12}^2}{c_{22}} - \frac{v^2}{c_s^2}\right)\sqrt{1 - \frac{v^2}{c_s^2}} - \frac{v^2}{c_s^2}\sqrt{1 - \frac{v^2}{c_{11}c_s^2}} = 0$$

which is the Rayleigh function for orthotropic materials (Ting, 1996). The roots of this function are $v = \pm c_R$.

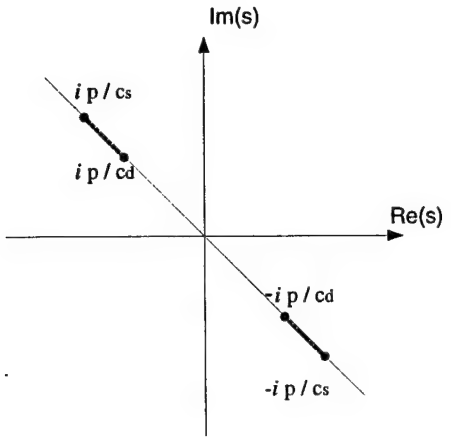

Figure 1.2: Branch cuts for $\hat{F}(s)$ in the $s-$plane.

Consequently, the first step in factoring $L(s)$ is to define

$$\hat{F}(s) = \frac{F(s,p)}{s^2 + p^2/c_R^2} \tag{1.46}$$

thus $\hat{F}(s) \to 1$ as $s \to \infty$, (the constant ξ in (1.29) was chosen to make this possible). The function $\hat{F}(s)$ is regular and $\hat{F}(s) \neq 0$ in the $s-$plane cut as shown in figure 1.2. The only singularities are the branch points shared with γ_1 and γ_2. It is readily shown that the branch points of γ_1 and γ_2 are

$$\begin{aligned} \text{for } \gamma_1; \quad s &= \pm\frac{ip}{c_s}, \\ \text{for } \gamma_2; \quad s &= \pm\frac{ip}{\sqrt{c_{11}}\, c_s} = \pm\frac{ip}{c_d}. \end{aligned}$$

It is well-known that factorization is accomplished most directly for functions that approach unity as $|s| \to \infty$ and that have neither zeros nor poles in the finite plane; $\hat{F}(s)$ is an example of such a function. Therefore, using Cauchy's integral formula it can be shown that (Freund 1990)

$$\hat{F}_{\pm}(s) = \exp\left\{\frac{1}{2\pi i}\int_{\Gamma_{\pm}} \frac{\log \hat{F}(z)}{z - s}\, dz\right\},$$

where Γ_- (Γ_+) is the contour enclosing the branch points $+ip/c_d$, $+ip/c_s$, ($-ip/c_d$, $-ip/c_s$). Using the fact that $\hat{F}(\bar{s}) = \overline{\hat{F}(s)}$ then

$$\hat{F}_{\pm}(s) = \exp\left\{\frac{-1}{\pi}\int_{1/c_d}^{1/c_s} \tan^{-1}\left(\frac{\mathrm{Im}[\hat{F}(ipw)]}{\mathrm{Re}[\hat{F}(ipw)]}\right)\frac{dw}{w \mp \frac{is}{p}}\right\}.$$

Returning to the factorization of $L(s)$ it is found that

$$L(s) = \frac{L_-(s)}{L_+(s)} = \mu_{12}\xi \frac{\hat{F}(s)(s^2 + p^2/c_R^2)}{\sqrt{s^2 + p^2/c_d^2}} \tag{1.47}$$

$$= \mu_{12}\xi \frac{\hat{F}_+(s)\hat{F}_-(s)(s + ip/c_R)(s - ip/c_R)}{\sqrt{s + ip/c_d}\sqrt{s - ip/c_d}} \tag{1.48}$$

therefore

$$L_-(s) = \mu_{12}\xi \frac{(s - ip/c_R)}{\sqrt{s - ip/c_d}} \hat{F}_-(s). \tag{1.49}$$

$$L_+(s) = \frac{\sqrt{s + ip/c_d}}{(s + ip/c_R)} \frac{1}{\hat{F}_+(s)}. \tag{1.50}$$

Decomposition of $D(s)$ follows easily,

$$D(s) = \frac{\sigma_0}{ips} L_+(s) = \frac{\sigma_0}{p} \left[\frac{L_+(s) - L_+(0)}{is} + \frac{L_+(0)}{is} \right] = D_+(s) + D_-(s) \tag{1.51}$$

with

$$D_+(s) = \frac{\sigma_0}{p} \left[\frac{L_+(s) - L_+(0)}{is} \right], \qquad D_-(s) = \frac{\sigma_0}{p} \left[\frac{L_+(0)}{is} \right]. \tag{1.52}$$

Each side of equation (1.45) is analytic in one of the overlapping half planes, and the sides coincide on the strip of overlap. Consequently each side of (1.45) is the analytic continuation of the other into its complementary half plane; so that the two sides together represent one and the same entire function $W(s)$. The entire function will be determined by its behavior at $|s| \to \infty$ which is related with the behavior of physical quantities near $x = 0$. First note that $L_+(s) \sim s^{-1/2}$ and $L_-(s) \sim s^{1/2}$ as $|s| \to \infty$, therefore, $D_+(s)$ and $D_-(s)$ in (1.52) are bounded in their respective planes of analyticity and vanish at infinity. Furthermore, $\sigma_+^*(x,p)$ is expected to be square root singular as $x \to 0^+$ and $v_-^*(x,p)$ is expected to vanish as $x \to 0^-$ to ensure continuity of displacement. Consequently from the Abel theorem (Noble, 1958) relating asymptotic properties of transforms

$$\lim_{x \to 0^+} x^{1/2} \sigma_+^*(x,p) \sim \lim_{s \to \infty} s^{1/2} \Sigma_+(s)$$

$$\lim_{x \to 0^-} |x|^{-q} v_-^*(x,p) \sim \lim_{s \to -\infty} |s|^{1+q} V_-(s)$$

for some $q > 0$. Therefore, it is expected that $\Sigma_+(s) \sim s^{-1/2}$ and $V_-(s) \sim s^{-1-q}$ as $|s| \to \infty$, thus the products $\Sigma_+(s)L_+(s)$ and $L_-(s)V_-(s)$ vanish at infinity. Therefore, each side of (1.45) vanishes as $|s| \to \infty$ in the corresponding half planes. According the the Lliouville's theorem, a bounded entire function is constant. In this case, $W(s)$ is bounded in the finite plane and $W(s) \to 0$ as $|s| \to \infty$ so that the constant must be zero; thus, $W(s) = 0$. By using then (1.45) and (1.52), the functions of interest are given by

$$\Sigma_+(s) = \frac{D_+(s)}{L_+(s)} = -\frac{\sigma_0}{p}\frac{1}{is}\left[\frac{L_+(0)}{L_+(s)} - 1\right]. \tag{1.53}$$

$$V_-(s) = \frac{D_-(s)}{L_-(s)} = \frac{\sigma_0}{p}\frac{1}{is}\frac{L_+(0)}{L_-(s)}. \tag{1.54}$$

1.3.2 Stress Intensity factor

To find the stress intensity factor, an asymptotic expression for the normal stress near the crack tip is sought. The Abel's theorem relating asymptotic expressions between a function and its Fourier transform is the following (Noble 1958)

$$\lim_{x\to 0^+} \sqrt{x}\ \sigma_+^*(x,p) = \lim_{s\to+\infty} e^{-i\pi/4}\sqrt{\frac{s}{\pi}}\ \Sigma_+(s). \tag{1.55}$$

Clearly, the behavior of $\Sigma_+(s)$ as $s \to \infty$ is needed. Note that

$$L_+(s) = \frac{1}{s^{1/2}} \quad \text{as} \quad s \to \infty$$

and since $\hat{F}_+(0) = \hat{F}_-(0) = \sqrt{\hat{F}(0)} = \frac{c_R}{p}\sqrt{F(0,p)}$ then

$$L_+(0) = \frac{p}{\sqrt{ipc_d}\sqrt{F(0,p)}}$$

therefore

$$\Sigma_+(s) = \frac{-\sigma_0}{(ip)^{3/2}}\frac{1}{s^{1/2}}\frac{p}{\sqrt{c_d}\sqrt{F(0,p)}} \quad \text{as} \quad s \to \infty. \tag{1.56}$$

Using this relation and the definition of the stress intensity factor in (1.55) gives

$$K_I^*(p) = \lim_{x\to 0^+} \sqrt{2\pi x}\ \sigma_+^*(x,p) = \lim_{s\to+\infty} e^{-i\pi/4}\sqrt{2s}\ \Sigma_+(s) \tag{1.57}$$

$$= \frac{\sigma_0\sqrt{2}}{p^{3/2}}\frac{p}{\sqrt{c_d}\sqrt{F(0,p)}}. \tag{1.58}$$

It is readily shown that

$$\sqrt{F(0,p)} = p\sqrt{\frac{\sqrt{c_{22}}}{c_s c_d \xi}} \tag{1.59}$$

so that

$$K_I^*(p) = \sigma_0 \sqrt{\frac{2c_s\xi}{\sqrt{c_{22}}}} \frac{1}{p^{3/2}} \tag{1.60}$$

and by Laplace inversion the dynamic stress intensity factor in the time domain for this loading mode is

$$\boxed{K_I(t) = 2\sigma_0 \sqrt{\frac{2c_s\xi}{\pi\sqrt{c_{22}}}}\ \sqrt{t}\ .} \tag{1.61}$$

For the isotropic case and with plane strain conditions, substituting $E_1 = E_2 = E$, $\nu_{12} = \nu_{13} = \nu_{23} = \nu$ and $\mu_{12} = E/2(1+\nu)$ in equations (1.4) and the results in (1.30) it is found that $c_{22} = 2(1-\nu)/(1-2\nu)$ and $\xi = 1/(1-\nu)$ and equation (1.61) reduces to the well known result for isotropic materials (Freund 1990)

$$K_I(t) = 2\sigma_0 \frac{\sqrt{c_d(1-2\nu)/\pi}}{(1-\nu)}\ \sqrt{t}.$$

1.4 In-Plane Shear Loading

Consider the crack geometry illustrated in figure 1.1(b). The crack faces are subjected to suddenly applied, spatially uniform shear traction of magnitude τ_0. Exploiting asymmetry and examining the half space $y \geq 0$, the corresponding boundary conditions are

$$\begin{aligned} \tau_{xy}(x,0,t) &= -\tau_0 H(t) \quad \text{for} \quad -\infty < x < 0, \\ \sigma_y(x,0,t) &= 0 \qquad \text{for} \quad -\infty < x < \infty, \\ u(x,0,t) &= 0 \qquad \text{for} \quad x > 0, \end{aligned} \tag{1.62}$$

where $H(t)$ is the Heaviside step function. In addition the condition of zero displacements at infinity and zero initial conditions are assumed.

The method of solution is similar to that used for normal impact. Applying Laplace transform to boundary conditions (1.62) gives

$$\begin{aligned} \tau^*_{xy}(x,0,p) &= -\tau_0/p \quad \text{for} \quad -\infty < x < 0, \\ \sigma^*_y(x,0,p) &= 0 \quad \text{for} \quad -\infty < x < \infty, \\ u^*(x,0,p) &= 0 \quad \text{for} \quad x > 0. \end{aligned} \tag{1.63}$$

Assuming the displacement field (1.12) and (1.13) yields the same system of ordinary differential equations (1.14) and (1.15) whose solution is given by equations (1.16) where α_j are defined by (1.17) and γ_j are obtained from the solution of (1.18). Using (1.19), (1.20) and (1.5) indicates that σ^*_y is given by

$$\sigma^*_y(x,y,p) = -\frac{i\mu_{12}}{2\pi}\int_{-\infty}^{\infty}[(s^2c_{12}-\alpha_1\gamma_1c_{22})A_1e^{-\gamma_1 y}+(s^2c_{12}-\alpha_2\gamma_2c_{22})A_2e^{-\gamma_2 y}]\frac{e^{-isx}}{s}\,ds. \tag{1.64}$$

Applying the second condition of (1.63) to equation (1.64) yields

$$\begin{aligned} A_2(s,p) &= -\beta_2 A_1(s,p), \\ \beta_2 &= \frac{s^2c_{12}-\alpha_1\gamma_1c_{22}}{s^2c_{12}-\alpha_2\gamma_2c_{22}}. \end{aligned} \tag{1.65}$$

Therefore, the expressions for the transformed components of displacement become

$$u^*(x,y,p) = \frac{1}{2\pi}\int_{-\infty}^{\infty}(e^{-\gamma_1 y}-\beta_2e^{-\gamma_2 y})A_1(s,p)e^{-isx}\,ds, \tag{1.66}$$

$$v^*(x,y,p) = \frac{-i}{2\pi}\int_{-\infty}^{\infty}(\alpha_1e^{-\gamma_1 y}-\beta_2\alpha_2e^{-\gamma_2 y})\frac{A_1(s,p)}{s}e^{-isx}\,ds, \tag{1.67}$$

and the associated stress components are given by

$$\sigma^*_x = \frac{-i\mu_{12}}{2\pi}\int_{-\infty}^{\infty}[(c_{11}s^2-\alpha_1\gamma_1c_{12})e^{-\gamma_1 y}-(c_{11}s^2-\alpha_2\gamma_2c_{12})\beta_2e^{-\gamma_2 y}]\frac{A_1(s,p)}{s}e^{-isx}ds, \tag{1.68}$$

$$\sigma^*_y = \frac{-i\mu_{12}}{2\pi}\int_{-\infty}^{\infty}(c_{12}s^2-\alpha_1\gamma_1c_{22})(e^{-\gamma_1 y}-e^{-\gamma_2 y})\frac{A_1(s,p)}{s}e^{-isx}ds, \tag{1.69}$$

$$\tau^*_{xy} = \frac{-\mu_{12}}{2\pi}\int_{-\infty}^{\infty}[(\alpha_1+\gamma_1)e^{-\gamma_1 y}-(\alpha_2+\gamma_2)\beta_2e^{-\gamma_2 y}]A_1(s,p)e^{-isx}ds. \tag{1.70}$$

Introducing the functions

$$C(s,p) = (1-\beta_2)A_1(s,p), \tag{1.71}$$

$$G(s,p) = \frac{\sqrt{s^2+p^2/c_s^2}}{(1-\beta_2)\eta}[(\alpha_1+\gamma_1)-\beta_2(\alpha_2+\gamma_2)], \tag{1.72}$$

$$\eta = \frac{c_{11}\xi}{c_{22}N_1N_2} \tag{1.73}$$

where ξ and $N_{1,2}$ are given in (1.30) and (1.31) and in view of the first and third boundary conditions in (1.63), equation (1.66) and (1.70) yield the following pair of dual integral equations for the determination of the function $C(s,p)$,

$$\tau^*_{xy}(x,0,p) = \frac{-\mu_{12}\eta}{2\pi}\int_{-\infty}^{\infty}\frac{G(s,p)}{\sqrt{s^2+p^2/c_s^2}}C(s,p)e^{-isx}\,ds = -\frac{\tau_0}{p} \qquad -\infty<x<0, \tag{1.74}$$

$$u^*(x,0,p) = \frac{1}{2\pi}\int_{-\infty}^{\infty}C(s,p)e^{-isx}\,ds = 0 \qquad 0<x<\infty, \tag{1.75}$$

Let $u^*_-(x,p)$ be the unknown Laplace transform of the displacement on the negative $x-$axis, and $\tau^*_+(x,p)$ be the unknown Laplace transform of the shear stress on the positive $x-$axis, so that

$$u^*(x,0,p) = \begin{cases} 0 & \text{for} \quad x>0 \\ u^*_-(x,p) & \text{for} \quad x<0 \end{cases} \qquad \tau^*_{xy}(x,0,p) = \begin{cases} \tau^*_+(x,p) & \text{for} \quad x>0 \\ -\tau_0/p & \text{for} \quad x<0. \end{cases} \tag{1.76}$$

Then, the Laplace transform of the shear stress and the displacement on the whole boundary $y=0$ is

$$\frac{-\mu_{12}\eta}{2\pi}\int_{-\infty}^{\infty}\frac{G(s,p)}{\sqrt{s^2+p^2/c_s^2}}C(s,p)e^{-isx}\,ds = -\frac{\tau_0}{p}H(-x)+\tau^*_+(x), \tag{1.77}$$

$$\frac{1}{2\pi}\int_{-\infty}^{\infty}C(s,p)e^{-isx}\,ds = u^*_-(x) \tag{1.78}$$

and by Fourier transform inversion, these equations give

$$-\mu_{12}\eta\frac{G(s,p)}{\sqrt{s^2+p^2/c_s^2}}C(s,p) = -\frac{\tau_0}{ips}+T_+(s) \tag{1.79}$$

$$C(s,p) = U_-(s) \tag{1.80}$$

where

$$T_+(s) = \int_0^{\infty}\tau^*_+(x)e^{isx}dx \tag{1.81}$$

$$U_-(s) = \int_{-\infty}^{0}u^*_-(x)e^{isx}dx \tag{1.82}$$

$$\int_{-\infty}^{0}\left(\frac{-\tau_0}{p}\right)e^{isx}dx = -\frac{\tau_0}{ips}$$

Eliminating $C(s,p)$ from (1.79) and (1.80) results in a Wiener-Hopf equation

$$\frac{\tau_0}{ips} - T_+(s) = \mu_{12}\eta \frac{G(s,p)}{\sqrt{s^2 + p^2/c_s^2}} U_-(s) \tag{1.83}$$

which contains only the two unknown functions, $T_+(s)$ and $U_-(s)$, and can be solved using the Wiener-Hopf technique as in the normal impact analysis. The result is

$$D_+(s) - T_+(s)L_+(s) = L_-(s)U_-(s) - D_-(s) = 0 \tag{1.84}$$

where

$$L_-(s) = -\mu_{12}\xi \frac{(s - ip/c_R)}{\sqrt{s - ip/c_s}} \hat{G}_-(s), \tag{1.85}$$

$$L_+(s) = \frac{\sqrt{s + ip/c_s}}{(s + ip/c_R)} \frac{1}{\hat{G}_+(s)}, \tag{1.86}$$

and

$$D(s) = \frac{\tau_0}{ips} L_+(s) = \frac{\tau_0}{p}\left[\frac{L_+(s) - L_+(0)}{is} + \frac{L_+(0)}{is}\right] = D_+(s) + D_-(s), \tag{1.87}$$

with

$$D_+(s) = \frac{\tau_0}{p}\left[\frac{L_+(s) - L_+(0)}{is}\right], \quad \text{and} \quad D_-(s) = \frac{\tau_0}{p}\left[\frac{L_+(0)}{is}\right]$$

where

$$\hat{G}(s) = \frac{G(s,p)}{s^2 + p^2/c_R^2}. \tag{1.88}$$

It can be shown that $\hat{G}(s) \to 1$ as $s \to \infty$. Thus, the solution of (1.84) is

$$T_+(s) = \frac{D_+(s)}{L_+(s)} = -\frac{\tau_0}{p}\frac{1}{is}\left[\frac{L_+(0)}{L_+(s)} - 1\right] \tag{1.89}$$

$$U_-(s) = \frac{D_-(s)}{L_-(s)} = \frac{\tau_0}{p}\frac{1}{is}\frac{L_+(0)}{L_-(s)}. \tag{1.90}$$

with $L_\pm(s)$ defined in (1.85) and (1.86) and $\hat{G}_\pm(s)$ given by

$$\hat{G}_\pm(s) = \exp\left\{\frac{-1}{\pi}\int_{1/c_d}^{1/c_s} \tan^{-1}\left(\frac{\mathrm{Im}[\hat{G}(ipw)]}{\mathrm{Re}[\hat{G}(ipw)]}\right)\frac{dw}{w \mp \frac{is}{p}}\right\}.$$

To calculate the stress intensity factor $T_+(s)$ as $s \to \infty$ is needed. First, note that

$$L_+(s) = \frac{1}{s^{1/2}} \quad \text{as} \quad s \to \infty$$

and since $\hat{G}_+(0) = \hat{G}_-(0) = \sqrt{\hat{G}(0)} = \frac{c_R}{p}\sqrt{G(0,p)}$ then

$$L_+(0) = \frac{p}{\sqrt{ipc_s}\sqrt{G(0,p)}}.$$

Therefore,

$$T_+(s) = \frac{-\tau_0}{(ip)^{3/2}}\frac{1}{s^{1/2}}\frac{p}{\sqrt{c_s}\sqrt{G(0,p)}} \quad \text{as} \quad s \to \infty. \tag{1.91}$$

Using (1.55) and the definition of the stress intensity factor gives

$$K^*_{II}(p) = \lim_{x\to 0^+}\sqrt{2\pi x}\,\tau^*_+(x,p) = \lim_{s\to+\infty} e^{-i\pi/4}\sqrt{2s}\,T_+(s) \tag{1.92}$$

$$= \frac{\tau_0\sqrt{2}}{p^{3/2}}\frac{p}{\sqrt{c_s}\sqrt{G(0,p)}}. \tag{1.93}$$

It can be shown that

$$\sqrt{G(0,p)} = \frac{p}{c_s\sqrt{\eta}}, \tag{1.94}$$

so that

$$K^*_{II}(p) = \tau_0\sqrt{2c_s\eta}\,\frac{1}{p^{3/2}}, \tag{1.95}$$

and by Laplace inversion

$$\boxed{K_{II}(t) = 2\tau_0\sqrt{2c_s\eta/\pi}\,\sqrt{t}.} \tag{1.96}$$

For the isotropic case and with plane strain conditions $\eta = 1/(1-\nu)$ and equation (1.96) reduces to the well known result for isotropic materials (Freund 1990)

$$K_{II}(t) = 2\tau_0\sqrt{\frac{2c_s}{\pi(1-\nu)}}\,\sqrt{t}.$$

1.5 Antiplane Shear

Consider a semi-infinite crack in orthotropic material shown in figure 1.3, subjected to antiplane shear loading of magnitude τ_0. The governing differential equation for two dimensional antiplane motions of homogeneous, orthotropic, linearly elastic solids is (Nayfeh 1995)

$$\beta^2\frac{\partial^2 w}{\partial x^2} + \frac{\partial^2 w}{\partial y^2} = \frac{1}{c_h^2}\frac{\partial^2 w}{\partial t^2}, \tag{1.97}$$

where

$$\beta^2 = \frac{C_{55}}{C_{44}} \quad \text{and} \quad c_h = \sqrt{C_{44}/\rho}.$$

Again, the principal material axes of orthotropy are chosen to coincide with the (x, y, z) axes, such that the in-plane and antiplane motions are not coupled. In terms of the engineering constants, C_{44} and C_{55} are given by $C_{44} = \mu_{23}$ and $C_{55} = \mu_{31}$. The non-zero stresses are related to the displacements by the equations

$$\tau_{xz} = C_{55}\frac{\partial w}{\partial x} \qquad \tau_{yz} = C_{44}\frac{\partial w}{\partial y}. \tag{1.98}$$

Exploiting symmetry and examining the upper half-plane $y \geq 0$, the boundary conditions for this loading mode are given as

$$\tau_{yz}(x, 0, t) = -\tau_0 H(t) \quad \text{for} \quad x < 0 \tag{1.99}$$

$$w(x, 0, t) = 0 \quad \text{for} \quad x > 0. \tag{1.100}$$

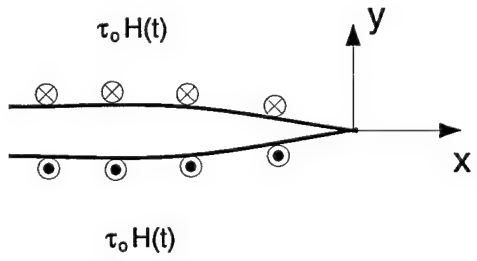

Figure 1.3: Schematic of the semi-infinite crack geometry. Antiplane shear loading.

The method of solution is very similar to that used for the in-plane problems. Applying Laplace transform to the governing equation gives

$$\beta^2\frac{\partial^2 w^*}{\partial x^2} + \frac{\partial^2 w^*}{\partial y^2} - \frac{p^2}{c_h^2}w^* = 0 \tag{1.101}$$

and to the boundary conditions gives

$$\tau^*_{yz}(x, 0, p) = -\tau_0/p \quad \text{for} \quad x < 0 \tag{1.102}$$

$$w^*(x, 0, p) = 0 \quad \text{for} \quad x > 0. \tag{1.103}$$

Assuming a displacement field of the form

$$w^*(x,y,p) = \frac{1}{2\pi}\int_{-\infty}^{\infty} A(s,y,p)e^{-isx}\,ds, \tag{1.104}$$

and inserting it into (1.101) results in the ordinary differential equation

$$\frac{d^2A}{dy^2} - (s^2\beta^2 + p^2/c_h^2)A = 0.$$

The solution of this equation which vanishes for $y \to \infty$ is

$$A(s,y,p) = A_1(s,p)e^{-\gamma y},$$

with

$$\gamma = \sqrt{\beta^2 s^2 + p^2/c_h^2}. \tag{1.105}$$

Therefore, the non-zero displacements and stresses are

$$w^*(x,y,p) = \frac{1}{2\pi}\int_{-\infty}^{\infty} A_1(s,p)e^{-\gamma y}e^{-isx}\,ds, \tag{1.106}$$

$$\tau_{xz}^*(x,y,p) = \frac{-iC_{55}}{2\pi}\int_{-\infty}^{\infty} s\,A_1(s,p)e^{-\gamma y}e^{-isx}\,ds, \tag{1.107}$$

$$\tau_{yz}^*(x,y,p) = \frac{-C_{44}}{2\pi}\int_{-\infty}^{\infty} \gamma\,A_1(s,p)e^{-\gamma y}e^{-isx}\,ds. \tag{1.108}$$

Applying the boundary conditions (1.102) and (1.103) yields a system of dual integral equations for the determination of the function $A_1(s,p)$

$$\begin{aligned}
\frac{1}{2\pi}\int_{-\infty}^{\infty} A_1(s,p)e^{-\gamma y}e^{-isx}\,ds &= 0 \quad \text{for} \quad x > 0,\\
\frac{-C_{44}}{2\pi}\int_{-\infty}^{\infty} \gamma\,A_1(s,p)e^{-\gamma y}e^{-isx}\,ds &= -\tau_0/p \quad \text{for} \quad x < 0,
\end{aligned}$$

or on the whole boundary $y = 0$

$$\begin{aligned}
\frac{1}{2\pi}\int_{-\infty}^{\infty} A_1(s,p)e^{-\gamma y}e^{-isx}\,ds &= -w_-^*(x,p),\\
\frac{-C_{44}}{2\pi}\int_{-\infty}^{\infty} \gamma\,A_1(s,p)e^{-\gamma y}e^{-isx}\,ds &= -\frac{\tau_0}{p}H(-x) + \tau_+^*(x,p).
\end{aligned}$$

By Fourier transform inversion

$$A_1(s,p) = W_-(s), \tag{1.109}$$

$$-C_{44}\gamma A_1(s,p) = -\frac{\tau_0}{ips} + T_+(s), \tag{1.110}$$

where

$$W_-(s) = \int_{-\infty}^{0} w_-^*(x,p)e^{isx}dx,$$
$$T_+(s) = \int_{0}^{\infty} \tau_+^*(x,p)e^{isx}dx.$$

Eliminating A_1 from equations (1.109) and (1.110) gives the Wiener-Hopf equation

$$\frac{\tau_0}{ips} - T_+(s) = C_{44}\gamma W_-(s). \tag{1.111}$$

Using the Wiener-Hopf technique as in the previous problems it is found that

$$T_+(s) = -\frac{\tau_0}{p}\frac{1}{is}\left[\frac{L_+(0)}{L_-(s)} - 1\right] \tag{1.112}$$

where

$$L_+(s) = \frac{1}{\gamma_+(s)}, \qquad L_-(s) = C_{44}\gamma_-(s),$$

and

$$\gamma_+(s) = \sqrt{\beta s + ip/c_h}, \qquad \gamma_-(s) = \sqrt{\beta s - ip/c_h}.$$

To find the stress intensity factor $T_+(s)$ as $s \to \infty$ is needed. This is given by

$$T_+(s) = -\frac{\tau_0}{(ip)^{3/2}}\frac{\sqrt{\beta c_h}}{s^{1/2}} \quad \text{as} \quad s \to \infty. \tag{1.113}$$

Therefore, the dynamic stress intensity factor is

$$K_{III}^*(p) = \frac{\tau_0\sqrt{2}}{p^{3/2}}\sqrt{\beta c_h}$$

and in the time domain

$$\boxed{K_{III}(t) = 2\tau_0\sqrt{2\beta c_h/\pi}\sqrt{t}.} \tag{1.114}$$

For transversely isotropic materials with fibers along the $x-$axis, $C_{55} = \mu_{12}$ and $\beta c_h = \sqrt{\mu_{12}/\rho} = c_s$, this equation becomes

$$K_{III}(t) = 2\tau_0\sqrt{2c_s/\pi}\sqrt{t}.$$

For isotopic materials, the same expression for $K_{III}(t)$, with the shear wave velocity $c_s = \sqrt{\mu/\rho}$ is found.

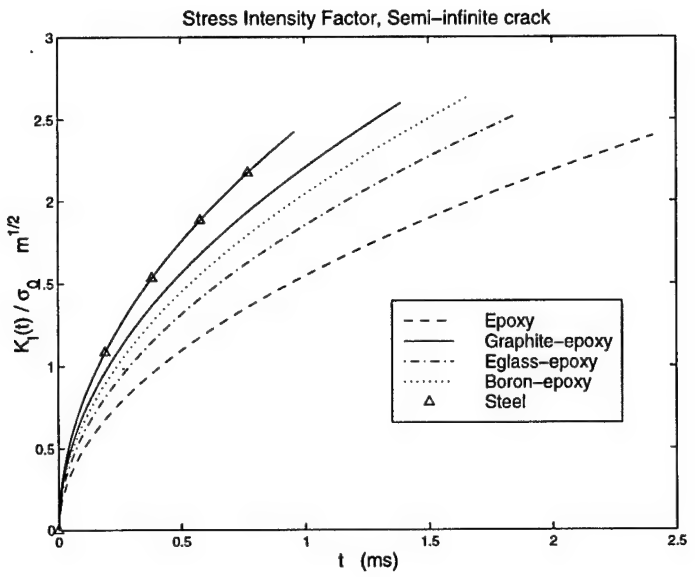

Figure 1.4: Stress intensity factor history for a semi-infinite crack in different materials, real time.

	Graphite Epoxy	E-Glass Epoxy	Boron Epoxy	Epoxy	Steel
c_{11}	20.77	8.38	32.67	3.91	3.5
c_{22}	2.18	2.29	3.12	3.91	3.5
c_{12}	0.49	0.52	0.79	1.91	1.5
μ_{12} (GPa)	7.48	5.5	6.4	1.96	76.92
ρ (Kg/m^3)	1600	2100	1990	1260	7840
$(c_{22}/c_{11})^{1/4}$	0.57	0.73	0.56	1	1

Table 1.1: Mechanical properties used for the analysis.

1.6 Results and Conclusions

Closed form expressions of the dynamic stress intensity factors $K_I(t)$, $K_{II}(t)$ and $K_{III}(t)$ have been determined for semi-infinite cracks in orthotropic materials under the three loading modes, i.e., opening, in-plane shear and antiplane shear loadings, respectively. The method of solution differs from that typically used in the isotropic case. The displacement formulation of the equations of motion is solved without the use of Helmholtz potentials. It has been shown that the orthotropic formulation includes the isotropic results as special cases. That is, for each loading mode the dynamic stress intensity factor for isotropic materials is recovered

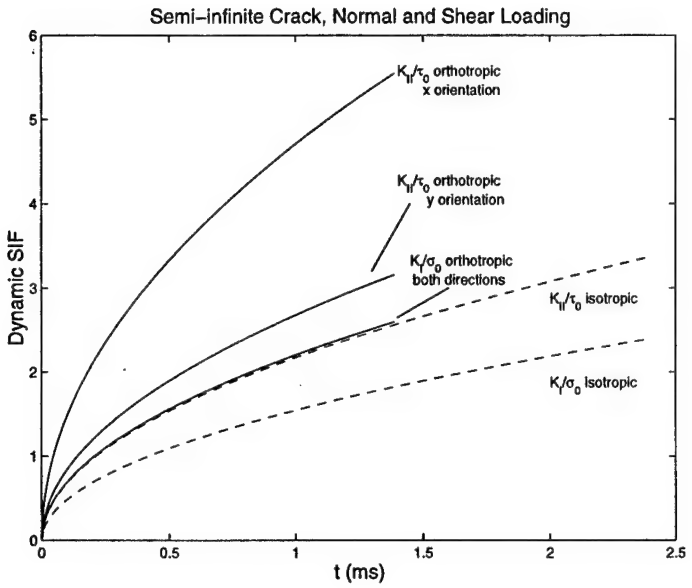

Figure 1.5: Stress intensity factor history $K_I(t)$ and $K_{II}(t)$ for a semi-infinite crack in different materials. The isotropic case corresponds to epoxy and the orthotropic to graphite-epoxy.

from the orthotropic expressions with the proper substitution of the elastic constants.

Figure 1.4 shows the stress intensity factor history for the opening mode for different materials. The material properties used are shown in table 1.1. As in the isotropic case, the stress intensity factors are proportional to the square root of time; hence there is no equivalent quasi-static problem for the semi-infinite crack under uniform loadings and there is no long-time equilibrium value. It can be seen that the fiber reinforcement of epoxy leads to an increase of the stress intensity factor for a given time, i.e., $K_I(t)$ for graphite-epoxy composite is greater than the corresponding $K_I(t)$ for epoxy at a given time t. Figure 1.5 shows the stress intensity factors $K_I(t)$ and $K_{II}(t)$ for isotropic (epoxy) and orthotropic (graphite-epoxy) materials, note that with same load amplitude the stress intensity factor $K_{II}(t)$ is greater than $K_I(t)$ at a given time. In both cases, the introduction of fibers results in an increase in the stress intensity factor.

It is interesting to note that $K_I(t)$ for a composite with fibers parallel to the $x-$axis and for a composite with fibers parallel to y-axis is the same. This result is contained in equation (1.61) since the ratio $\xi/\sqrt{c_{22}}$ is invariant to the replacement of c_{22} by c_{11} and c_{11}

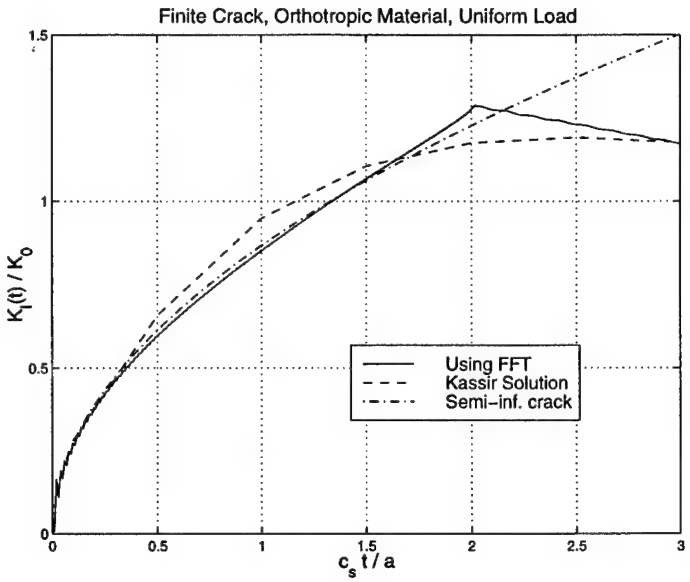

Figure 1.6: Comparison of the stress intensity factor $K_I(t)$ for a semi-infinite crack and a finite crack of length $2a$ in orthotropic material, the latter is a numerical solution obtained using integral transform methods by Kassir and Bandyopadhyay (1983) and by Rubio-Gonzalez and Mason (1998) using FFT for Laplace transform inversion. $K_0 = \sigma_0\sqrt{\pi a}$.

by c_{22}. This result does not hold for the in-plane shear loading however, since $K_{II}(t)$ for the fibers oriented along the $y-$axis is less than that for fibers oriented along the $x-$axis by a factor of $(c_{22}/c_{11})^{1/4}$. This factor is given in Table 1.1 for the materials examined here.

Integral transform methods have been applied to solve dynamic problems dealing with finite cracks in orthotropic materials. Figure 1.6 shows the stress intensity factor for a finite crack of length $2a$ in orthotropic material under uniform impact loading, this is an approximated solution obtained by Kassir and Bandyopadhyay (1983) and by Rubio-Gonzalez and Mason (1998) using a more suitable technique for numerical inversion of the Laplace transform. It is known that for short times the finite crack behaves like a semi-infinite crack. As illustrated in the figure, the closed form solution derived here agrees with the numerical solution for short times ($c_s t/a < 2$) as expected.

Acknowledgment

Support of this work by the Office of Naval Research Young Investigator Program under grant N00014-96-1-0774 supervised by Dr. Y. Rajapakse and by the Mexican Government through CONACYT (Consejo Nacional de Ciencia y Tecnologia) is gratefully acknowledged.

Bibliography

[1] Baker B.R., 1962, *Dynamic Stresses Created by a Moving Crack*, ASME, J. Appl. Mech. v.29, pp.449-458.

[2] Chen, E.P., and Sih, G.C. 1977, *Transient Response of Cracks to Impact Loads* in Elastodynamic Crack Problems, ed. G.C. Sih, Noordhoff International Publishing. Leyden.

[3] Freund, L.B., 1990, *Dynamic Fracture Mechanics*, Cambridge University Press. New York.

[4] Kassir, M.K., and Bandyopadhyay, K.K., 1983, *Impact Response of a Cracked Orthotropic Medium*, ASME, J. Appl. Mech. v.50, pp.630-636.

[5] Maue A.W., 1954 *Die Entspannungswelle bei plotzlichem Einschnitt eines gespannten elastischen Korpes* ZAMM v34, n1/2, pp.1-10.

[6] Nayfeh, A.H., 1995, *Wave Propagation in Anisotropic Media with Applications to Composites*, North-Holland Publishing Company. Amsterdam.

[7] Noble B., 1958, *Methods Based on the Wiener-Hopf Technique*, Elmsford, N.Y., Pergamon.

[8] Rubio-Gonzalez, C. and Mason, J.J., 1998, *Fundamental Solutions for the Stress Intensity Factor Evolution in Finite Cracks in Orthotropic Materials.*, Submitted to Int. J. of Fracture.

[9] Rubio-Gonzalez, C. and Mason, J.J., 1998, *Response of Finite Cracks in Orthotropic Materials due to Concentrated Impact Shear Loads.*, Submitted to J. Appl. Mech.

[10] Shindo, Y. and Nozaki, H., 1991a, *Impact Response of a Finite Crack in an Orthotropic Strip*, Acta Mechanica, v.62, pp.87-104.

[11] Ting, T.C.T., 1996, *Anisotropic Elasticity*, Oxford University Press, New York.

Chapter 2

Dynamic Stress Intensity Factor for a Propagating Semi-infinite Crack in Orthotropic Materials.

co-authored with C. Rubio-Gonzalez

The elastodynamic response of an infinite orthotropic material with a semi-infinite crack propagating at constant speed is examined. Solution for the stress intensity factor history around the crack tip is found for the loading modes I and II. Laplace and Fourier transforms along with the Wiener-Hopf technique are employed to solve the equations of motion. The asymptotic expression for the stress near the crack tip is analyzed which lead to a closed-form solution of the dynamic stress intensity factor. It is found that the stress intensity factor for the propagating crack is proportional to the stress intensity factor for a stationary crack by a factor similar to the universal function $k(v)$ from the isotropic case. Results are presented for orthotropic materials as well as for the isotropic case.

2.1 Introduction

Problems of crack propagation at constant speed can be classified into three classes depending on the boundary conditions [5]. The first class is the steady state crack growth. Here, the crack tip moves at constant speed for all the time and the mechanical fields are invariant with respect to an observer moving with the crack tip. The second class of problems is the self-similar crack growth subjected to time-independent loading. In this case, the crack tip moves at constant speed from some initial instant, and certain mechanical fields are invariant with respect to an observer moving steadily away from the process being observed. The third category of problems corresponds crack growth due to time-dependent loading usually in the form of crack face pressure or normally incident stress pulse.

The prototype problem of the first category is the two dimensional Yoffe problem [15] of a crack of fixed length propagating in an isotropic body subjected to uniform remote tensile loading. Even though this mathematical problem is not a realistic model of a physical situation because of the feature that the crack closes at one end at the same rate at which it opens at the other end; it is important because some field quantities are independent of the fictitious crack length $2a$, in particular the angular variation of the near tip stress field. Propagating finite cracks under steady state conditions have also been considered for orthotropic materials by several authors using different techniques. Kassir and Tse [6] through an integral transform technique reduced the related boundary value problem to a system of dual integral equations. Piva and Viola [11] solved the same problem through a complex variable approach reducing the equations of motion to a first order elliptic system of the Cauchy-Riemann type. More recently, Lee, *et al* [8] obtained higher order expressions for the stress and displacements around the tip of a crack propagating in orthotropic materials. In that work a power series representation of complex potentials was used. Atkinson [1] studied the steady-state propagation of a semi-infinite crack in aelotropic materials by means of the Cauchy integral formula. In all of these works the emphasis was in the angular variation of the stress field near the crack tip. Kousiounelos and Williams [7] analyzed the

problem of a dynamically propagating crack in a highly orthotropic fiber composite infinite strip subjected to constant displacement mode I loading. The basic assumption was to neglect the strain along the fibers and simplify substantially the mathematical treatment. Using Fourier transforms and the Wiener-Hopf technique they obtained expressions for the dynamic stress intensity factor and dynamic energy release rate under this simplified model.

The Broberg problem [3] is the prototype of the second category. In self-similar problems attention is focused on the symmetric expansion of a crack at constant rate from zero initial length. A thorough discussion of the analysis of self-similar mixed boundary value problems in elastodynamics was presented by Willis [14]. He considered problems in both two and three space dimensions as well as isotropic and anisotropic materials.

The prototype of the third category is the Baker problem [2] for isotropic materials. He considered a transient problem in which a semi-infinite crack extends at constant velocity after a step stress loading on the crack faces is applied at time $t = 0$. This type of loading induces a transient traction distribution on the crack plane ahead of the crack tip. If the material is of limited strength, the crack will begin to extend at some later time, $t = t_0$, after the application of the load, where t_0 is the delay time for the process. Freund [4] showed that the stress intensity factor is independent of the time delay and that it has the form of the stress intensity factor for a stationary crack subjected to the same stress wave loading multiplied by the stress universal function $k_I(v)$, i.e.

$$K_I(t, v) = k_I(v) K_I(t, 0). \tag{2.1}$$

Furthermore, Freund [4] also demonstrated that the relation (2.1) holds for crack propagation at non-uniform speed being v the instantaneous crack tip velocity and $K_I(t, 0)$ the stress intensity factor for the crack as it had been at the instantaneous position for all time. Note the importance of the universal function of the crack tip velocity $k_I(v)$ in problems of arbitrary loading and non-uniform crack speed, even though $k_I(v)$ could have been obtained in the solution of a less general problem like that of a semi-infinite crack propagating at constant velocity and under a step loading (Baker problem).

The extension of the Baker problem to orthotropic materials under mode I and mode II loading is the aim of this work. That is, the problem to be examined consists of an unloaded crack propagating at constant velocity v in an undeformed unloaded orthotropic material that remains at rest. At some time, $t = 0$, uniform stress is applied to the crack faces. The resulting history of the stress intensity factor at the crack tip is a function of the velocity as well as the material properties and time, $K_i = K_i(t, c_{ij}, v)$ where i =I, II. As will be shown here, the dynamic stress intensity factor for the stationary semi-infinite crack due to Rubio-Gonzalez and Mason [12] is recovered letting $v = 0$. In [12] it was shown that

$$K_I(t,0) = 2\sigma_0\sqrt{\frac{2c_s\xi(0)}{\pi\sqrt{c_{22}}}}\,\sqrt{t}, \tag{2.2}$$

$$K_{II}(t,0) = 2\tau_0\sqrt{2c_s\eta(0)/\pi}\,\sqrt{t}, \tag{2.3}$$

which represent one of the few available closed form solutions for the dynamic stress intensity factors for cracks in orthotropic materials. Making use of these results, it will be possible to write $K_I(t,v)$ and $K_{II}(t,v)$ in the form of (2.1) and consequently derive expressions for the universal functions of the crack speed $k_I(v)$ and $k_{II}(v)$ in orthotropic materials. The motivation to achieve this task is that $k_I(v)$ and $k_{II}(v)$ may be useful in more general problems as in the case of isotropic materials.

2.2 Governing Equations, in-plane problems

Consider the plane problem of an infinite orthotropic medium containing a semi-infinite crack, Figure 2.1, propagating at constant velocity, v along the $x'-$axis. Let E_i, μ_{ij} and ν_{ij} $(i,j = 1,2,3)$ be the engineering elastic constants of the material where the indices 1, 2, and 3 correspond the Cartesian coordinates (x', y', z') chosen to coincide with the axes of material orthotropy. The crack faces are parallel to $x'-$axis.

Restricting the problem to two dimensions with wave propagation limited to the $x' - y'$ plane by setting all the derivatives with respect to z to be zero, it is readily shown that the

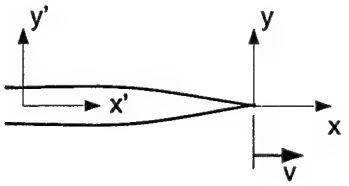

Figure 2.1: Schematic of the semi-infinite crack propagating at constant speed.

displacement equations of motion [9] reduce to

$$c_{11}\frac{\partial^2 u_x}{\partial x'^2} + \frac{\partial^2 u_x}{\partial y'^2} + (1+c_{12})\frac{\partial^2 u_y}{\partial x' \partial y'} = \frac{1}{c_s^2}\frac{\partial^2 u_x}{\partial t^2}, \tag{2.4}$$

$$\frac{\partial^2 u_y}{\partial x'^2} + c_{22}\frac{\partial^2 u_y}{\partial y'^2} + (1+c_{12})\frac{\partial^2 u_x}{\partial x' \partial y'} = \frac{1}{c_s^2}\frac{\partial^2 u_y}{\partial t^2}, \tag{2.5}$$

where u_x and u_y are the x and y components of the displacement vector and c_{11}, c_{12} and c_{22} are non-dimensional parameters related to the elastic constants by the relations:

$$\begin{aligned} c_{11} &= \frac{E_1}{\mu_{12}[1-(E_2/E_1)\nu_{12}^2]}, \\ c_{22} &= (E_2/E_1)c_{11}, \\ c_{12} &= \nu_{12}c_{22} = \nu_{21}c_{11}, \end{aligned} \tag{2.6}$$

for generalized plane stress, and by

$$\begin{aligned} c_{11} &= \frac{E_1}{\mu_{12}\Delta}(1-\nu_{23}\nu_{32}), \\ c_{22} &= \frac{E_2}{\mu_{12}\Delta}(1-\nu_{13}\nu_{31}), \\ c_{12} &= \frac{E_1}{\mu_{12}\Delta}(\nu_{21}+\frac{E_2}{E_1}\nu_{13}\nu_{32}), \\ \Delta &= 1-\nu_{12}\nu_{21}-\nu_{23}\nu_{32}-\nu_{31}\nu_{13}-\nu_{12}\nu_{23}\nu_{31}-\nu_{13}\nu_{21}\nu_{32}, \end{aligned} \tag{2.7}$$

for plane strain. In the orthotropic solid, $c_s = \sqrt{\mu_{12}/\rho}$ represents the velocity of the in-plane shear wave propagating along the the principal material axes and ρ is the mass density.

A new coordinate system (x, y) is attached to the propagating crack tip, the relation between the fixed and moving coordinates are

$$x = x' - vt \qquad y = y'.$$

Steady-state conditions are not assumed, consequently the motion equations in the moving coordinates are

$$\left(c_{11}-\frac{v^2}{c_s^2}\right)\frac{\partial^2 u_x}{\partial x^2}+\frac{\partial^2 u_x}{\partial y^2}+(1+c_{12})\frac{\partial^2 u_y}{\partial x\partial y} = \frac{1}{c_s^2}\left(\frac{\partial^2 u_x}{\partial t^2}-2v\frac{\partial^2 u_x}{\partial x\partial t}\right), \tag{2.8}$$

$$\left(1-\frac{v^2}{c_s^2}\right)\frac{\partial^2 u_y}{\partial x^2}+c_{22}\frac{\partial^2 u_y}{\partial y^2}+(1+c_{12})\frac{\partial^2 u_x}{\partial x\partial y} = \frac{1}{c_s^2}\left(\frac{\partial^2 u_y}{\partial t^2}-2v\frac{\partial^2 u_y}{\partial x\partial t}\right), \tag{2.9}$$

The stresses are related to the displacements by the equations:

$$\begin{aligned}\frac{\sigma_x}{\mu_{12}} &= c_{11}\frac{\partial u_x}{\partial x}+c_{12}\frac{\partial u_y}{\partial y},\\ \frac{\sigma_y}{\mu_{12}} &= c_{12}\frac{\partial u_x}{\partial x}+c_{22}\frac{\partial u_y}{\partial y},\\ \frac{\tau_{xy}}{\mu_{12}} &= \frac{\partial u_x}{\partial y}+\frac{\partial u_y}{\partial x}.\end{aligned} \tag{2.10}$$

2.3 Normal Impact

A spatially uniform pressure of magnitude σ_0 is applied suddenly on the crack faces at $t=0$. Exploiting symmetry and taking only the upper half plane $y \geq 0$, the corresponding boundary conditions are

$$\begin{aligned}\sigma_y(x,0,t) &= -\sigma_0 H(t) \quad \text{for} \quad -\infty < x < 0,\\ \tau_{xy}(x,0,t) &= 0 \quad \text{for} \quad -\infty < x < \infty,\\ u_y(x,0,t) &= 0 \quad \text{for} \quad x > 0,\end{aligned} \tag{2.11}$$

where $H(t)$ is the Heaviside step function. In addition the condition of zero displacements at infinity and zero initial conditions are assumed.

The method of solution of the governing equations presented here follows that described by Baker [2] for the isotropic case with some significant differences; displacement potentials are not used. In equations (2.8) and (2.9), the time variable may be removed by application of the Laplace transform

$$f^*(p)=\int_0^\infty f(t)\,e^{-pt}\,dt, \quad f(t)=\frac{1}{2\pi i}\int_{Br} f^*(p)\,e^{pt}\,dt, \tag{2.12}$$

where Br denotes the Bromwich path of integration which is a line parallel to the imaginary axis in the p-plane. Applying relations (2.12) to equations (2.8) and (2.9) and assuming zero initial conditions for the displacements and velocities, the transformed field equations become

$$\left(c_{11}-\frac{v^2}{c_s^2}\right)c_{11}\frac{\partial^2 u_x^*}{\partial x^2}+\frac{\partial^2 u_x^*}{\partial y^2}+(1+c_{12})\frac{\partial^2 u_y^*}{\partial x\partial y}-\frac{1}{c_s^2}\left(p^2u_x^*-2vp\frac{\partial u_x^*}{\partial x}\right) = 0, \quad (2.13)$$

$$\left(1-\frac{v^2}{c_s^2}\right)\frac{\partial^2 u_y^*}{\partial x^2}+c_{22}\frac{\partial^2 u_y^*}{\partial y^2}+(1+c_{12})\frac{\partial^2 u_x^*}{\partial x\partial y}-\frac{1}{c_s^2}\left(p^2u_y^*-2vp\frac{\partial u_y^*}{\partial x}\right) = 0, \quad (2.14)$$

where the transformed displacement components, u_x^* and u_y^*, are now functions of the variables x, y, and p. The application of the Laplace transform to the boundary conditions (2.11) gives

$$\begin{aligned}
\sigma_y^*(x,0,p) &= -\sigma_0\frac{1}{p} \quad \text{for} \quad -\infty<x<0,\\
\tau_{xy}^*(x,0,p) &= 0 \qquad \text{for} \quad -\infty<x<\infty, \qquad (2.15)\\
u_y^*(x,0,p) &= 0 \qquad \text{for} \quad x>0.
\end{aligned}$$

To obtain a solution of the differential equations (2.13) and (2.14) subject to conditions (2.15), the Fourier transform is applied,

$$F(s)=\int_{-\infty}^{\infty}f(x)\,e^{isx}\,dx, \quad f(x)=\frac{1}{2\pi}\int_{-\infty}^{\infty}F(s)\,e^{-isx}\,ds. \quad (2.16)$$

It is assumed that the displacements in the Laplace transform domain have the form

$$u_x^*(x,y,p) = \frac{1}{2\pi}\int_{-\infty}^{\infty}A(s,y,p)e^{-isx}\,ds, \quad (2.17)$$

$$u_y^*(x,y,p) = \frac{1}{2\pi}\int_{-\infty}^{\infty}B(s,y,p)e^{-isx}\,ds, \quad (2.18)$$

where A and B are the Fourier transforms of the Laplace transform of the displacements, u_x^* and u_y^*, respectively, and are yet to be determined. Substituting these transforms into equations (2.13) and (2.14), the functions A and B are found to satisfy the simultaneous ordinary differential equations

$$\left[\left(c_{11}-\frac{v^2}{c_s^2}\right)s^2+\frac{2vpis}{c_s^2}+\frac{p^2}{c_s^2}\right]A-\frac{d^2A}{dy^2}+(1+c_{12})is\frac{dB}{dy} = 0, \quad (2.19)$$

$$\left[\left(1-\frac{v^2}{c_s^2}\right)s^2+\frac{2vpis}{c_s^2}+\frac{p^2}{c_s^2}\right]B-c_{22}\frac{d^2B}{dy^2}+(1+c_{12})is\frac{dA}{dy} = 0. \quad (2.20)$$

The solution of these equations which vanishes for $y \to \infty$ is

$$\begin{aligned} A(s,y,p) &= A_1(s,p)e^{-\gamma_1 y} + A_2(s,p)e^{-\gamma_2 y}, \\ B(s,y,p) &= \frac{-i\alpha_1}{s}A_1(s,p)e^{-\gamma_1 y} - \frac{i\alpha_2}{s}A_2(s,p)e^{-\gamma_2 y}, \end{aligned} \tag{2.21}$$

where A_1 and A_2 are arbitrary functions and $\alpha_j(s,p)$ stands for the functions

$$\alpha_j(s,p) = \frac{\left(c_{11} - \frac{v^2}{c_s^2}\right)s^2 + \frac{2vpis}{c_s^2} + \frac{p^2}{c_s^2} - \gamma_j^2}{(1+c_{12})\gamma_j}, \quad j = 1,2 \tag{2.22}$$

with γ_1^2 and γ_2^2 being two distinct roots of the quadratic equation

$$\begin{aligned} c_{22}\gamma^4 + \left\{\left[\frac{v^2}{c_s^2} - c_{22}\left(c_{11} - \frac{v^2}{c_s^2}\right) + c_{12}^2 + 2c_{12}\right]s^2 - (1+c_{22})\frac{p^2}{c_s^2} - (1+c_{22})\frac{2vpis}{c_s^2}\right\}\gamma^2 + \\ \left[\left(c_{11} - \frac{v^2}{c_s^2}\right)s^2 + \frac{2vpis}{c_s^2} + \frac{p^2}{c_s^2}\right]\left[\left(1 - \frac{v^2}{c_s^2}\right)s^2 + \frac{2vpis}{c_s^2} + \frac{p^2}{c_s^2}\right] = 0. \end{aligned} \tag{2.23}$$

It can be shown that for many materials the roots γ_1 and γ_2 are real and positive and the expressions for the displacements in the Laplace transform domain become:

$$u_x^* = \frac{1}{2\pi}\int_{-\infty}^{\infty}(A_1e^{-\gamma_1 y} + A_2e^{-\gamma_2 y})e^{-isx}\,ds, \tag{2.24}$$

$$u_y^* = \frac{-i}{2\pi}\int_{-\infty}^{\infty}(\alpha_1 A_1e^{-\gamma_1 y} + \alpha_2 A_2e^{-\gamma_2 y})\frac{e^{-isx}}{s}ds, \tag{2.25}$$

and using (2.10) the corresponding expression for τ_{xy}^* is given by

$$\tau_{xy}^* = -\frac{\mu_{12}}{2\pi}\int_{-\infty}^{\infty}[(\alpha_1+\gamma_1)A_1e^{-\gamma_1 y} + (\alpha_2+\gamma_2)A_2e^{-\gamma_2 y}]e^{-isx}\,ds. \tag{2.26}$$

Applying the second condition of (2.15) to equation (2.26) yields

$$\begin{aligned} A_2(s,p) &= -\beta_1 A_1(s,p), \\ \beta_1 &= \frac{\alpha_1+\gamma_1}{\alpha_2+\gamma_2}. \end{aligned} \tag{2.27}$$

Therefore the expressions for the transformed components of displacement become

$$u_x^*(x,y,p) = \frac{1}{2\pi}\int_{-\infty}^{\infty}(e^{-\gamma_1 y} - \beta_1 e^{-\gamma_2 y})A_1(s,p)e^{-isx}\,ds, \tag{2.28}$$

$$u_y^*(x,y,p) = \frac{-i}{2\pi}\int_{-\infty}^{\infty}(\alpha_1 e^{-\gamma_1 y} - \beta_1\alpha_2 e^{-\gamma_2 y})\frac{A_1(s,p)}{s}e^{-isx}\,ds, \tag{2.29}$$

and the associated stress components are given by

$$\sigma_x^* = \frac{-i\mu_{12}}{2\pi}\int_{-\infty}^{\infty}[(c_{11}s^2-\alpha_1\gamma_1c_{12})e^{-\gamma_1 y}-(c_{11}s^2-\alpha_2\gamma_2c_{12})\beta_1e^{-\gamma_2 y}]\frac{A_1(s,p)}{s}e^{-isx}ds, \quad (2.30)$$

$$\sigma_y^* = \frac{-i\mu_{12}}{2\pi}\int_{-\infty}^{\infty}[(c_{12}s^2-\alpha_1\gamma_1c_{22})e^{-\gamma_1 y}-(c_{12}s^2-\alpha_2\gamma_2c_{22})\beta_1e^{-\gamma_2 y}]\frac{A_1(s,p)}{s}e^{-isx}ds, \quad (2.31)$$

$$\tau_{xy}^* = \frac{-\mu_{12}}{2\pi}\int_{-\infty}^{\infty}(\alpha_1+\gamma_1)[e^{-\gamma_1 y}-e^{-\gamma_2 y}]A_1(s,p)e^{-isx}ds. \quad (2.32)$$

Introducing the functions

$$E(s,p) = \frac{1}{s}(\alpha_1-\beta_1\alpha_2)A_1(s,p), \quad (2.33)$$

$$F(s,p) = -\frac{\theta_d}{(\alpha_1-\beta_1\alpha_2)\xi}[c_{12}s^2-\alpha_1\gamma_1c_{22}-\beta_1(c_{12}s^2-\alpha_2\gamma_2c_{22})], \quad (2.34)$$

$$\theta_d(v) = \sqrt{\left(1-\frac{v^2}{c_d^2}\right)s^2+\frac{2vpis}{c_d^2}+\frac{p^2}{c_d^2}} \quad (2.35)$$

$$\xi(v) = \frac{-\sqrt{1-v^2/c_d^2}}{(c_{11}-v^2/c_s^2)(1+c_{12})(N_1+N_2)(1-v^2/c_R^2)}\{(c_{12}^2+c_{12}-c_{11}c_{22}+c_{22}v^2/c_s^2)$$
$$(c_{12}N_1N_2-c_{11}+v^2/c_s^2)-c_{22}[c_{12}N_1^2N_2^2+(c_{11}-v^2/c_s^2)(N_1^2+N_1N_2+N_2^2)]\}, \quad (2.36)$$

$$N_{1,2}^2(v) = \frac{1}{2c_{22}}\{-v^2/c_s^2+c_{22}(c_{11}-v^2/c_s^2)-c_{12}^2-2c_{12}\pm[(v^2/c_s^2$$
$$-c_{22}(c_{11}-v^2/c_s^2)+c_{12}^2+2c_{12})^2-4c_{22}(c_{11}-v^2/c_s^2)(1-v^2/c_s^2)]^{1/2}\}, \quad (2.37)$$

where the velocity $c_d=\sqrt{c_{11}}c_s$ represents the dilatational wave speed along the $x-$axis and in view of the first and third boundary conditions in (2.15), equation (2.29) and (2.31) yield the following pair of dual integral equations for the determination of the function $E(s,p)$

$$\sigma_y^*(x,0,p)=\frac{i\mu_{12}\xi}{2\pi}\int_{-\infty}^{\infty}\frac{F(s,p)}{\theta_d}E(s,p)e^{-isx}\,ds = -\frac{\sigma_0}{p} \qquad -\infty<x<0, \quad (2.38)$$

$$u_y^*(x,0,p)=\frac{-i}{2\pi}\int_{-\infty}^{\infty}E(s,p)e^{-isx}\,ds = 0 \qquad 0<x<\infty. \quad (2.39)$$

Let $u_{y-}^*(x,p)$ be the unknown Laplace transform of the vertical displacement on the negative $x-$axis, and $\sigma_+^*(x,p)$ be the unknown Laplace transform of the normal stress on the positive $x-$axis, so that

$$u_y^*(x,0,p)=\begin{cases}0 & \text{for } x>0\\ u_{y-}^*(x,p) & \text{for } x<0\end{cases} \qquad \sigma_y^*(x,0,p)=\begin{cases}\sigma_+^*(x,p) & \text{for } x>0\\ -\sigma_0/p & \text{for } x<0.\end{cases} \quad (2.40)$$

Then the Laplace transform of the normal stress and the vertical displacement on the whole boundary $y = 0$ is given by

$$\frac{i\mu_{12}\xi}{2\pi}\int_{-\infty}^{\infty}\frac{F(s,p)}{\theta_d}E(s,p)e^{-isx}\,ds = -\frac{\sigma_0}{p}H(-x)+\sigma_+^*(x,p), \tag{2.41}$$

$$\frac{-i}{2\pi}\int_{-\infty}^{\infty}E(s,p)e^{-isx}\,ds = u_{y-}^*(x,p), \tag{2.42}$$

and by Fourier transform inversion, these equations give

$$i\mu_{12}\xi\frac{F(s,p)}{\theta_d}E(s,p) = -\frac{\sigma_0}{pis}+\Sigma_+(s), \tag{2.43}$$

$$-iE(s,p) = V_-(s), \tag{2.44}$$

where

$$\Sigma_+(s) = \int_0^{\infty}\sigma_+^*(x,p)e^{isx}dx, \tag{2.45}$$

$$V_-(s) = \int_{-\infty}^{0}u_{y-}^*(x,p)e^{isx}dx, \tag{2.46}$$

$$\int_{-\infty}^{0}\left(\frac{-\sigma_0}{p}\right)e^{isx}dx = -\frac{\sigma_0}{ips}.$$

From the physics of the problem it is reasonable to assume that the function $\sigma_+^*(x,p)$ and $u_{y-}^*(x,p)$ are exponentially bounded at infinity and this ensures the existence of their Fourier transform (2.45) and (2.46). In particular it is shown in [10] that

$$\text{if } |\sigma_+^*(x,p)| < M_1e^{\lambda_- x} \text{ as } x\to+\infty \text{ then } \quad \Sigma_+(s) \text{ is analytic in } \mathrm{Im}(s)=\lambda>\lambda_-,$$

$$\text{and if } |u_{y-}^*(x,p)| < M_2e^{\lambda_+ x} \text{ as } x\to-\infty \text{ then } \quad V_-(s) \text{ is analytic in } \mathrm{Im}(s)=\lambda<\lambda_+.$$

2.3.1 Wiener-Hopf technique

Eliminating $E(s,p)$ from (2.43) and (2.44) yields a Wiener-Hopf equation

$$\frac{\sigma_0}{ips}-\Sigma_+(s) = \mu_{12}\xi\frac{F(s,p)}{\theta_d}V_-(s) \tag{2.47}$$

which contains only the two unknown functions $\Sigma_+(s)$ and $V_-(s)$, and now the Wiener-Hopf technique can be applied as follows. Suppose that the function $L(s)$ is defined and factored as

$$L(s) = \frac{L_-(s)}{L_+(s)} = \mu_{12}\xi\frac{F(s,p)}{\theta_d} \tag{2.48}$$

then equation (2.47) becomes

$$\frac{\sigma_0}{ips}L_+(s) - \Sigma_+(s)L_+(s) = L_-(s)V_-(s). \tag{2.49}$$

Assume that the function $D(s)$ can be defined and decomposed as

$$\frac{\sigma_0}{ips}L_+(s) = D(s) = D_+(s) + D_-(s), \tag{2.50}$$

then equation (2.49) becomes

$$D_+(s) - \Sigma_+(s)L_+(s) = L_-(s)V_-(s) - D_-(s) = W(s). \tag{2.51}$$

The first member of this equation is analytic in the upper half plane $\mathrm{Im}(s) = \lambda > \lambda_-$ and the second member in the lower half plane $\mathrm{Im}(s) = \lambda < \lambda_+$. Therefore, if $\lambda_+ > \lambda_-$ the regions of analyticity overlap. Using the Liouville's theorem to determine $W(s)$, solutions for $\Sigma_+(s)$ and $V_-(s)$ can be found.

The only zeros of the function $F(s,p)$ are of the form $s = ip/(\pm c_R + v)$ where c_R is the Rayleigh wave speed. This can be seen by substituting $s = ip/(c+v)$ in $F(s,p)$, letting $F(s,p) = 0$ and dividing by the non-zero factors, then $F(ip/(c+v),p) = 0$ reduces to

$$\sqrt{\frac{c_{22}}{c_{11}}}\left(\frac{c_{11}c_{22} - c_{12}^2}{c_{22}} - \frac{c^2}{c_s^2}\right)\sqrt{1 - \frac{c^2}{c_s^2}} - \frac{c^2}{c_s^2}\sqrt{1 - \frac{c^2}{c_{11}c_s^2}} = 0$$

which is the Rayleigh function for orthotropic materials [13]. The roots of this function are $c = \pm c_R$.

Consequently, the first step in factoring $L(s)$ is to define

$$\hat{F}(s) = \frac{F(s,p)}{\theta_R} \tag{2.52}$$

where

$$\theta_R = \left(1 - \frac{v^2}{c_R^2}\right)s^2 + \frac{2vpis}{c_R^2} + \frac{p^2}{c_R^2}. \tag{2.53}$$

It can be shown that $\hat{F}(s) \to 1$ as $s \to \infty$, (the function $\xi(v)$ in (2.34) was chosen to make this possible). The function $\hat{F}(s)$ is regular and $\hat{F}(s) \neq 0$ in the $s-$plane cut as shown in

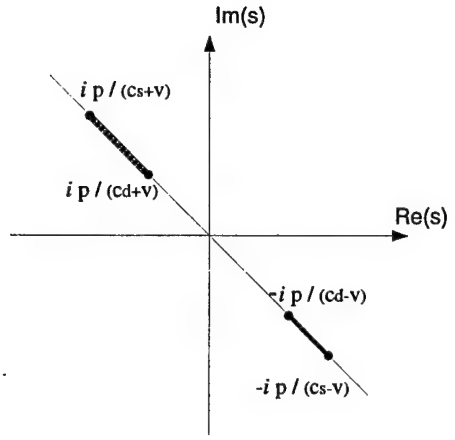

Figure 2.2: Branch cuts of $\hat{F}(s)$ in the $s-$plane.

figure 2.2, the only singularities are the branch points shared with γ_1 and γ_2. Where the branch points of γ_1 and γ_2 are

$$\begin{aligned} \text{for } \gamma_1; \quad s &= \frac{ip}{c_s+v}, \ \frac{-ip}{c_s-v}, \\ \text{for } \gamma_2; \quad s &= \frac{ip}{c_d+v}. \ \frac{-ip}{c_d-v}, \end{aligned}$$

It is well-known that factorization is accomplished most directly for functions that approach unity as $|s| \to \infty$ and that have neither zeros nor poles in the finite plane; $\hat{F}(s)$ is an example of such a function. Therefore, using Cauchy's integral formula it can be shown that [5]

$$\hat{F}_{\pm}(s) = \exp\left\{\frac{1}{2\pi i}\int_{\Gamma_{\pm}} \frac{\log \hat{F}(z)}{z-s}\, dz\right\}$$

where $\hat{F}(s) = \hat{F}_{+}(s)\hat{F}_{-}(s)$ and Γ_{-} $[\Gamma_{+}]$ is the contour enclosing the cut between the branch points $+ip/(c_s+v)$ and $+ip/(c_d+v)$, $[-ip/(c_s-v)$ and $-ip/(c_d-v)]$. Using the fact that $\hat{F}(\bar{s}) = \overline{\hat{F}(s)}$ one can write

$$\hat{F}_{\pm}(s) = \exp\left\{\frac{-1}{\pi}\int_{1/c_d \mp v}^{1/c_s \mp v} \tan^{-1}\left(\frac{\mathrm{Im}[\hat{F}(ipw)]}{\mathrm{Re}[\hat{F}(ipw)]}\right)\frac{dw}{w \mp \frac{is}{p}}\right\}.$$

From equations (2.35) and (2.53) note that

$$\begin{aligned} \theta_d &= \sqrt{\left(1-\frac{v^2}{c_d^2}\right)s^2 + \frac{2vpis}{c_d^2} + \frac{p^2}{c_d^2}} = \sqrt{\left(1-\frac{v}{c_d}\right)s + \frac{ip}{c_d}}\sqrt{\left(1+\frac{v}{c_d}\right)s - \frac{ip}{c_d}} = \theta_d^{+}\theta_d^{-}, \\ \theta_R &= \left(1-\frac{v^2}{c_R^2}\right)s^2 + \frac{2vpis}{c_R^2} + \frac{p^2}{c_R^2} = \left[\left(1-\frac{v}{c_R}\right)s + \frac{ip}{c_R}\right]\left[\left(1+\frac{v}{c_R}\right)s - \frac{ip}{c_R}\right] = \theta_R^{+}\theta_R^{-}. \end{aligned}$$

Returning to the factorization of $L(s)$ we have

$$L(s) = \frac{L_-(s)}{L_+(s)} = \mu_{12}\xi\frac{\hat{F}(s)\theta_R}{\theta_d} \tag{2.54}$$

$$= \mu_{12}\xi\frac{\hat{F}_+(s)\hat{F}_-(s)\theta_R^+\theta_R^-}{\theta_d^+\theta_d^-} \tag{2.55}$$

therefore

$$L_-(s) = \mu_{12}\xi\frac{\theta_R^-}{\theta_d^-}\hat{F}_-(s) \tag{2.56}$$

$$L_+(s) = \frac{\theta_d^+}{\theta_R^+}\frac{1}{\hat{F}_+(s)} \tag{2.57}$$

and

$$D(s) = \frac{\sigma_0}{ips}L_+(s) = \frac{\sigma_0}{p}\left[\frac{L_+(s)-L_+(0)}{is} + \frac{L_+(0)}{is}\right] = D_+(s) + D_-(s) \tag{2.58}$$

with

$$D_+(s) = \frac{\sigma_0}{p}\left[\frac{L_+(s)-L_+(0)}{is}\right], \qquad D_-(s) = \frac{\sigma_0}{p}\left[\frac{L_+(0)}{is}\right]. \tag{2.59}$$

Each side of equation (2.51) is analytic in one of the overlapping half planes, and the sides coincide on the strip of overlap. Consequently each side of (2.51) is the analytic continuation of the other into its complementary half plane; so that the two sides together represent one and the same entire function $W(s)$. The entire function will be determined by its behavior at $|s| \to \infty$ which is related with the behavior of physical quantities near $x = 0$. First note that $L_+(s) \sim s^{-1/2}$ and $L_-(s) \sim s^{1/2}$ as $|s| \to \infty$, and, $D_+(s)$ and $D_-(s)$ in (2.59) are bounded in their respective planes of analyticity and vanish at infinity. Furthermore, $\sigma_+^*(x,p)$ is expected to be square root singular as $x \to 0^+$ and $u_{y-}^*(x,p)$ is expected to vanish as $x \to 0^-$ to ensure continuity of displacement. As a result, from the Abel theorem [10] relating asymptotic properties of transforms, we know

$$\lim_{x\to 0^+} x^{1/2}\sigma_+^*(x,p) \sim \lim_{s\to\infty} s^{1/2}\Sigma_+(s),$$

$$\lim_{x\to 0^-} |x|^{-q}v_-^*(x,p) \sim \lim_{s\to-\infty} |s|^{1+q}V_-(s),$$

for some $q > 0$. Therefore, it is expected that $\Sigma_+(s) \sim s^{-1/2}$ and $V_-(s) \sim s^{-1-q}$ as $|s| \to \infty$, thus the products $\Sigma_+(s)L_+(s)$ and $L_-(s)V_-(s)$ vanish at infinity. Therefore, each side of

(2.51) vanishes as $|s| \to \infty$ in the corresponding half planes. According the the Liouville's theorem, a bounded entire function is constant. In this case, $W(s)$ is bounded in the finite plane and $W(s) \to 0$ as $|s| \to \infty$ so that the constant must be zero; thus, $W(s) = 0$. By using (2.51) and (2.59), the functions of interest are then given by

$$\Sigma_+(s) = \frac{D_+(s)}{L_+(s)} = -\frac{\sigma_0}{p}\frac{1}{is}\left[\frac{L_+(0)}{L_+(s)} - 1\right] \tag{2.60}$$

$$V_-(s) = \frac{D_-(s)}{L_-(s)} = \frac{\sigma_0}{p}\frac{1}{is}\frac{L_+(0)}{L_-(s)}. \tag{2.61}$$

2.3.2 Stress Intensity factor

To find the stress intensity factor, an asymptotic expression for the normal stress near the crack tip is sought. The Abel's theorem relating asymptotic expressions between a function and its Fourier transform is the following [10]

$$\lim_{x\to 0^+} \sqrt{x}\ \sigma_+^*(x,p) = \lim_{s\to+\infty} e^{-i\pi/4}\sqrt{\frac{s}{\pi}}\ \Sigma_+(s). \tag{2.62}$$

Clearly, the behavior of $\Sigma_+(s)$ as $s \to \infty$ is needed. Note that

$$L_+(s) = \frac{\sqrt{1 - v/c_d}}{1 - v/c_R}\frac{1}{s^{1/2}} \quad \text{as} \quad s \to \infty$$

and since $\hat{F}_+(0) = \hat{F}_-(0) = \sqrt{\hat{F}(0)} = \frac{c_R}{p}\sqrt{F(0,p)}$ then

$$L_+(0) = \frac{p}{\sqrt{ipc_d}\sqrt{F(0,p)}}$$

therefore

$$\Sigma_+(s) = \frac{-\sigma_0}{(ip)^{3/2}}\frac{1}{s^{1/2}}\frac{1 - v/c_R}{\sqrt{1 - v/c_d}}\frac{p}{\sqrt{c_d}\sqrt{F(0,p)}} \quad \text{as} \quad s \to \infty. \tag{2.63}$$

Using this relation and the definition of the stress intensity factor in (2.62) gives

$$K_I^*(p) = \lim_{x\to 0^+} \sqrt{2\pi x}\ \sigma_+^*(x,p) = \lim_{s\to+\infty} e^{-i\pi/4}\sqrt{2s}\ \Sigma_+(s) \tag{2.64}$$

$$= \frac{\sigma_0\sqrt{2}}{p^{3/2}}\frac{1 - c/c_R}{\sqrt{1 - c/c_d}}\frac{p}{\sqrt{c_d}\sqrt{F(0,p)}} \tag{2.65}$$

it is readily shown that

$$\sqrt{F(0,p)} = p\sqrt{\frac{\sqrt{c_{22}}}{c_s c_d \xi}} \tag{2.66}$$

so that

$$K_I^*(p) = \sigma_0 \frac{1 - c/c_R}{\sqrt{1 - c/c_d}} \sqrt{\frac{2c_s\xi}{\sqrt{c_{22}}}} \frac{1}{p^{3/2}} \tag{2.67}$$

and by Laplace inversion the dynamic stress intensity factor in the time domain for this loading mode is

$$K_I(t,v) = 2\sigma_0 \frac{1 - v/c_R}{\sqrt{1 - v/c_d}} \sqrt{\frac{2c_s\xi(v)}{\pi\sqrt{c_{22}}}}\ \sqrt{t}. \tag{2.68}$$

Denoting $\xi(0)$ the function ξ evaluated at $v = 0$, equation (2.68) can be rearranged

$$K_I(t,v) = \frac{1 - v/c_R}{\sqrt{1 - v/c_d}} \sqrt{\frac{\xi(v)}{\xi(0)}} \left[2\sigma_0 \sqrt{\frac{2c_s\xi(0)}{\pi\sqrt{c_{22}}}}\ \sqrt{t} \right] \tag{2.69}$$

The expression in brackets corresponds to the dynamic stress intensity factor for a stationary semi-infinite crack in orthotropic materials derived in [12], and the remaining factor will be $k_I(v)$, the universal function of the crack tip speed that relates the stress intensity factor for stationary and propagating crack. That is

$$k_I(v) = \frac{1 - v/c_R}{\sqrt{1 - v/c_d}} \sqrt{\frac{\xi(v)}{\xi(0)}}, \qquad K_I(t,v) = k_I(v) K_I(t,0) \tag{2.70}$$

The expression for $k_I(v)$ can be approximated, for $0 \le v \le c_R$, by

$$k_I(v) \approx \frac{1 - v/c_R}{\sqrt{1 - v/c_d}} \tag{2.71}$$

as in the case of isotropic materials.

2.4 In-Plane Shear Loading

Consider the crack geometry illustrated in figure 2.1(b). The crack faces are subjected to suddenly applied, spatially uniform shear traction of magnitude τ_0 at time $t = 0$. Exploiting asymmetry and examining the half space $y \ge 0$, the corresponding boundary conditions are

$$\tau_{xy}(x,0,t) \;=\; -\tau_0 H(t) \quad \text{for} \quad -\infty < x < 0,$$

$$\begin{aligned} \sigma_y(x,0,t) &= 0 \quad \text{for} \quad -\infty < x < \infty, \\ u_x(x,0,t) &= 0 \quad \text{for} \quad x > 0, \end{aligned} \tag{2.72}$$

where $H(t)$ is the Heaviside step function. In addition the condition of zero displacements at infinity and zero initial conditions are assumed.

The method of solution is similar to that used for normal impact. Applying Laplace transform to boundary conditions (2.72) gives

$$\begin{aligned} \tau^*_{xy}(x,0,p) &= -\tau_0/p \quad \text{for} \quad -\infty < x < 0, \\ \sigma^*_y(x,0,p) &= 0 \quad \text{for} \quad -\infty < x < \infty, \\ u^*_x(x,0,p) &= 0 \quad \text{for} \quad x > 0. \end{aligned} \tag{2.73}$$

Assuming the displacement field (2.17) and (2.18) yields the same system of ordinary differential equations (2.19) and (2.20) whose solution is given by equations (2.21) where α_j are defined by (2.22) and γ_j are obtained from the solution of (2.23). Using (2.24), (2.25) and (2.10) indicates that σ^*_y is given by

$$\sigma^*_y(x,y,p) = -\frac{i\mu_{12}}{2\pi}\int_{-\infty}^{\infty}[(s^2c_{12}-\alpha_1\gamma_1c_{22})A_1e^{-\gamma_1 y}+(s^2c_{12}-\alpha_2\gamma_2c_{22})A_2e^{-\gamma_2 y}]\frac{e^{-isx}}{s}\,ds. \tag{2.74}$$

Applying the second condition of (2.73) to equation (2.74) yields

$$\begin{aligned} A_2(s,p) &= -\beta_2 A_1(s,p), \\ \beta_2 &= \frac{s^2c_{12}-\alpha_1\gamma_1c_{22}}{s^2c_{12}-\alpha_2\gamma_2c_{22}}. \end{aligned} \tag{2.75}$$

Therefore, the expressions for the transformed components of displacement become

$$u^*_x(x,y,p) = \frac{1}{2\pi}\int_{-\infty}^{\infty}(e^{-\gamma_1 y}-\beta_2e^{-\gamma_2 y})A_1(s,p)e^{-isx}\,ds, \tag{2.76}$$

$$u^*_y(x,y,p) = \frac{-i}{2\pi}\int_{-\infty}^{\infty}(\alpha_1e^{-\gamma_1 y}-\beta_2\alpha_2e^{-\gamma_2 y})\frac{A_1(s,p)}{s}e^{-isx}\,ds, \tag{2.77}$$

and the associated stress components are given by

$$\sigma^*_x = \frac{-i\mu_{12}}{2\pi}\int_{-\infty}^{\infty}[(c_{11}s^2-\alpha_1\gamma_1c_{12})e^{-\gamma_1 y}-(c_{11}s^2-\alpha_2\gamma_2c_{12})\beta_2e^{-\gamma_2 y}]\frac{A_1(s,p)}{s}e^{-isx}ds, \tag{2.78}$$

$$\sigma^*_y = \frac{-i\mu_{12}}{2\pi}\int_{-\infty}^{\infty}(c_{12}s^2-\alpha_1\gamma_1c_{22})(e^{-\gamma_1 y}-e^{-\gamma_2 y})\frac{A_1(s,p)}{s}e^{-isx}ds, \tag{2.79}$$

$$\tau^*_{xy} = \frac{-\mu_{12}}{2\pi}\int_{-\infty}^{\infty}[(\alpha_1+\gamma_1)e^{-\gamma_1 y}-(\alpha_2+\gamma_2)\beta_2e^{-\gamma_2 y}]A_1(s,p)e^{-isx}ds. \tag{2.80}$$

Introducing the functions

$$C(s,p) = (1-\beta_2)A_1(s,p), \tag{2.81}$$

$$G(s,p) = \frac{-\theta_s}{(1-\beta_2)\eta}[(\alpha_1+\gamma_1)-\beta_2(\alpha_2+\gamma_2)], \tag{2.82}$$

$$\theta_s(v) = \sqrt{\left(1-\frac{v^2}{c_s^2}\right)s^2+\frac{2vpis}{c_s^2}+\frac{p^2}{c_s^2}}, \tag{2.83}$$

$$\eta(v) = \frac{c_{11}\sqrt{1-v^2/c_s^2}\sqrt{1-v^2/c_d^2}}{c_{22}N_1N_2}\xi(v) \tag{2.84}$$

where ξ and $N_{1,2}$ are given in (2.36) and (2.37) and in view of the first and third boundary conditions in (2.73), equation (2.76) and (2.80) yield the following pair of dual integral equations for the determination of the function $C(s,p)$,

$$\tau_{xy}^*(x,0,p) = \frac{\mu_{12}\eta}{2\pi}\int_{-\infty}^{\infty}\frac{G(s,p)}{\theta_s}C(s,p)e^{-isx}\,ds = -\frac{\tau_0}{p} \qquad -\infty < x < 0, \tag{2.85}$$

$$u_x^*(x,0,p) = \frac{1}{2\pi}\int_{-\infty}^{\infty}C(s,p)e^{-isx}\,ds = 0 \qquad 0 < x < \infty. \tag{2.86}$$

Let $u_{x-}^*(x,p)$ be the unknown Laplace transform of the displacement on the negative $x-$axis, and $\tau_+^*(x,p)$ be the unknown Laplace transform of the shear stress on the positive $x-$axis, so that

$$u_x^*(x,0,p) = \begin{cases} 0 & \text{for } x>0 \\ u_{x-}^*(x,p) & \text{for } x<0 \end{cases} \qquad \tau_{xy}^*(x,0,p) = \begin{cases} \tau_+^*(x,p) & \text{for } x>0 \\ -\tau_0/p & \text{for } x<0. \end{cases} \tag{2.87}$$

Then, the Laplace transform of the shear stress and the displacement on the whole boundary $y=0$ is

$$\frac{\mu_{12}\eta}{2\pi}\int_{-\infty}^{\infty}\frac{G(s,p)}{\theta_s}C(s,p)e^{-isx}\,ds = -\frac{\tau_0}{p}H(-x)+\tau_+^*(x), \tag{2.88}$$

$$\frac{1}{2\pi}\int_{-\infty}^{\infty}C(s,p)e^{-isx}\,ds = u_{x-}^*(x) \tag{2.89}$$

and by Fourier transform inversion, these equations give

$$\mu_{12}\eta\frac{G(s,p)}{\theta_s}C(s,p) = -\frac{\tau_0}{ips}+T_+(s) \tag{2.90}$$

$$C(s,p) = U_-(s) \tag{2.91}$$

where

$$T_+(s) = \int_0^\infty \tau_+^*(x)e^{isx}dx \tag{2.92}$$

$$U_-(s) = \int_{-\infty}^0 u_{x-}^*(x)e^{isx}dx \tag{2.93}$$

$$\int_{-\infty}^0 \left(\frac{-\tau_0}{p}\right) e^{isx}dx = -\frac{\tau_0}{ips}$$

Eliminating $C(s,p)$ from (2.90) and (2.91) results in a Wiener-Hopf equation

$$\frac{\tau_0}{ips} - T_+(s) = -\mu_{12}\eta\frac{G(s,p)}{\theta_s}U_-(s) \tag{2.94}$$

which contains only the two unknown functions, $T_+(s)$ and $U_-(s)$, and can be solved using the Wiener-Hopf technique as in the normal impact analysis. The result is

$$D_+(s) - T_+(s)L_+(s) = L_-(s)U_-(s) - D_-(s) = 0 \tag{2.95}$$

where

$$L_-(s) = -\mu_{12}\xi\frac{\theta_R^-}{\theta_s^-}\hat{G}_-(s), \tag{2.96}$$

$$L_+(s) = \frac{\theta_s^+}{\theta_R^+}\frac{1}{\hat{G}_+(s)}, \tag{2.97}$$

and

$$D(s) = \frac{\tau_0}{ips}L_+(s) = \frac{\tau_0}{p}\left[\frac{L_+(s) - L_+(0)}{is} + \frac{L_+(0)}{is}\right] = D_+(s) + D_-(s), \tag{2.98}$$

with

$$D_+(s) = \frac{\tau_0}{p}\left[\frac{L_+(s) - L_+(0)}{is}\right], \quad \text{and} \quad D_-(s) = \frac{\tau_0}{p}\left[\frac{L_+(0)}{is}\right],$$

where

$$\hat{G}(s) = \frac{G(s,p)}{\theta_R}, \tag{2.99}$$

and

$$\theta_s = \sqrt{\left(1 - \frac{v^2}{c_s^2}\right)s^2 + \frac{2vpis}{c_s^2} + \frac{p^2}{c_s^2}} = \sqrt{\left(1 - \frac{v}{c_s}\right)s + \frac{ip}{c_s}}\sqrt{\left(1 + \frac{v}{c_s}\right)s - \frac{ip}{c_s}} = \theta_s^+\theta_s^-.$$

It can be shown that $\hat{G}(s) \to 1$ as $s \to \infty$. Thus, the solution of (2.95) is

$$T_+(s) = \frac{D_+(s)}{L_+(s)} = -\frac{\tau_0}{p}\frac{1}{is}\left[\frac{L_+(0)}{L_+(s)} - 1\right] \tag{2.100}$$

$$U_-(s) = \frac{D_-(s)}{L_-(s)} = \frac{\tau_0}{p}\frac{1}{is}\frac{L_+(0)}{L_-(s)}. \tag{2.101}$$

with $L_\pm(s)$ defined in (2.96) and (2.97) and $\hat{G}_\pm(s)$ given by

$$\hat{G}_\pm(s) = \exp\left\{\frac{-1}{\pi}\int_{1/c_d \mp v}^{1/c_s \mp v} \tan^{-1}\left(\frac{\mathrm{Im}[\hat{G}(ipw)]}{\mathrm{Re}[\hat{G}(ipw)]}\right)\frac{dw}{w \mp \frac{is}{p}}\right\}.$$

To calculate the stress intensity factor, $T_+(s)$ as $s \to \infty$ is needed. First, note that

$$L_+(s) = \frac{\sqrt{1 - v/c_s}}{1 - v/c_R}\frac{1}{s^{1/2}} \quad \text{as} \quad s \to \infty$$

and since $\hat{G}_+(0) = \hat{G}_-(0) = \sqrt{\hat{G}(0)} = \frac{c_R}{p}\sqrt{G(0,p)}$ then

$$L_+(0) = \frac{p}{\sqrt{ipc_s}\sqrt{G(0,p)}}.$$

Therefore,

$$T_+(s) = \frac{-\tau_0}{(ip)^{3/2}}\frac{1}{s^{1/2}}\frac{1 - v/c_R}{\sqrt{1 - v/c_s}}\frac{p}{\sqrt{c_s}\sqrt{G(0,p)}} \quad \text{as} \quad s \to \infty. \tag{2.102}$$

Using (2.62) and the definition of the stress intensity factor gives

$$K^*_{II}(p) = \lim_{x \to 0^+}\sqrt{2\pi x}\,\tau^*_+(x,p) = \lim_{s \to +\infty} e^{-i\pi/4}\sqrt{2s}\,T_+(s) \tag{2.103}$$

$$= \frac{\tau_0\sqrt{2}}{p^{3/2}}\frac{1 - v/c_R}{\sqrt{1 - v/c_s}}\frac{p}{\sqrt{c_s}\sqrt{G(0,p)}}. \tag{2.104}$$

It can be shown that

$$\sqrt{G(0,p)} = \frac{p}{c_s\sqrt{\eta}}, \tag{2.105}$$

so that

$$K^*_{II}(p) = \tau_0\sqrt{2c_s\eta}\,\frac{1}{p^{3/2}}\frac{1 - v/c_R}{\sqrt{1 - v/c_s}}, \tag{2.106}$$

and by Laplace inversion the dynamic stress intensity factor in the time domain for this loading mode is

$$K_{II}(t,v) = 2\tau_0\frac{1 - v/c_R}{\sqrt{1 - v/c_s}}\sqrt{2c_s\eta(v)/\pi}\,\sqrt{t}. \tag{2.107}$$

	Graphite Epoxy	E-Glass Epoxy	Boron Epoxy	Epoxy
c_{11}	20.77	8.38	32.67	3.91
c_{22}	2.18	2.29	3.12	3.91
c_{12}	0.49	0.52	0.79	1.91
μ_{12} (GPa)	7.48	5.5	6.4	1.96
ρ (Kg/m^3)	1600	2100	1990	1260

Table 2.1: Mechanical properties used for the analysis.

Denoting $\eta(0)$ the function η evaluated at $v = 0$, equation (2.107) can be rearranged as

$$K_{II}(t,v) = \frac{1 - v/c_R}{\sqrt{1 - v/c_s}} \sqrt{\frac{\eta(v)}{\eta(0)}} \left[2\tau_0 \sqrt{2c_s \eta(0)/\pi}\ \sqrt{t} \right]. \tag{2.108}$$

The expression in brackets corresponds to the stress intensity factor for a stationary semi-infinite crack in orthotropic materials under impact shear loading derived in [12], and the remaining factor will be $k_{II}(v)$, the universal function of the crack tip speed that relates the stress intensity factor for stationary and propagating crack. That is

$$k_{II}(v) = \frac{1 - v/c_R}{\sqrt{1 - v/c_s}} \sqrt{\frac{\eta(v)}{\eta(0)}}, \qquad K_{II}(t,v) = k_{II}(v) K_{II}(t,0) \tag{2.109}$$

The expression for $k_{II}(v)$ can be approximated, for $0 \leq v \leq c_R$, by

$$k_{II}(v) \approx \frac{1 - v/c_R}{\sqrt{1 - v/c_s}} \tag{2.110}$$

as in the case of isotropic materials.

2.5 Results and Conclusions

Closed form expressions for the dynamic stress intensity factors $K_I(t,v)$ and $K_{II}(t,v)$ due to suddenly applied uniform loads on the crack faces have been determined for semi-infinite cracks propagating at constant velocity v in orthotropic materials. The results presented here are consistent with those for stationary cracks, i.e. for $v = 0$, $K_I(t,0)$ and $K_{II}(t,0)$ developed in a previous work by Rubio-Gonzalez and Mason [12] for semi-infinite cracks in orthotropic

materials subjected to spatially uniform step loads on the crack faces are obtained. Using these results it has been possible to find expressions for the universal function of the crack tip speed $k_I(v)$ and $k_{II}(v)$ which may be written in approximated manner as

$$k_I(v) \approx \frac{1 - v/c_R}{\sqrt{1 - v/c_d}}$$
$$k_{II}(v) \approx \frac{1 - v/c_R}{\sqrt{1 - v/c_s}}.$$

Note that these equations conserve the same form as those for isotropic materials [5], where the wave speeds c_s and c_d should be computed and understood properly for orthotropic materials with the planes of orthotropy assumed here.

Figures 2.3 and 2.5 illustrate $k_I(v)$ and $k_{II}(v)$ for different materials for which the properties are given in Table 2.1. They also show that for orthotropic materials the functions $k_I(v)$ and $k_{II}(v)$ given by equations (2.70) and (2.109) may be approximated by the simplified expressions (2.71) and (2.110), respectively as usually it is for isotropic materials. They are very close each other for several materials. In fact, the factor $\sqrt{\xi(v)/\xi(0)}$ is close to one over a large interval of speeds as shown by figure 2.4. It can be shown that $\xi(v)/\xi(0) = \eta(v)/\eta(0)$ and therefore Figure 2.4 applies to the in-plane shear loading too.

It was assumed tacitly in the method of solution of the equations of motion that the crack speed propagation is subsonic, $v < c_R$, in order to maintain elliptic differential equations.

Acknowledgment

Support of this work by the Office of Naval Research Young Investigator Program under grant N00014-96-1-0774 supervised by Dr. Y. Rajapakse and by the Mexican Government through CONACYT (Consejo Nacional de Ciencia y Tecnologia) are gratefully acknowledged.

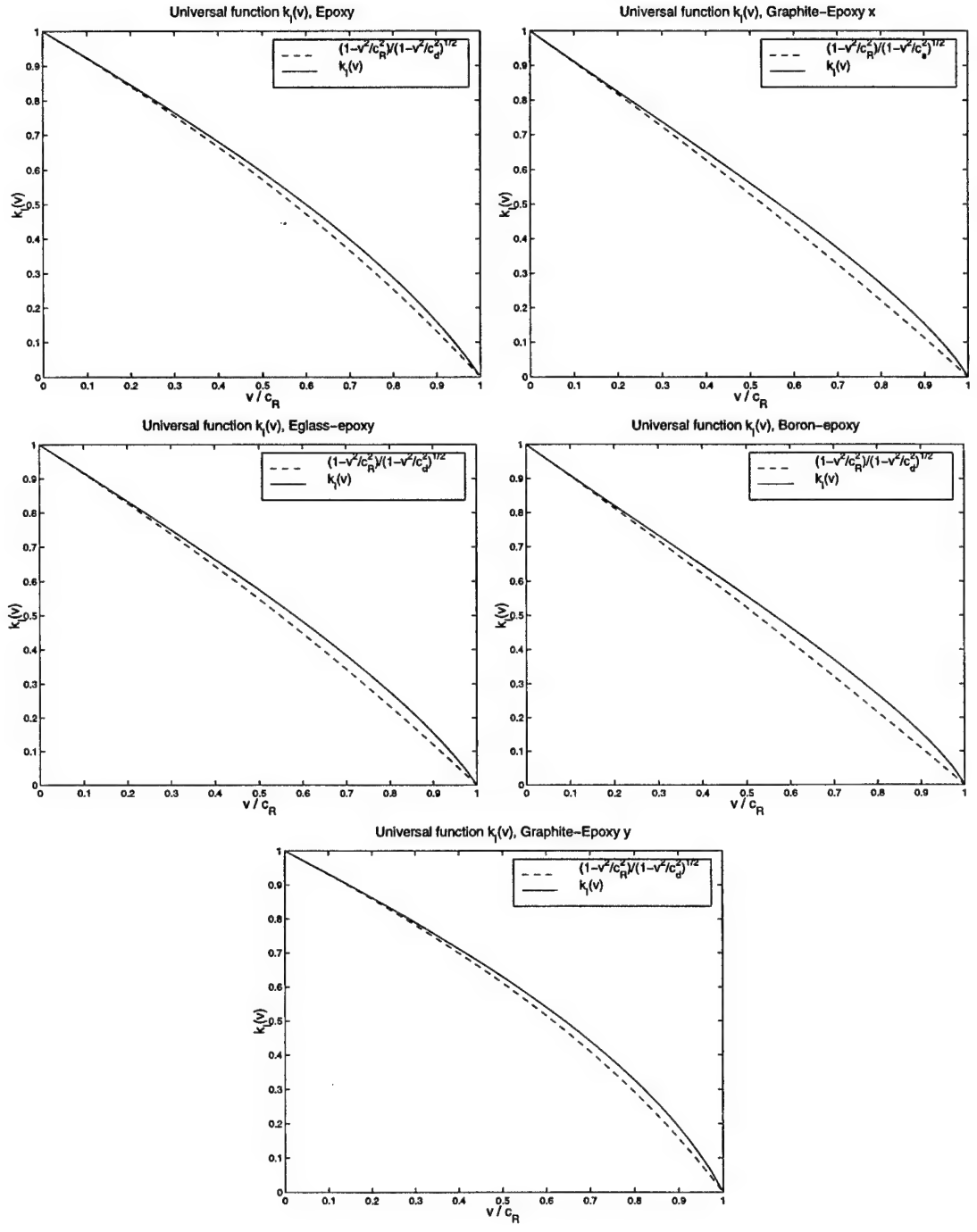

Figure 2.3: Comparison of the universal function $k_I(v)$ and its approximated expression (2.71) for different materials in mode I loading.

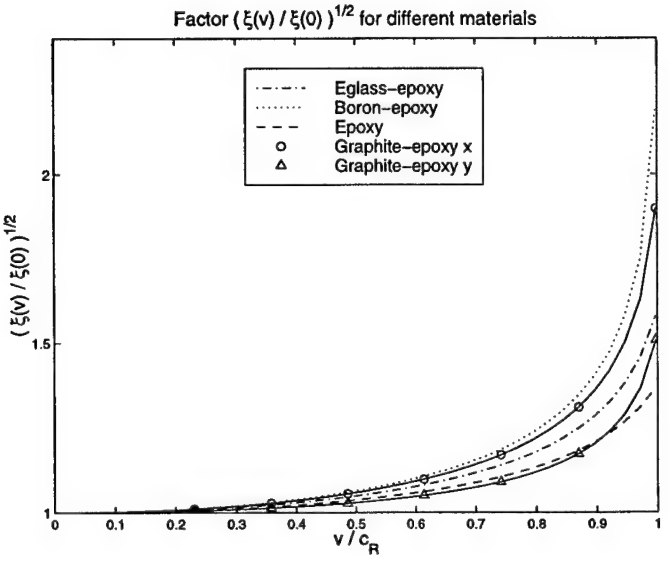

Figure 2.4: Factor $\sqrt{\xi(v)/\xi(0)}$ for different materials. Graphite-epoxy x or y means that the fibers are parallel to the $x-$ or $y-$axis, respectively.

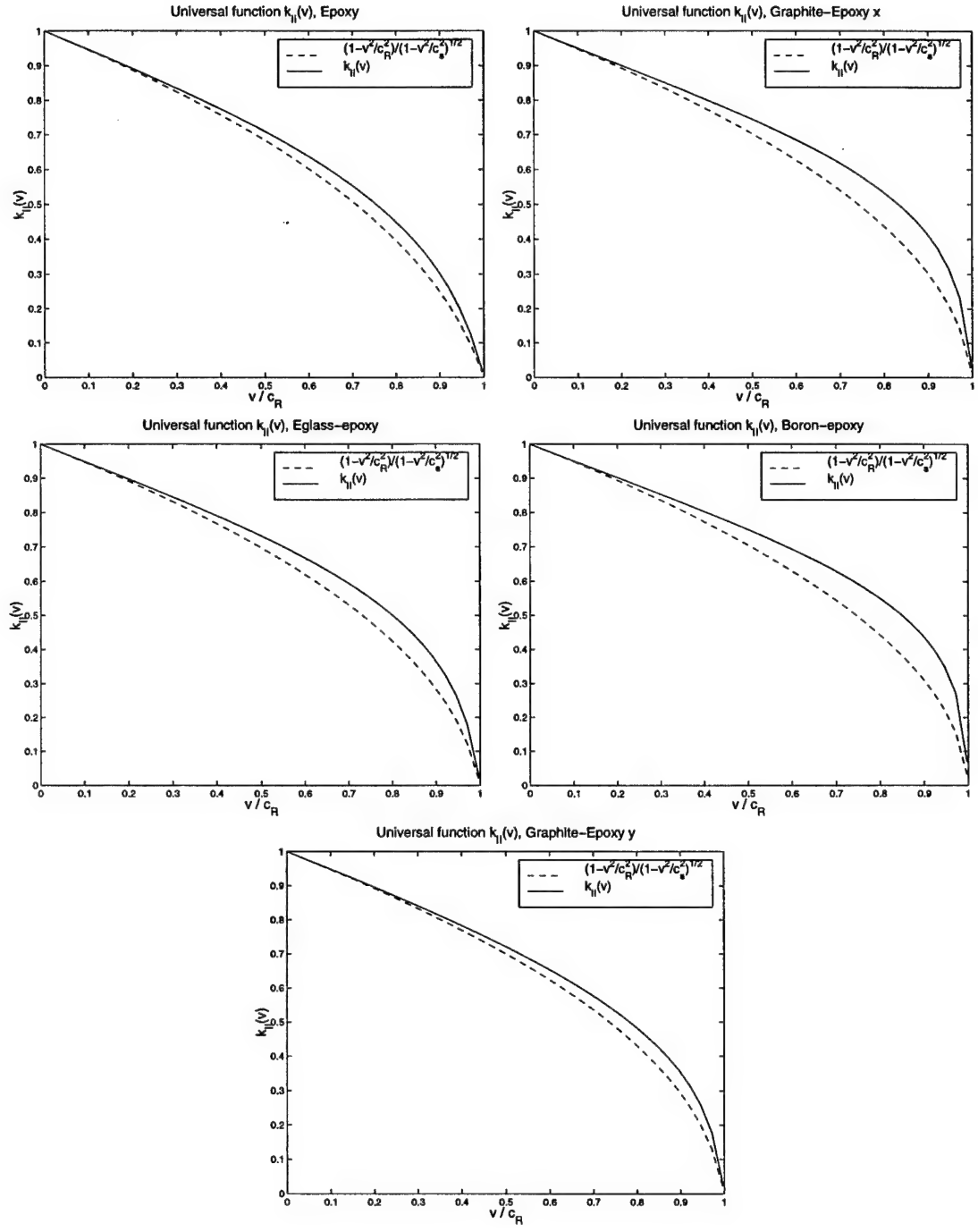

Figure 2.5: Comparison of the universal function $k_{II}(v)$ and its approximated expression (2.110) for different materials in mode II loading.

Bibliography

[1] Atkinson C., 1965, *The Propagation of Fracture in Aelotropic Materials.* Int. J. Fracture Mech., v.53, n.1, pp.119-140.

[2] Baker B.R., 1962, *Dynamic Stresses Created by a Moving Crack,* ASME, J. Appl. Mech. v.29, pp.449-458.

[3] Broberg K.B., 1960, *The Propagation of a Brittle Crack.* Arch. fur Fysik, v.18, pp.159-192.

[4] Freund, L. B., 1973, *Crack Propagation in an Elastic Solid Subjected to General Loading. III. Stress Wave Loading.* J.Mech. Phys. Solids, v.21, pp.47-61.

[5] Freund, L.B., 1990, *Dynamic Fracture Mechanics,* Cambridge University Press. New York.

[6] Kassir M.K. and Tse S., 1983, *Moving Griffith Crack in an Orthotropic Material.* Int. J. Engng. Sci., v.21, n.4, pp.315-325.

[7] Kousiounelos P.N., and Williams J.H., 1982, *Dynamic Fracture of Unidirectional Graphite Fiber Composite Strips.* Int. J. Fracture, v.20, pp.47-63.

[8] Lee K.H., Hawong J.S. and Choi S.H., 1996, *Dynamic Stress Intensity Factors K_I, K_{II} and Dynamic Crack Propagation Characteristics of Orthotropic Material.* Eng. Fracture Mech. v.53, n.1, pp.119-140.

[9] Nayfeh, A.H., 1995, *Wave Propagation in Anisotropic Media with Applications to Composites*, North-Holland Publishing Company. Amsterdam.

[10] Noble B., 1958, *Methods Based on the Wiener-Hopf Technique*, Elmsford, N.Y., Pergamon.

[11] Piva A., and Viola E., 1988, *Crack Propagation in an Orthotropic Medium*, Eng. Fracture Mech., v.29, n.5, pp.535-548.

[12] Rubio-Gonzalez, C. and Mason, J.J., 1998, *Closed Form Solutions for the Dynamic Stress Intensity Factors at the Tip of Uniformly Loaded Semi-infinite Cracks in Orthotropic Materials.*, Submitted to J. Mech. Phys. Solids.

[13] Ting, T.C.T., 1996, *Anisotropic Elasticity*, Oxford University Press, New York.

[14] Willis J.R., 1973, *Self-similar Problems in Elastodynamics.* Phil. Trans. Royal Soc. (London), v.272, pp.435-491.

[15] Yoffe, E.H., 1951, *The Moving Griffith Crack.* Phil. Mag., v.42, pp.739-750.

Chapter 3

Dynamic Stress Intensity Factor due to Concentrated Normal Loads on Semi-infinite Cracks in Orthotropic Materials.

Co-authored with C. Rubio-Gonzalez and submitted to the Journal of Composite Materials

The transient elastodynamic response due to concentrated normal impact load on the faces of a a semi-infinite crack in an orthotropic material is examined. In contrast to earlier papers where numerical approximations were used, a closed form solution for the stress intensity factor history around the crack tip is found here. Laplace and Fourier transforms together with the Wiener-Hopf technique are employed to solve the equations of motion in terms of displacements. Even though the problem has characteristic length, it has been shown in previous works that the Wiener-Hopf technique can be applied. The asymptotic expression for the stress near the crack tip is analyzed which leads to the dynamic stress intensity factor in mode I. Similarly to the isotropic case, it is found that the stress intensity factor has a singularity and discontinuity when the Rayleigh wave emitted from the load arrives at the crack tip. Results are presented for orthotropic materials as well as for the isotropic materials. The closed form solution is given by simple integral and algebraic expressions and does not exhibit the spurious oscillations seen in earlier numerical solutions.

Keywords: stress intensity factor, dynamic fracture, orthotropic materials.

3.1 Introduction

The growing use of composites in many engineering applications demands the fundamental understanding of the response of cracked orthotropic bodies under impact loads. The behavior of finite cracks with concentrated loads on its faces in orthotropic materials has been analyzed by Rubio-Gonzalez and Mason [8, 9] using integral transform methods. In that work, the problem is reduced to a Fredholm integral equation in the Laplace transform domain which is solved numerically, and the stress intensity factor is recovered in the time domain by numerical Laplace inversion. Although this approach can be quite accurate, the solution obtained is approximated and restricted to finite cracks. It would be desirable to have an exact solution for the stress intensity factor in cracks in orthotropic materials subjected to impact concentrated loads that can be used as a Green's function in dynamic crack problems in orthotropic materials.

In the present work a semi-infinite crack with impact concentrated loads on its faces in orthotropic material is analyzed, an exact, closed-form solution for the dynamic stress intensity factor is obtained for the opening loading mode. Laplace and Fourier transforms are used along with the Wiener-Hopf technique to find the stress ahead of the crack tip and the displacements of the crack faces. Asymptotic expression for the stress near the crack tip leads to the stress intensity factor $K_I(t)$. The equivalent problem for isotropic materials was solved by Freund [2] by superposition of two different problems with no characteristic fixed length. The superposed problems were solved employing the Wiener-Hopf technique. Kuo and Chen [4, 5] have shown that the direct application of the Wiener-Hopf technique may be used to solve that problem in a more straightforward manner. The latter approach is used in this paper to extend the solution of Freund to orthotropic materials.

3.2 Governing Equations

Consider the plane problem of an infinite orthotropic medium containing a semi-infinite crack, Figure 3.1. Let E_i, μ_{ij} and ν_{ij} $(i,j = 1,2,3)$ be the engineering elastic constants of the material where the indices 1, 2, and 3 correspond to the directions (x, y, z) of a system of Cartesian coordinates chosen to coincide with the axes of material orthotropy. The crack faces are along the negative $x-$axis and the origin of the xy axes is the crack tip. The crack faces are suddenly loaded by a pair of concentrated normal forces of magnitude σ_0 located a distance l away from the crack tip, as shown in Figure 3.1.

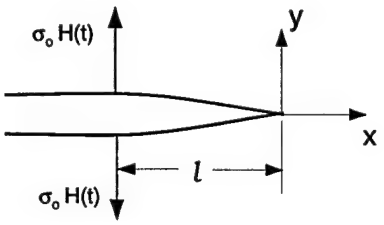

Figure 3.1: Schematic of the semi-infinite crack geometry.

The problem is restricted to two dimensions with wave propagation in the $x-y$ plane only. By setting all the derivatives with respect to z to be zero, it is readily shown that the displacement equations of motion [6] reduce to

$$c_{11}\frac{\partial^2 u}{\partial x^2} + \frac{\partial^2 u}{\partial y^2} + (1+c_{12})\frac{\partial^2 v}{\partial x \partial y} = \frac{1}{c_s^2}\frac{\partial^2 u}{\partial t^2}, \tag{3.1}$$

$$\frac{\partial^2 v}{\partial x^2} + c_{22}\frac{\partial^2 v}{\partial y^2} + (1+c_{12})\frac{\partial^2 u}{\partial x \partial y} = \frac{1}{c_s^2}\frac{\partial^2 v}{\partial t^2}, \tag{3.2}$$

where u and v are the x and y components of the displacement vector and c_{11}, c_{12} and c_{22} are non-dimensional parameters related to the elastic constants by the relations:

$$\begin{aligned} c_{11} &= \frac{E_1}{\mu_{12}[1-(E_2/E_1)\nu_{12}^2]}, \\ c_{22} &= (E_2/E_1)c_{11}, \\ c_{12} &= \nu_{12}c_{22} = \nu_{21}c_{11}, \end{aligned} \tag{3.3}$$

for generalized plane stress, and by

$$\begin{aligned} c_{11} &= \frac{E_1}{\mu_{12}\Delta}(1-\nu_{23}\nu_{32}), \\ c_{22} &= \frac{E_2}{\mu_{12}\Delta}(1-\nu_{13}\nu_{31}), \\ c_{12} &= \frac{E_1}{\mu_{12}\Delta}(\nu_{21}+\frac{E_2}{E_1}\nu_{13}\nu_{32}), \\ \Delta &= 1-\nu_{12}\nu_{21}-\nu_{23}\nu_{32}-\nu_{31}\nu_{13}-\nu_{12}\nu_{23}\nu_{31}-\nu_{13}\nu_{21}\nu_{32}, \end{aligned} \tag{3.4}$$

for plane strain. In the orthotropic solid, $c_s = \sqrt{\mu_{12}/\rho}$ represents the velocity of the in-plane shear wave propagating along the the principal material axes and ρ is the mass density. The stresses are related to the displacements by the equations:

$$\begin{aligned} \frac{\sigma_x}{\mu_{12}} &= c_{11}\frac{\partial u}{\partial x}+c_{12}\frac{\partial v}{\partial y}, \\ \frac{\sigma_y}{\mu_{12}} &= c_{12}\frac{\partial u}{\partial x}+c_{22}\frac{\partial v}{\partial y}, \\ \frac{\tau_{xy}}{\mu_{12}} &= \frac{\partial u}{\partial y}+\frac{\partial v}{\partial x}. \end{aligned} \tag{3.5}$$

3.3 Method of Solution

Exploiting symmetry and taking only the upper half plane $y \geq 0$, the corresponding boundary conditions are

$$\begin{aligned} \sigma_y(x,0,t) &= -\sigma_0 H(t)\delta(x+l) \quad \text{for} \quad -\infty < x < 0, \\ \tau_{xy}(x,0,t) &= 0 \qquad \text{for} \quad -\infty < x < \infty, \\ v(x,0,t) &= 0 \qquad \text{for} \quad x > 0, \end{aligned} \tag{3.6}$$

where $H(t)$ is the Heaviside step function. In addition, the condition of zero displacements at infinity and zero initial conditions are assumed.

The method of solution of the governing equations presented here follows that described in Kuo and Chen [4, 5] for the isotropic case with some significant differences. Displacement potentials are not used and no assumptions are made about the form of the unknown functions. In equations (3.1) and (3.2), the time variable may be removed by application of the

Laplace transform

$$f^*(p) = \int_0^\infty f(t)\, e^{-pt}\, dt, \quad f(t) = \frac{1}{2\pi i}\int_{Br} f^*(p)\, e^{pt}\, dt, \tag{3.7}$$

where Br denotes the Bromwich path of integration which is a line parallel to the imaginary axis in the p-plane. Applying relations (3.7) to equations (3.1) and (3.2) and using zero initial conditions for the displacements and velocities, the transformed field equations become

$$c_{11}\frac{\partial^2 u^*}{\partial x^2} + \frac{\partial^2 u^*}{\partial y^2} + (1+c_{12})\frac{\partial^2 v^*}{\partial x \partial y} - \frac{p^2}{c_s^2}u^* = 0, \tag{3.8}$$

$$\frac{\partial^2 v^*}{\partial x^2} + c_{22}\frac{\partial^2 v^*}{\partial y^2} + (1+c_{12})\frac{\partial^2 u^*}{\partial x \partial y} - \frac{p^2}{c_s^2}v^* = 0, \tag{3.9}$$

where the transformed displacement components, u^* and v^*, are now functions of the variables x, y, and p. The application of the Laplace transform to the boundary conditions (3.6) gives

$$\begin{aligned} \sigma_y^*(x,0,p) &= -\sigma_0\frac{1}{p}\delta(x+l) \quad \text{for} \quad -\infty < x < 0, \\ \tau_{xy}^*(x,0,p) &= 0 \qquad \text{for} \quad -\infty < x < \infty, \\ v^*(x,0,p) &= 0 \qquad \text{for} \quad x > 0. \end{aligned} \tag{3.10}$$

To obtain a solution of the differential equations (3.8) and (3.9) subject to conditions (3.10), the Fourier transform is applied,

$$F(s) = \int_{-\infty}^{\infty} f(x)\, e^{isx}\, dx, \quad f(x) = \frac{1}{2\pi}\int_{-\infty}^{\infty} F(s)\, e^{-isx}\, ds. \tag{3.11}$$

It is assumed that the displacements in the Laplace transform domain have the form

$$u^*(x,y,p) = \frac{1}{2\pi}\int_{-\infty}^{\infty} A(s,y,p)e^{-isx}\, ds, \tag{3.12}$$

$$v^*(x,y,p) = \frac{1}{2\pi}\int_{-\infty}^{\infty} B(s,y,p)e^{-isx}\, ds, \tag{3.13}$$

where A and B are the Fourier transforms of the Laplace transform of the displacements, u^* and v^*, respectively, and are yet to be determined. Substituting these transforms into

equations (3.8) and (3.9), the functions A and B are found to satisfy the simultaneous ordinary differential equations

$$(c_{11}s^2 + p^2/c_s^2)A - \frac{d^2A}{dy^2} + (1 + c_{12})is\frac{dB}{dy} = 0, \tag{3.14}$$

$$(s^2 + p^2/c_s^2)B - c_{22}\frac{d^2B}{dy^2} + (1 + c_{12})is\frac{dA}{dy} = 0. \tag{3.15}$$

The solution of these equations which vanishes for $y \to \infty$ is

$$\begin{aligned} A(s,y,p) &= A_1(s,p)e^{-\gamma_1 y} + A_2(s,p)e^{-\gamma_2 y}, \\ B(s,y,p) &= \frac{-i\alpha_1}{s}A_1(s,p)e^{-\gamma_1 y} - \frac{i\alpha_2}{s}A_2(s,p)e^{-\gamma_2 y}, \end{aligned} \tag{3.16}$$

where A_1 and A_2 are arbitrary functions and $\alpha_j(s,p)$ stands for the functions

$$\alpha_j(s,p) = \frac{c_{11}s^2 + p^2/c_s^2 - \gamma_j^2}{(1 + c_{12})\gamma_j}, \quad j = 1,2 \tag{3.17}$$

with γ_1^2 and γ_2^2 being two distinct roots of the quadratic equation

$$c_{22}\gamma^4 + [(c_{12}^2 + 2c_{12} - c_{11}c_{22})s^2 - (1 + c_{22})p^2/c_s^2]\gamma^2 + (c_{11}s^2 + p^2/c_s^2)(s^2 + p^2/c_s^2) = 0. \tag{3.18}$$

It can be shown that for many materials the roots γ_1 and γ_2 are real and positive and the expressions for the displacements in the Laplace transform domain become:

$$u^* = \frac{1}{2\pi}\int_{-\infty}^{\infty}(A_1e^{-\gamma_1 y} + A_2e^{-\gamma_2 y})e^{-isx}\,ds, \tag{3.19}$$

$$v^* = \frac{-i}{2\pi}\int_{-\infty}^{\infty}(\alpha_1A_1e^{-\gamma_1 y} + \alpha_2A_2e^{-\gamma_2 y})\frac{e^{-isx}}{s}ds, \tag{3.20}$$

and using (3.5) the corresponding expression for τ_{xy}^* is given by

$$\tau_{xy}^* = -\frac{\mu_{12}}{2\pi}\int_{-\infty}^{\infty}[(\alpha_1 + \gamma_1)A_1e^{-\gamma_1 y} + (\alpha_2 + \gamma_2)A_2e^{-\gamma_2 y}]e^{-isx}\,ds. \tag{3.21}$$

Applying the second condition of (3.10) to equation (3.21) yields

$$\begin{aligned} A_2(s,p) &= -\beta_1 A_1(s,p), \\ \beta_1 &= \frac{\alpha_1 + \gamma_1}{\alpha_2 + \gamma_2}. \end{aligned} \tag{3.22}$$

Therefore, the expressions for the transformed components of displacement become

$$u^*(x,y,p) = \frac{1}{2\pi}\int_{-\infty}^{\infty}(e^{-\gamma_1 y} - \beta_1 e^{-\gamma_2 y})A_1(s,p)e^{-isx}\,ds, \tag{3.23}$$

$$v^*(x,y,p) = \frac{-i}{2\pi}\int_{-\infty}^{\infty}(\alpha_1 e^{-\gamma_1 y} - \beta_1\alpha_2 e^{-\gamma_2 y})\frac{A_1(s,p)}{s}e^{-isx}\,ds, \tag{3.24}$$

and the associated stress components are given by

$$\sigma_x^* = \frac{-i\mu_{12}}{2\pi}\int_{-\infty}^{\infty}[(c_{11}s^2 - \alpha_1\gamma_1 c_{12})e^{-\gamma_1 y} - (c_{11}s^2 - \alpha_2\gamma_2 c_{12})\beta_1 e^{-\gamma_2 y}]\frac{A_1(s,p)}{s}e^{-isx}ds, \tag{3.25}$$

$$\sigma_y^* = \frac{-i\mu_{12}}{2\pi}\int_{-\infty}^{\infty}[(c_{12}s^2 - \alpha_1\gamma_1 c_{22})e^{-\gamma_1 y} - (c_{12}s^2 - \alpha_2\gamma_2 c_{22})\beta_1 e^{-\gamma_2 y}]\frac{A_1(s,p)}{s}e^{-isx}ds, \tag{3.26}$$

$$\tau_{xy}^* = \frac{-\mu_{12}}{2\pi}\int_{-\infty}^{\infty}(\alpha_1+\gamma_1)[e^{-\gamma_1 y} - e^{-\gamma_2 y}]A_1(s,p)e^{-isx}ds. \tag{3.27}$$

The following functions are introduced,

$$E(s,p) = \frac{1}{s}(\alpha_1 - \beta_1\alpha_2)A_1(s,p), \tag{3.28}$$

$$F(s,p) = -\frac{\sqrt{s^2 + p^2/c_d^2}}{(\alpha_1 - \beta_1\alpha_2)\xi}[c_{12}s^2 - \alpha_1\gamma_1 c_{22} - \beta_1(c_{12}s^2 - \alpha_2\gamma_2 c_{22})], \tag{3.29}$$

$$\xi = \frac{-1}{c_{11}(1+c_{12})(N_1+N_2)}\{(c_{12}^2 + c_{12} - c_{11}c_{22})(c_{12}N_1N_2 - c_{11}) - c_{22}[c_{12}N_1^2N_2^2 + c_{11}(N_1^2 + N_1N_2 + N_2^2)]\}, \tag{3.30}$$

$$N_{1,2}^2 = \frac{1}{2c_{22}}\{c_{11}c_{22} - c_{12}^2 - 2c_{12} \pm [(c_{11}c_{22} - c_{12}^2 - 2c_{12})^2 - 4c_{11}c_{22}]^{1/2}\}, \tag{3.31}$$

where the velocity $c_d = \sqrt{c_{11}}c_s$ represents the dilatational wave speed along the $x-$axis. In view of the first and third boundary conditions in (3.10), equation (3.24) and (3.26) now yield the following pair of dual integral equations for the determination of the function $E(s,p)$

$$\sigma_y^*(x,0,p) = \frac{i\mu_{12}\xi}{2\pi}\int_{-\infty}^{\infty}\frac{F(s,p)}{\sqrt{s^2+p^2/c_d^2}}E(s,p)e^{-isx}\,ds = -\frac{\sigma_0}{p}\delta(x+l) \qquad -\infty < x < 0, \tag{3.32}$$

$$v^*(x,0,p) = \frac{-i}{2\pi}\int_{-\infty}^{\infty}E(s,p)e^{-isx}\,ds = 0 \qquad 0 < x < \infty, \tag{3.33}$$

Let $v_-^*(x,p)$ be the unknown Laplace transform of the vertical displacement on the negative $x-$axis, and $\sigma_+^*(x,p)$ be the unknown Laplace transform of the normal stress on the positive $x-$axis, so that

$$v^*(x,0,p) = \begin{cases} 0 & \text{for } x > 0 \\ v_-^*(x,p) & \text{for } x < 0 \end{cases} \qquad \sigma_y^*(x,0,p) = \begin{cases} \sigma_+^*(x,p) & \text{for } x > 0 \\ -(\sigma_0/p)\delta(x+l) & \text{for } x < 0 \end{cases} \tag{3.34}$$

then we can write the Laplace transform of the normal stress and the vertical displacement on the whole boundary $y = 0$ as

$$\frac{i\mu_{12}\xi}{2\pi}\int_{-\infty}^{\infty}\frac{F(s,p)}{\sqrt{s^2+p^2/c_d^2}}E(s,p)e^{-isx}\,ds = -\frac{\sigma_0}{p}\delta(x+l)+\sigma_+^*(x,p), \tag{3.35}$$

$$\frac{-i}{2\pi}\int_{-\infty}^{\infty}E(s,p)e^{-isx}\,ds = v_-^*(x,p), \tag{3.36}$$

and by Fourier transform inversion, these equations give

$$i\mu_{12}\xi\frac{F(s,p)}{\sqrt{s^2+p^2/c_d^2}}E(s,p) = -\frac{\sigma_0}{p}e^{-isl}+\Sigma_+(s), \tag{3.37}$$

$$-iE(s,p) = V_-(s), \tag{3.38}$$

where

$$\Sigma_+(s) = \int_0^{\infty}\sigma_+^*(x,p)e^{isx}dx, \tag{3.39}$$

$$V_-(s) = \int_{-\infty}^{0}v_-^*(x,p)e^{isx}dx, \tag{3.40}$$

From the physics of the problem it is reasonable to assume that the function $\sigma_+^*(x,p)$ and $v_-^*(x,p)$ are exponentially bounded at infinity and this ensures the existence of their Fourier transform (3.39) and (3.40). In particular it is shown by Noble [7] that

$$\text{if } |\sigma_+^*(x,p)| < M_1e^{\lambda_- x} \text{ as } x\to+\infty \text{ then } \quad \Sigma_+(s) \text{ is analytic in } \mathrm{Im}(s)=\lambda>\lambda_-,$$

$$\text{and if } |v_-^*(x,p)| < M_2e^{\lambda_+ x} \text{ as } x\to-\infty \text{ then } \quad V_-(s) \text{ is analytic in } \mathrm{Im}(s)=\lambda<\lambda_+.$$

3.3.1 Wiener-Hopf technique

Eliminating $E(s,p)$ from (3.37) and (3.38) we obtain a Wiener-Hopf equation

$$\frac{\sigma_0}{p}e^{-isl}-\Sigma_+(s) = \mu_{12}\xi\frac{F(s,p)}{\sqrt{s^2+p^2/c_d^2}}V_-(s) \tag{3.41}$$

which contains only the two unknown functions $\Sigma_+(s)$ and $V_-(s)$, and now the Wiener-Hopf technique can be applied as follows. Suppose that the function $L(s)$ is defined and factored as

$$L(s) = \frac{L_-(s)}{L_+(s)} = \mu_{12}\xi\frac{F(s,p)}{\sqrt{s^2+p^2/c_d^2}} \tag{3.42}$$

then equation (3.41) becomes

$$\frac{\sigma_0}{p}e^{-isl}L_+(s) - \Sigma_+(s)L_+(s) = L_-(s)V_-(s). \tag{3.43}$$

Assume that the function $D(s)$ can be decomposed as

$$\frac{\sigma_0}{p}e^{-isl}L_+(s) = D(s) = D_+(s) + D_-(s), \tag{3.44}$$

then equation (3.43) becomes

$$D_+(s) - \Sigma_+(s)L_+(s) = L_-(s)V_-(s) - D_-(s) = W(s). \tag{3.45}$$

The first member of this equation is analytic in the upper half of the $s-$plane $\mathrm{Im}(s) = \lambda > \lambda_-$ and the second member is analytic in the lower half of the $s-$plane $\mathrm{Im}(s) = \lambda < \lambda_+$. Therefore, if $\lambda_+ > \lambda_-$ the regions of analyticity overlap. Using the Liouville's theorem to determine $W(s)$, solutions for $\Sigma_+(s)$ and $V_-(s)$ can be found.

After algebraic manipulation it is found that the function $F(s,p)$ reduces to

$$\begin{aligned} F(s,p) \;=\; & \frac{1}{\xi\sqrt{c_{11}}\sqrt{c_{11}s^2 + p^2/c_s^2}(\gamma_1+\gamma_2)(1+c_{12})}\Big\{c_{22}c_{12}\gamma_1^2\gamma_2^2 - \gamma_1\gamma_2(1+c_{12})c_{12}^2s^2 + \\ & (c_{11}s^2 + p^2/c_s^2)\left[c_{22}(\gamma_1^2+\gamma_2^2) + \gamma_1\gamma_2(1+c_{12})c_{22} + s^2(c_{12}+c_{12}^2 - c_{11}c_{22}) - c_{22}p^2/c_s^2\right]\Big\} \end{aligned}$$

The only zeros of $F(s,p)$ are of the form $s = \pm ip/c_R$ where c_R is the Rayleigh wave speed. This can be seen by substituting $s = ip/v$ in $F(s,p)$, letting $F(s,p) = 0$ and dividing by the non-zero factors, then $F(ip/v,p) = 0$ reduces to

$$\sqrt{\frac{c_{22}}{c_{11}}}\left(\frac{c_{11}c_{22} - c_{12}^2}{c_{22}} - \frac{v^2}{c_s^2}\right)\sqrt{1 - \frac{v^2}{c_s^2}} - \frac{v^2}{c_s^2}\sqrt{1 - \frac{v^2}{c_{11}c_s^2}} = 0$$

which is the Rayleigh function for orthotropic materials [10]. The roots of this function are $v = \pm c_R$.

Consequently, the first step in factoring $L(s)$ is to define

$$\hat{F}(s) = \frac{F(s,p)}{s^2 + p^2/c_R^2}. \tag{3.46}$$

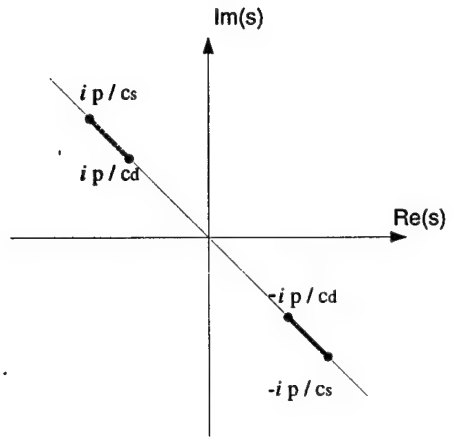

Figure 3.2: Branch cuts of $\hat{F}(s)$ in the $s-$plane.

It can be shown that $\hat{F}(s) \to 1$ as $s \to \infty$, (the constant ξ in (3.29) was chosen to make this possible). The function $\hat{F}(s)$ is regular and $\hat{F}(s) \neq 0$ in the $s-$plane cut as shown in figure 3.2, the only singularities are the branch points shared with γ_1 and γ_2. Where the branch points of γ_1 and γ_2 are

$$\begin{aligned} \text{for } \gamma_1; \quad s &= \pm\frac{ip}{c_s}, \\ \text{for } \gamma_2; \quad s &= \pm\frac{ip}{\sqrt{c_{11}}\, c_s} = \pm\frac{ip}{c_d}. \end{aligned}$$

It is well-known that factorization is accomplished most directly for functions that approach unity as $|s| \to \infty$ and that have neither zeros nor poles in the finite plane; $\hat{F}(s)$ is an example of such a function. Therefore, using Cauchy's integral formula it can be shown that [3]

$$\hat{F}_{\pm}(s) = \exp\left\{\frac{1}{2\pi i}\int_{\Gamma_{\pm}} \frac{\log \hat{F}(z)}{z-s}\, dz\right\}$$

where $\hat{F}(s) = \hat{F}_{+}(s)\hat{F}_{-}(s)$ and Γ_{-} (Γ_{+}) is the contour enclosing the branch cut between $+ip/c_d$ and $+ip/c_s$, ($-ip/c_d$ and $-ip/c_s$). Using the fact that $\hat{F}(\bar{s}) = \overline{\hat{F}(s)}$, one can write

$$\hat{F}_{\pm}(s) = \exp\left\{\frac{-1}{\pi}\int_{1/c_d}^{1/c_s} \tan^{-1}\left(\frac{\mathrm{Im}[\hat{F}(ipw)]}{\mathrm{Re}[\hat{F}(ipw)]}\right)\frac{dw}{w \mp \frac{is}{p}}\right\}$$

Note that by making $s = ip\zeta$ in this equation, $\hat{F}_{\pm}(s = ip\zeta) = \tilde{F}_{\pm}(\zeta)$ becomes a function only

of ζ. That is

$$\tilde{F}_{\pm}(\zeta) = \exp\left\{\frac{-1}{\pi}\int_{1/c_d}^{1/c_s} \tan^{-1}\left[R(w)\right]\frac{dw}{w \pm \zeta}\right\} \tag{3.47}$$

where

$$R(w) = \frac{\mathrm{Im}[\hat{F}(ipw)]}{\mathrm{Re}[\hat{F}(ipw)]}.$$

Returning to the factorization of $L(s)$ we have

$$L(s) = \frac{L_-(s)}{L_+(s)} = \mu_{12}\xi\frac{\hat{F}(s)(s^2+p^2/c_R^2)}{\sqrt{s^2+p^2/c_d^2}} \tag{3.48}$$

$$= \mu_{12}\xi\frac{\hat{F}_+(s)\hat{F}_-(s)(s+ip/c_R)(s-ip/c_R)}{\sqrt{s+ip/c_d}\sqrt{s-ip/c_d}} \tag{3.49}$$

therefore

$$L_-(s) = \mu_{12}\xi\frac{(s-ip/c_R)}{\sqrt{s-ip/c_d}}\hat{F}_-(s), \tag{3.50}$$

$$L_+(s) = \frac{\sqrt{s+ip/c_d}}{(s+ip/c_R)}\frac{1}{\hat{F}_+(s)}. \tag{3.51}$$

Using the sum splitting formula [7] for the function $D(s)$ defined in (3.44) along with the result (3.51) it is found that

$$D_+(s) = \frac{1}{2\pi i}\int_{-\infty+i\lambda_0}^{\infty+i\lambda_0}\frac{D(z)}{z-s}dz = \frac{\sigma_0}{p}\frac{1}{2\pi i}\int_{-\infty+i\lambda_0}^{\infty+i\lambda_0}\frac{(z+ip/c_d)^{1/2}e^{-izl}}{(z-s)(z+ip/c_R)\hat{F}_+(z)}dz, \tag{3.52}$$

$$D_-(s) = D(s) - D_+(s) \tag{3.53}$$

where λ_0 is such that $\lambda_- < \lambda_0 < \lambda_+$.

Each side of equation (3.45) is analytic in one of the overlapping half planes, and the sides coincide on the strip of overlap. Consequently each side of (3.45) is the analytic continuation of the other into its complementary half plane; so that the two sides together represent one and the same entire function $W(s)$. The entire function will be determined by its behavior at $|s| \to \infty$ which is related with the behavior of physical quantities near $x = 0$. First note that $L_+(s) \sim s^{-1/2}$ and $L_-(s) \sim s^{1/2}$ as $|s| \to \infty$, and, $D_+(s)$ and $D_-(s)$ in (3.52) and (3.53) are bounded in their respective planes of analyticity and vanish at infinity. Furthermore,

$\sigma_+^*(x,p)$ is expected to be square root singular as $x \to 0^+$ and $v_-^*(x,p)$ is expected to vanish as $x \to 0^-$ to ensure continuity of displacement. Consequently from the Abel theorem [7] relating asymptotic properties of transforms

$$\lim_{x\to 0^+} x^{1/2}\sigma_+^*(x,p) \sim \lim_{s\to\infty} s^{1/2}\Sigma_+(s)$$
$$\lim_{x\to 0^-} |x|^{-q} v_-^*(x,p) \sim \lim_{s\to-\infty} |s|^{1+q} V_-(s)$$

for some $q > 0$. Therefore, it is expected that $\Sigma_+(s) \sim s^{-1/2}$ and $V_-(s) \sim s^{-1-q}$ as $|s| \to \infty$, thus the products $\Sigma_+(s)L_+(s)$ and $L_-(s)V_-(s)$ vanish at infinity. Therefore, each side of (3.45) vanishes as $|s| \to \infty$ in the corresponding half planes. According the the Liouville's theorem, a bounded entire function is constant. In this case, $W(s)$ is bounded in the finite plane and $W(s) \to 0$ as $|s| \to \infty$ so that the constant must be zero; thus, $W(s) = 0$. By using (3.45) and (3.52), the functions of interest are then given by

$$\Sigma_+(s) = \frac{D_+(s)}{L_+(s)} \tag{3.54}$$
$$V_-(s) = \frac{D_-(s)}{L_-(s)}. \tag{3.55}$$

3.3.2 Stress Intensity factor

To find the stress intensity factor, an asymptotic expression for the normal stress near the crack tip is sought. The Abel's theorem relating asymptotic expressions between a function and its Fourier transform is the following [7]

$$\lim_{x\to 0^+} \sqrt{x}\ \sigma_+^*(x,p) = \lim_{s\to+\infty} e^{-i\pi/4}\sqrt{\frac{s}{\pi}}\ \Sigma_+(s). \tag{3.56}$$

Clearly, the behavior of $\Sigma_+(s)$ as $s \to \infty$ is needed. Note from (3.51), (3.52) and (3.54) that

$$\Sigma_+(s) = \frac{-\sigma_0}{p}\frac{1}{s^{1/2}}\frac{1}{2\pi i}\int_{-\infty+i\lambda_0}^{\infty+i\lambda_0} \frac{(z+ip/c_d)^{1/2}e^{-izl}}{(z+ip/c_R)\hat{F}_+(z)}dz \quad \text{as} \quad s\to\infty \tag{3.57}$$

by making $z = ip\zeta$ this equation becomes

$$\Sigma_+(s) = \frac{-\sigma_0\sqrt{i}}{p^{1/2}}\frac{1}{s^{1/2}}\frac{1}{2\pi i}\int_{\tau_0-i\infty}^{\tau_0+i\infty} \frac{(\zeta+1/c_d)^{1/2}e^{p\zeta l}}{(\zeta+1/c_R)\tilde{F}_+(\zeta)}d\zeta \quad \text{as} \quad s\to\infty \tag{3.58}$$

where τ_0 is real and $-1/c_d < \tau_0 < 0$. Using this relation, the definition of the stress intensity factor gives

$$K_I^*(p) = \lim_{x\to 0^+} \sqrt{2\pi x}\, \sigma_+^*(x,p) = \lim_{s\to+\infty} e^{-i\pi/4}\sqrt{2s}\, \Sigma_+(s) \tag{3.59}$$

$$= \frac{\sqrt{2}\sigma_0}{p^{1/2}} \left\{ \frac{1}{2\pi i} \int_{\tau_0-i\infty}^{\tau_0+i\infty} I(\zeta) e^{p\zeta l}\, d\zeta \right\}, \tag{3.60}$$

where

$$I(\zeta) = \frac{(\zeta + 1/c_d)^{1/2}}{(\zeta + 1/c_R)\tilde{F}_+(\zeta)}. \tag{3.61}$$

To perform the inversion of $K_I^*(p)$ the Cagniard-de Hoop method can be applied. The central idea of the Cagniard-de Hoop scheme [1, 3] is to convert the integral in (3.60) to a form which allow inversion of the one-sided Laplace transform *by observation.* The path of integration is modified to form a closed contour, figure 3.3, such that the integrand in (3.60) is analytic inside of this contour. Applying Cauchy's theorem, Jordan's lemma and the fact that $I(\bar{\zeta}) = \overline{I(\zeta)}$ one can write $K_I^*(p)$ as

$$K_I^*(p) = \frac{\sqrt{2}\sigma_0}{p^{1/2}} \left\{ \frac{1}{\pi} \int_{-1/c_d}^{-\infty} \mathrm{Im}\left[I(\zeta)\right] e^{p\zeta l}\, d\zeta \right\}. \tag{3.62}$$

Letting $\zeta l = -\eta$ this equation becomes

$$K_I^*(p) = \frac{-\sqrt{2}\sigma_0}{p^{1/2}} \frac{1}{l\pi} \int_0^{\infty} \mathrm{Im}\left[I(-\eta/l)\right] H(\eta - l/c_d) e^{-p\eta}\, d\eta. \tag{3.63}$$

and the inversion of the Laplace transform becomes obvious. Equation (3.63) is a product of two transforms, so that $K_I(t)$ is a convolution of the inverse of the two transforms, i.e.

$$K_I(t) = -\frac{\sigma_0}{\pi}\sqrt{\frac{2}{\pi l}} \int_{1/c_d}^{t/l} \mathrm{Im}\left\{ \frac{(1/c_d - \eta)^{1/2}}{(1/c_R - \eta)\tilde{F}_-(\eta)(t/l - \eta)^{1/2}} \right\} d\eta \tag{3.64}$$

where it has been used the result $\tilde{F}_+(-\zeta) = \tilde{F}_-(\zeta)$.

Note that for time $t > l/c_s$, equation(3.64) can be evaluated by complex integration as shown by Freund [3]. It equals the sum of contributions from the pole at $\zeta = 1/c_R$ and the integral taken along a closed contour of infinitely large radius by using Cauchy's theorem. The final result for the intervals $l/c_s < t < l/c_R$ and $t > l/c_R$ is

$$K_I(t) = \sigma_0\sqrt{\frac{2}{\pi l}} \left[1 - \frac{(1/c_R - 1/c_d)}{(1/c_R - t/l)^{1/2}\tilde{F}_-(1/c_R)} H(1/c_R - t/l) \right]. \tag{3.65}$$

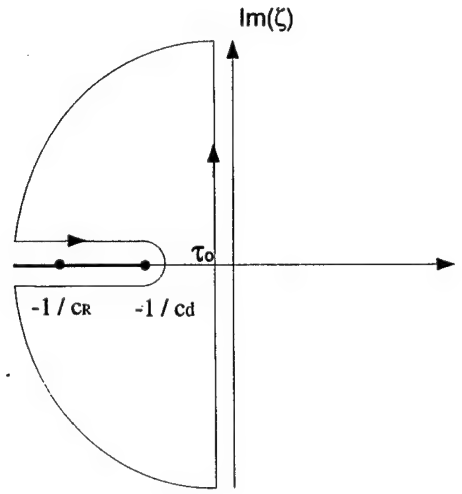

Figure 3.3: Contour of integration to evaluate the integral in (3.60) in the $\zeta-$ plane.

The second term in equation (3.65) becomes zero for $t > l/c_R$ and the remaining first term is the corresponding static solution for a semi-infinite crack under normal concentrated forces applied on its faces. For the interval $l/c_d < t < l/c_s$, the stress intensity factor is obtained by numerical evaluation of the integral in equation (3.64).

3.4 Results and Conclusions

The stress intensity factor $K_I(t)$ computed according to equations (3.64) and (3.65) are shown in figures 3.4 to 3.6 for different materials. The mechanical properties used for the analysis are given in table 3.1.

Figure 3.4 shows $K_I(t)$ for an isotropic material, in this case epoxy. The normalization factor is the long time limit $K_I(\infty) = \sigma_0\sqrt{2/\pi l}$ and the normalized time is $c_s t/l$. The behavior illustrated in the plot is the typical for isotropic materials as described by [3]. After the arrival of the dilatational wave generated by the load, the stress intensity factor takes on a small negative value, reflecting the tendency of the crack faces to move toward each other. The small negative value persists until the shear wave front arrives at time $t = l/c_s$. Thereafter, the stress intensity factor decreases rapidly to a negative square root singularity at time $t = l/c_R$, which is the instant of the arrival of the Rayleigh wave traveling

along the crack faces from the load to the crack tip. For time $t > l/c_R$, the stress intensity factor takes on the constant value $\sigma_0\sqrt{2/\pi l}$, which is the equilibrium stress intensity factor for the specified applied loading.

Figures 3.5(a) and 3.5(b) show the stress intensity factor history for a graphite/epoxy composite with fibers parallel to the $x-$axis and $y-$axis, respectively. A similar behavior is observed to that shown by the isotropic material. After the time $t = l/c_d$, $K_I(t)$ takes a small negative value until $t = l/c_s$ and then decreases rapidly to a singularity at time $t = l/c_R$. After the arrival of the Rayleigh wave at the crack tip emitted by the load, $K_I(t)$ takes its long time limit $K_I(\infty) = \sigma_0\sqrt{2/\pi l}$. The difference between $K_I(t)$ for isotropic and orthotropic materials are in the small negative value; for the orthotropic case this value is almost zero over an ample range of the interval $l/c_d < t < l/c_s$. This fact explains why figures 3.5(a) and 3.5(b) are almost identical. That is, even though c_d is different for the composite with fibers parallel to the $x-$axis and to the $y-$axis, the arrival of the dilatational wave front on the crack tip is almost imperceptible and $K_I(t)$ exhibits no appreciable difference in both cases.

Figure 3.6 shows the stress intensity factor history for E-glass epoxy composite. The behavior of $K_I(t)$ is very similar to that shown by graphite/epoxy. The difference is the instant when the singularity occurs. Again a very small negative value is observed for $K_I(t)$ in the interval $l/c_d < t < l/c_s$. Under closed inspection, however, as shown in figure 3.6(b), it is observed that the shape of the curve after the arrival of the dilatational wave front is similar to that for isotropic material but with different scale.

Finite cracks can be considered as semi-infinite for a short period of time. Figure 3.7 shows the stress intensity factor history for a finite crack under impact concentrated loads on its faces for orthotropic material obtained by Rubio-Gonzalez and Mason [8] using a different method of solution that involves numerical solution of a Fredholm integral equation for the Laplace transform of the stress intensity factor followed by numerical Laplace transform inversion. This numerical solution suffers from spurious oscillations, due to the

Laplace transform inversion technique, at the discontinuity in $K_I(t)$ and at $t = 0$. The closed form solution is much simpler to evaluate because of its simple algebraic and integral representation, equations (3.64) and (3.65), and does not exhibit spurious oscillations. The two methods show a good agreement, (Figure 3.7(b)), in the appropriate time interval.

Acknowledgment

Support of this work by the Office of Naval Research Young Investigator Program under grant N00014-96-1-0774 supervised by Dr. Y. Rajapakse and by the Mexican Government through CONACYT (Consejo Nacional de Ciencia y Tecnologia) is gratefully acknowledged.

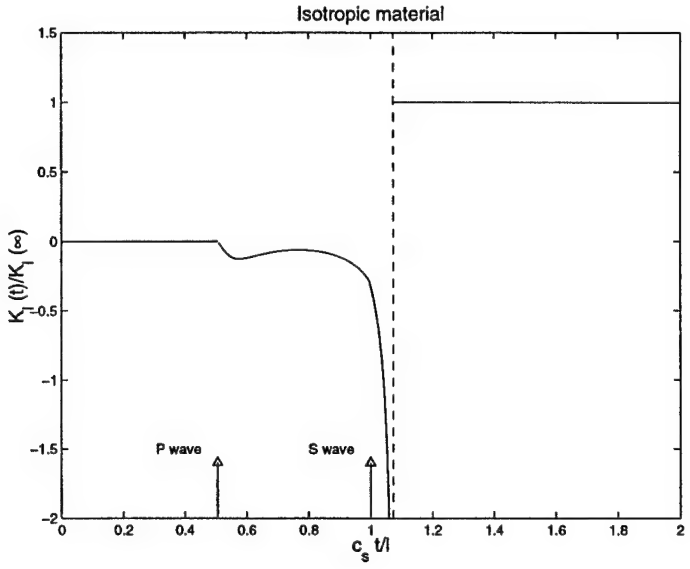

Figure 3.4: Stress intensity factor history for a semi-infinite crack in isotropic material, concentrated loads.

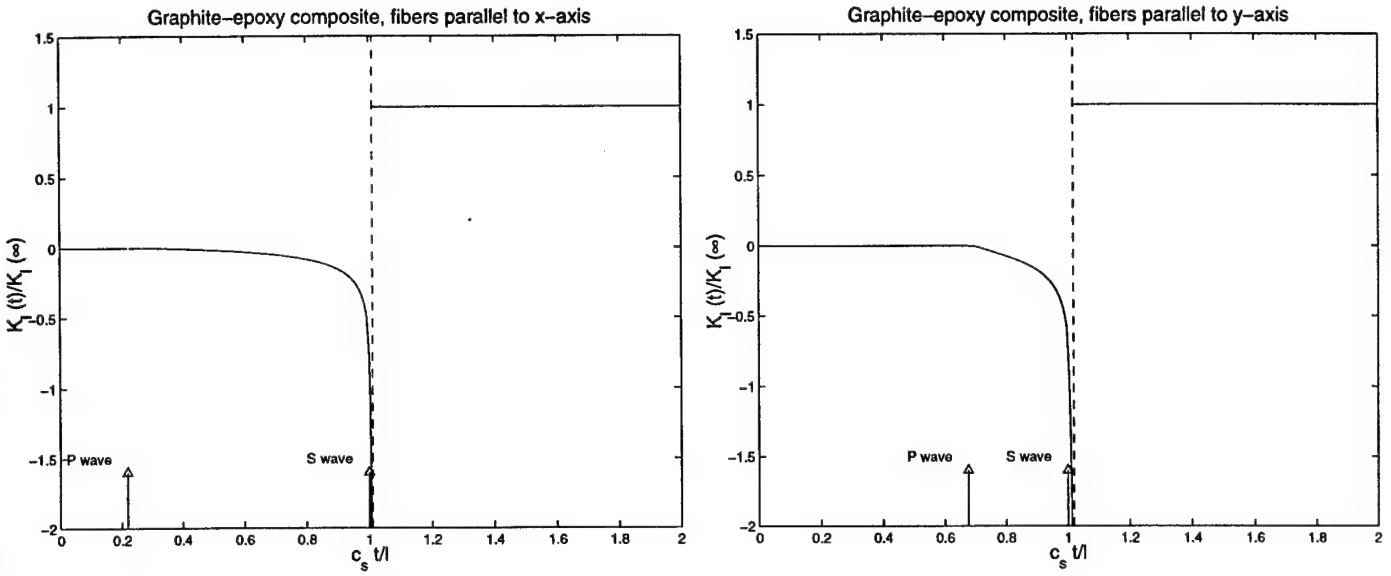

Figure 3.5: Stress intensity factor history for a semi-infinite crack in graphite/epoxy composite, concentrated loads. Fibers parallel to the (a) $x-$axis, (b) $y-$axis

	Graphite Epoxy	E-Glass Epoxy	Boron Epoxy	Epoxy
c_{11}	20.77	8.38	32.67	3.91
c_{22}	2.18	2.29	3.12	3.91
c_{12}	0.49	0.52	0.79	1.91
μ_{12} (GPa)	7.48	5.5	6.4	1.96
ρ (Kg/m^3)	1600	2100	1990	1260

Table 3.1: Mechanical properties used for the analysis.

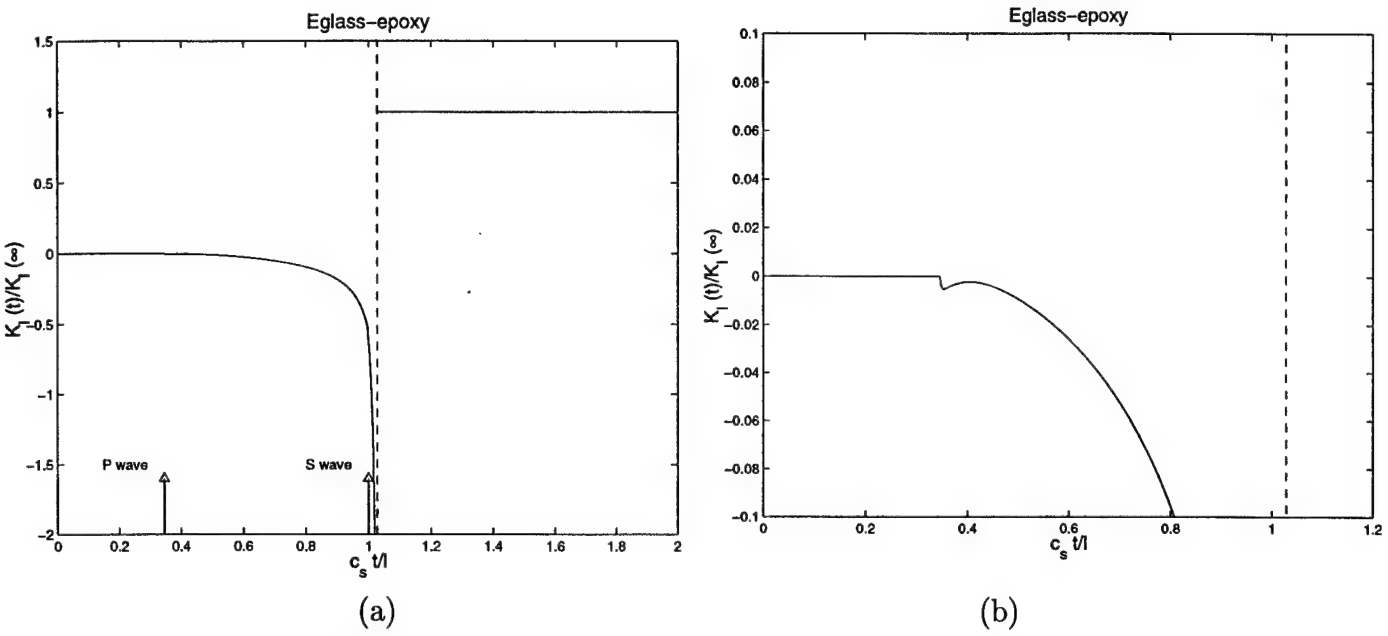

Figure 3.6: Stress intensity factor history for a semi-infinite crack in E-glass/epoxy composite, concentrated loads. (b) Under closer inspection.

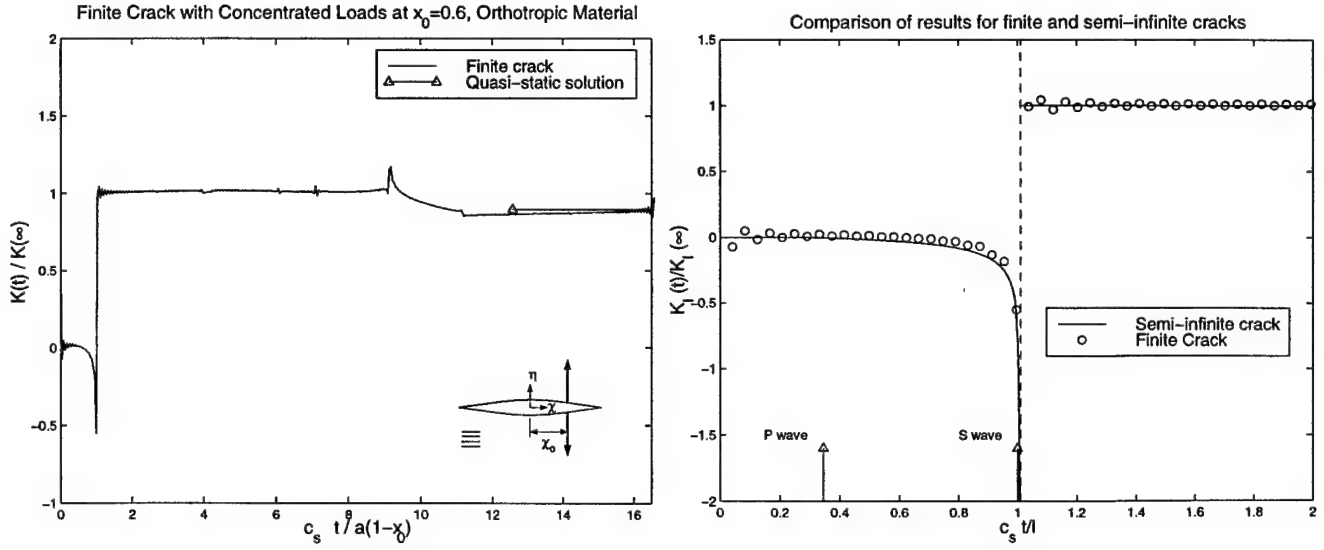

Figure 3.7: Comparison between the stress intensity factor for a finite crack of length $2a$ [8] and a semi-infinite crack under concentrated loads in orthotropic materials.

Bibliography

[1] Achenbach, J.D., 1973, *Wave Propagation in Elastic Solids*, North-Holland Publishing Company.

[2] Freund, L.B., 1974, *The Stress Intensity Factor due to Normal Impact Loading on the Faces of a Crack*, Int. J. Engng. Sci., v12, pp.179-189.

[3] Freund, L.B., 1990, *Dynamic Fracture Mechanics*, Cambridge University Press. New York.

[4] Kuo, M.K. and Chen T.Y., 1991, *Elastodynamic Responses due to Anti-plane Point Impact Loadings on the Faces of an Interface Crack along Dissimilar Anisotropic Materials*, Int. J. Solids Structures, v.28, pp.751-768.

[5] Kuo, M.K. and Chen T.Y., 1992, *The Wiener-Hopf Technique in Elastodynamic Crack Problems with Characteristic Lengths in Loading*, Engng. Fracture Mech. v.42, No.5, pp.805-813.

[6] Nayfeh, A.H., 1995, *Wave Propagation in Anisotropic Media with Applications to Composites*, North-Holland Publishing Company. Amsterdam.

[7] Noble B., 1958, *Methods Based on the Wiener-Hopf Technique*, Elmsford, N.Y., Pergamon.

[8] Rubio-Gonzalez, C. and Mason, J.J., 1998, *Fundamental Solutions for the Stress Intensity Factor Evolution in Finite Cracks in Orthotropic Materials.*, Submitted to Int. J. of Fracture.

[9] Rubio-Gonzalez, C. and Mason, J.J., 1998, *Response of Finite Cracks in Orthotropic Materials due to Concentrated Impact Shear Loads.*, Submitted to J. Appl. Mech.

[10] Ting, T.C.T., 1996, *Anisotropic Elasticity*, Oxford University Press, New York.

Chapter 4

Dynamic Stress Intensity Factor for Semi-infinite Cracks in Orthotropic Materials due to Concentrated Shear Impact Load

co-authored with C. Y. Wang and C. Rubio-Gonzalez and accepted for publication in International Journal of Solids and Structures

The transient elastodynamic response of an orthotropic material due to concentrated shear impact loads on the faces of a semi-infinite crack is examined, and the solution for the stress intensity factor history around the crack tip is found. Laplace and Fourier transforms together along with the Wiener-Hopf technique are employed to solve the equations of motion. Even though the problem has characteristic length, it has been shown in previous works that the Wiener-Hopf technique can be applied. The asymptotic expression of stress near the crack tip is analyzed, which leads to the dynamic mode II stress intensity factor. The results are presented for orthotropic materials as well as for an isotropic material.

1 Introduction

The growing use of composites in many engineering applications demands a fundamental understanding of the response of cracked orthotropic bodies to impact loading. By using the integral transform methods, the dynamic behavior for a finite crack under concentrated loads [1, 2] as well as for a semi-infinite crack under concentrated or uniform normal loads [3, 4] on its faces in orthotropic materials have been analyzed by Rubio-Gonzalez and Mason. In the former, the finite crack problem is reduced to a Fredholm integral equation in the Laplace transform domain which is solved numerically, and in the latter for the Weiner-Hopf technique was used to find the stress ahead of the crack tip and the displacement on the crack faces. The asymptotic expression for the stress near the crack tip leads to the stress intensity factor $K(t)$.

Many solutions for various loadings of cracks in orthotropic materials have been found by applying transforms to the displacement formulation of the equations of motion. Where previous researchers (for example, [5]) following this approach had solved the resulting dual integral equations using the method of Sneddon [6, 7], Rubio-Gonzalez and Mason [3] solve the same equations by converting the dual integral equations to a Weiner-Hopf equation. Solution of that equation requires only a straight forward application of the method of Noble [8]. In this paper, the problem of concentrated shear impact loads on the faces of a semi-infinite crack in orthotropic materials is analyzed using the same method. While it was been thought that the Weiner-Hopf technique could not be applied to problems such as this [9, 10], this approach has recently been shown to be valid in such cases [11]. Through Laplace and Fourier transforms combined with the Weiner-Hopf technique, a solution for the stress ahead of the crack tip is sought. The

asymptotic expression for the stress near the crack tip leads to the mode II stress intensity factor, $K_{II}(t)$.

2 Description of the problem

The plane problem of an infinite orthotropic body containing a semi-infinite crack is considered in Figure 1. Let E_i, μ_{ij} and v_{ij} $(i, j = 1, 2, 3)$ be the engineering elastic constants of the material where in the indices (1, 2, and 3) respectively stand for the directions (x, y, z) of a Cartesian coordinate system chosen to coincide with the orthotropic axes of material. The crack faces are suddenly loaded by a pair of concentrated shear forces with a magnitude (q) located a distance (a) away from the crack tip, as shown in Figure 1.

2.1 Equations of motion

The following problem is limited to a two-dimensional case with the inertial effect in the x-y plane only. By setting all the derivatives with respect to z-direction to be zero, it is readily shown that the displacement equations of motion [12] reduce to

$$\begin{aligned} c_{11}\frac{\partial^2 u}{\partial x^2}+\frac{\partial^2 u}{\partial y^2}+(1+c_{12})\frac{\partial^2 v}{\partial x\partial y}&=\frac{1}{c_s^{\,2}}\frac{\partial^2 u}{\partial t^2},\\ \frac{\partial^2 v}{\partial x^2}+c_{22}\frac{\partial^2 v}{\partial y^2}+(1+c_{12})\frac{\partial^2 u}{\partial x\partial y}&=\frac{1}{c_s^{\,2}}\frac{\partial^2 v}{\partial t^2}, \end{aligned} \tag{1}$$

where u and v are the x and y components of the displacement vector. In the orthotropic solids, $c_s=\sqrt{\mu_{12}/\rho}$ represents the velocity of the shear wave propagating along the principle material axes in xy-plane and ρ is the mass density. Here also, we introduce the

velocity $c_d = \sqrt{c_{11}}c_s$, which will appear later, representing the dilational wave speed along the x-axis. The non-dimensional parameters c_{11}, c_{12} and c_{22} are related to the elastic constants by the following relations. For a generalized plane stress problem,

$$\begin{aligned} c_{11} &= \frac{E_1}{\mu_{12}[1-(E_2/E_1)\nu_{12}^2]}, \\ c_{22} &= (E_2/E_1)c_{11}, \\ c_{12} &= \nu_{12}c_{22} = \nu_{21}c_{11}. \end{aligned} \tag{2}$$

For a plane strain problem,

$$\begin{aligned} c_{11} &= \frac{E_1}{\mu_{12}\Delta}(1-\nu_{23}\nu_{32}), \\ c_{22} &= \frac{E_2}{\mu_{12}\Delta}(1-\nu_{13}\nu_{31}), \\ c_{12} &= \frac{E_1}{\mu_{12}\Delta}(\nu_{21}+\frac{E_2}{E_1}\nu_{13}\nu_{32}), \\ \Delta &= 1-\nu_{12}\nu_{21}-\nu_{23}\nu_{32}-\nu_{31}\nu_{13}-\nu_{12}\nu_{23}\nu_{31}-\nu_{13}\nu_{21}\nu_{32}, \\ \frac{\nu_{ji}}{E_j} &= \frac{\nu_{ij}}{E_i}, \ (i, j=1, 2, 3). \end{aligned} \tag{3}$$

Finally, the stresses are related to the displacements by the equations,

$$\begin{aligned} \frac{\sigma_x}{\mu_{12}} &= c_{11}\frac{\partial u}{\partial x}+c_{12}\frac{\partial v}{\partial y}, \\ \frac{\sigma_y}{\mu_{12}} &= c_{12}\frac{\partial u}{\partial x}+c_{22}\frac{\partial v}{\partial y}, \\ \frac{\tau_{xy}}{\mu_{12}} &= \frac{\partial u}{\partial y}+\frac{\partial v}{\partial x}. \end{aligned} \tag{4}$$

2.2 Boundary conditions and Initial conditions

For the case shown Figure 1, the pair of spatially concentrated shear loads is applied suddenly on the crack faces. Exploiting symmetry and limiting ourselves to upper half-plane, $y>0$, the corresponding boundary conditions become

$$\begin{aligned} &\sigma_y(x,\ 0\ ,\ t)=0\ , && -\infty<x<+\infty\ , \\ &\tau_{xy}(x,\ 0,\ t)=-qH(t)\delta(x+a)\ , && -\infty<x<0\ , \\ &\mathrm{u}(x,\ 0,\ t)=0\ , && 0<x<+\infty\ , \end{aligned} \tag{5}$$

where q is the force per unit length in the z-direction of the opposed line loads acting on the crack faces and H(t) is the unit step function. The dirac delta function, $\delta(x+a)$, has the dimension of $length^{-1}$. In addition, the displacement at infinity is zero, and the body is stress free and at rest everywhere for $t\le 0$.

3 Integral transforms

3.1 Laplace transform

In equations (1), the time variable may be replaced by application of Laplace transform

$$f^*(s)=\int_0^\infty f(t)\,e^{-st}dt\ , \qquad f(\mathrm{t})=\frac{1}{2\pi i}\int_{\mathrm{Br}} f^*(s)\,e^{st}ds=\frac{1}{2\pi i}\int_{\sigma-i\infty}^{\sigma+i\infty} f^*(s)\,e^{st}ds\ , \tag{6}$$

where Br denotes the Bromwich path of integration which is a line parallel to the imaginary axis in the s-plane. Thus, using the Laplace transform representation, the displacements have the form

$$\begin{aligned} \mathrm{u}(x,\ y,\ t)&=\frac{1}{2\pi i}\int_{\mathrm{Br}}\mathrm{u}^*(x,\ y,\ s)\,e^{st}ds\ , \\ \mathrm{v}(x,\ y,\ t)&=\frac{1}{2\pi i}\int_{\mathrm{Br}}\mathrm{v}^*(x,\ y,\ s)\,e^{st}ds\ . \end{aligned} \tag{7}$$

Applying the relations (7) to equations (1) and assuming zero initial condition, the transformed domain equations become

$$
\begin{aligned}
&c_{11}\frac{\partial^2 u^*}{\partial x^2}+\frac{\partial^2 u^*}{\partial y^2}+(1+c_{12})\frac{\partial^2 v^*}{\partial x\partial y}-\frac{s^2}{c_s^{\,2}}u^*=0,\\
&\frac{\partial^2 v^*}{\partial x^2}+c_{22}\frac{\partial^2 v^*}{\partial y^2}+(1+c_{12})\frac{\partial^2 u^*}{\partial x\partial y}-\frac{s^2}{c_s^{\,2}}v^*=0.
\end{aligned}
\tag{8}
$$

Applying the relations (7) to equations (4), the transformed domain relations between stresses and displacements become

$$
\begin{aligned}
&\frac{\sigma_x^*}{\mu_{12}}=c_{11}\frac{\partial u^*}{\partial x}+c_{12}\frac{\partial v^*}{\partial y},\\
&\frac{\sigma_y^*}{\mu_{12}}=c_{12}\frac{\partial u^*}{\partial x}+c_{22}\frac{\partial v^*}{\partial y},\\
&\frac{\tau_{xy}^*}{\mu_{12}}=\frac{\partial u^*}{\partial y}+\frac{\partial v^*}{\partial x}.
\end{aligned}
\tag{9}
$$

Finally, the application of the Laplace transform to the boundary conditions (5) gives,

$$
\begin{aligned}
&\sigma_y^*(x,\,0\,,\,s)=0\,, && -\infty<x<+\infty\,,\\
&\tau_{xy}^*(x,\,0,\,s)=-q/s\,\delta(x+a)\,, && -\infty<x<0\,,\\
&u^*(x,\,0,\,s)=0\,, && 0<x<+\infty\,.
\end{aligned}
\tag{10}
$$

3.2 Fourier transform

To obtain a solution of the differential equations (8) subject to conditions (10), the Fourier transform is applied,

$$
\tilde{f}(\omega)=\int_{-\infty}^{\infty}f(x)\,e^{i\omega x}dx\,,\qquad f(x)=\frac{1}{2\pi}\int_{-\infty}^{\infty}\tilde{f}(\omega)\,e^{-i\omega x}d\omega \tag{11}
$$

It is noted that the boundary conditions (10) are explicitly defined only on half of the range of x. Consequently, the Fourier transform can not be applied to these boundary

conditions. To remedy this situation, the boundary conditions must be extended to apply on the full range of x. Two-unknown functions $u_-^*(x,s)$ and $\tau_+^*(x,s)$ are introduced. The function $u_-^*(x,s)$ is defined to be the x- direction displacement of the crack face, y=0, for $-\infty < x < 0$ and $0 < t < \infty$, and to be identically zero for $0 < x < +\infty$ and $0 < t < \infty$. Likewise, the function $\tau_+^*(x,s)$ is defined to be the shear stress in the x direction on the plane, y=0, for $0 < x < \infty$ and $0 < t < \infty$, and to be identically zero for $-\infty < x < 0$ and $0 < t < \infty$. With these definitions, the boundary conditions (10) can be rewritten as

$$\begin{aligned} &\sigma_y^*(\mathrm{x},\ 0\ ,\ \mathrm{s}) = 0\ , && \text{for } -\infty < x < \infty, \\ &\tau_{xy}^*(x,0,s) = -q/s\,\delta(x+a) + \tau_+^*(x,s)\ , && \text{for } -\infty < x < \infty, \\ &u^*(x,0,s) = u_-^*(x,s)\ , && \text{for } -\infty < x < \infty. \end{aligned} \tag{12}$$

Thus, the Laplace transformed displacements have the form

$$\begin{aligned} u^*(x,\ y,\ \mathrm{s}) &= \frac{1}{2\pi}\int_{-\infty}^{\infty} \tilde{\mathrm{u}}^*(\omega,\ y,\ \mathrm{s})\, e^{-i\omega x} d\omega\ , \\ \mathrm{v}^*(x,\ y,\ \mathrm{s}) &= \frac{1}{2\pi}\int_{-\infty}^{\infty} \tilde{\mathrm{v}}^*(\omega,\ y,\ \mathrm{s})\, e^{-i\omega x} d\omega\ . \end{aligned} \tag{13}$$

Substituting these transforms into equations (8), the functions $\tilde{u}^*$ and $\tilde{\mathrm{v}}^*$ are found to satisfy the ordinary differential equations

$$\begin{aligned} &\frac{d^2\tilde{\mathrm{u}}^*}{dy^2} - (1+c_{22})\omega i\frac{d\tilde{\mathrm{v}}^*}{dy} - (c_{11}\omega^2 + \frac{s^2}{c_s^{\ 2}})\tilde{\mathrm{u}}^* = 0\ , \\ &c_{22}\frac{d^2\tilde{\mathrm{v}}^*}{dy^2} - (1+c_{12})\omega i\frac{d\tilde{\mathrm{u}}^*}{dy} - (\omega^2 + \frac{s^2}{c_s^{\ 2}})\tilde{\mathrm{v}}^* = 0\ . \end{aligned} \tag{14}$$

The solution of equations (14) under the condition of zero displacement at infinity is

$$\tilde{u}^*(\omega,y,s)=A_1(\omega,s)e^{-\gamma_1 y}+A_2(\omega,s)e^{-\gamma_2 y},$$
$$\tilde{v}^*(\omega,y,s)=-\frac{i\alpha_1}{\omega}A_1(\omega,s)e^{-\gamma_1 y}-\frac{i\alpha_2}{\omega}A_2(\omega,s)e^{-\gamma_2 y}, \tag{15}$$

where $A_1(\omega,s)$ and $A_2(\omega,s)$ are arbitrary functions, and $\alpha_i(\omega,s)$ stands for the functions

$$\alpha_i(\omega,s)=\frac{c_{11}\omega^2+s^2/c_s^{\,2}-\gamma_i^{\,2}}{(1+c_{12})\gamma_i}, \qquad (i=1,\ 2), \tag{16}$$

with $\gamma_1^{\,2}$ and $\gamma_2^{\,2}$ being two roots of the quadratic equation,

$$c_{22}\gamma^4+[(c_{12}^{\,2}+2c_{12}-c_{11}c_{22})\omega^2-(1+c_{22})s^2/c_s^{\,2}]\gamma^2+(c_{11}\omega^2+s^2/c_s^{\,2})(\omega^2+s^2/c_s^{\,2})=0. \tag{17}$$

From (17), it is readily found that the functions $\gamma_1(\omega)$ and $\gamma_2(\omega)$ are multiple valued functions of ω in the complex ω-plane with branch points at $\omega=\pm is/c_s$ and $\omega=\pm is/\sqrt{c_{11}}c_s=\pm is/c_d$, respectively. It can be shown that for many materials that γ_1 and γ_2 are real and positive. Thus, the expressions for the displacements in the Laplace transform domain become

$$u^*=\frac{1}{2\pi}\int_{-\infty}^{\infty}(A_1e^{-\gamma_1 y}+A_2e^{-\gamma_2 y})e^{-i\omega x}d\omega,$$
$$v^*=\frac{-i}{2\pi}\int_{-\infty}^{\infty}(\alpha_1A_1e^{-\gamma_1 y}+\alpha_2A_2e^{-\gamma_2 y})\frac{e^{-i\omega x}}{\omega}d\omega. \tag{18}$$

Substituting these displacements into the constitutive law, (9), we obtain

$$\frac{\sigma_x^{\,*}}{\mu_{12}}=-\frac{ic_{11}}{2\pi}\int_{-\infty}^{\infty}(A_1e^{-\gamma_1 y}+A_2e^{-\gamma_2 y})e^{-i\omega x}d\omega+\frac{ic_{12}}{2\pi}\int_{-\infty}^{\infty}(\alpha_1\gamma_1A_1e^{-\gamma_1 y}+\alpha_2\gamma_2A_2e^{-\gamma_2 y})\frac{e^{-i\omega x}}{\omega}d\omega,$$

$$\frac{\sigma_y^{\,*}}{\mu_{12}}=-\frac{ic_{12}\omega}{2\pi}\int_{-\infty}^{\infty}(A_1e^{-\gamma_1 y}+A_2e^{-\gamma_2 y})e^{-i\omega x}d\omega+\frac{ic_{22}}{2\pi}\int_{-\infty}^{\infty}(\alpha_1\gamma_1A_1e^{-\gamma_1 y}+\alpha_2\gamma_2A_2e^{-\gamma_2 y})\frac{e^{-i\omega x}}{\omega}d\omega,$$

$$\frac{\tau_{xy}^{*}}{\mu_{12}} = -\frac{1}{2\pi}\int_{-\infty}^{\infty}(\gamma_1 A_1 e^{-\gamma_1 y} + \gamma_2 A_2 e^{-\gamma_2 y})e^{-i\omega x}d\omega - \frac{1}{2\pi}\int_{-\infty}^{\infty}(\alpha_1 A_1 e^{-\gamma_1 y} + \alpha_2 A_2 e^{-\gamma_2 y})e^{-i\omega x}d\omega .$$

(19)

Substitution of the expression for σ_y^*, the second of equations (19), into the boundary condition for σ_y^*, the first of equations (12), yields

$$A_2(\omega, s) = -\beta A_1(\omega, s) ,$$
$$\beta = \frac{c_{22}\alpha_1\gamma_1 - c_{12}\omega^2}{c_{22}\alpha_2\gamma_2 - c_{12}\omega^2} = \frac{c_{22}(c_{11}\omega^2 + s^2/c_s^{\,2} - \gamma_1^{\,2}) - c_{12}(1+c_{12})\omega^2}{c_{22}(c_{11}\omega^2 + s^2/c_s^{\,2} - \gamma_2^{\,2}) - c_{12}(1+c_{12})\omega^2} . \qquad (20)$$

Using this result in the expression for shear stress, the third of equations (19), and the expression for horizontal displacement, the first of equations (18), we obtain

$$\tau_{xy}^{\,*} = -\frac{\mu_{12}}{2\pi}\int_{-\infty}^{\infty}[(\alpha_1 + \gamma_1)e^{-\gamma_1 y} - \beta(\alpha_2 + \gamma_2)e^{-\gamma_2 y}]A_1 e^{-i\omega x}d\omega ,$$
$$u^* = \frac{1}{2\pi}\int_{-\infty}^{\infty}[e^{-\gamma_1 y} - \beta e^{-\gamma_2 y}]A_1 e^{-i\omega x}d\omega . \qquad (21)$$

Applying the remaining boundary conditions yields

$$-\frac{\mu_{12}}{2\pi}\int_{-\infty}^{\infty}[(\alpha_1 + \gamma_1) - \beta(\alpha_2 + \gamma_2)]A_1 e^{-i\omega x}d\omega = -q/s\,\delta(x+a) + \tau_+^{\,*}(x,s) ,$$
$$\frac{1}{2\pi}\int_{-\infty}^{\infty}[1-\beta]A_1 e^{-i\omega x}d\omega = u_-^{\,*}(x,s) . \qquad (22)$$

By Fourier transform inversion, these equations become

$$-\mu_{12}[(\alpha_1 + \gamma_1) - \beta(\alpha_2 + \gamma_2)]A_1 = -q/s\,e^{-i\omega a} + \Sigma_+(\omega) ,$$
$$(1-\beta)A_1 = U_-(\omega) , \qquad (23)$$

where

$$\Sigma_+(\omega) = \int_0^{\infty}\tau_+^{\,*}(x,s)e^{i\omega x}dx ,$$
$$U_-(\omega) = \int_{-\infty}^{0}u_-^{\,*}(x,s)e^{i\omega x}dx . \qquad (24)$$

Eliminating A_1 from equation, (23), we obtain a Wiener-Hopf equation,

$$\mu_{12} C \frac{R(\omega,s)}{\sqrt{\omega^2 + s^2/c_s^2}} U_-(\omega) = -q/s\, e^{-i\omega a} + \Sigma_+(\omega)\,, \tag{25}$$

where we have introduced the function

$$R(\omega,s) = -\frac{\sqrt{\omega^2 + s^2/c_s^2}}{(1-\beta)C}[(\alpha_1+\gamma_1) - \beta(\alpha_2+\gamma_2)]\,, \tag{26}$$

$$\begin{aligned} C = -\frac{1}{c_{22}(1+c_{12})N_1N_2(N_1+N_2)}\{&c_{12}c_{22}N_1^2N_2^2 - c_{12}^2(1+c_{12})N_1N_2 + \\ &c_{11}[c_{22}(N_1^2+N_2^2) + c_{22}(1+c_{12})N_1N_2 + (c_{12}+c_{12}^2 - c_{11}c_{22})]\}\,, \end{aligned} \tag{27}$$

$$N_{1,2}^2 = \frac{1}{2c_{22}}\left\{(c_{11}c_{22} - c_{12}^2 - 2c_{12}) \pm [(c_{11}c_{22} - c_{12}^2 - 2c_{12})^2 - 4c_{11}c_{22}]^{1/2}\right\}. \tag{28}$$

After algebraic manipulation, it is found that function $R(\omega,s)$ can be written as

$$\begin{aligned} R(\omega,s) = -\frac{\sqrt{\omega^2 + s^2/c_s^2}}{c_{22}(1+c_{12})\gamma_1\gamma_2(\gamma_1+\gamma_2)C}&\{c_{12}c_{22}\gamma_1^2\gamma_2^2 - c_{12}^2(1+c_{12})\gamma_1\gamma_2\omega^2 + (c_{11}\omega^2 + s^2/c_s^2) \\ &[c_{22}(\gamma_1^2+\gamma_2^2) + c_{22}(1+c_{12})\gamma_1\gamma_2 + (c_{12}+c_{12}^2 - c_{11}c_{22})\omega^2 - c_{22}\, s^2/c_s^2]\}\,. \end{aligned} \tag{29}$$

From the physics of the problem, it is reasonable to assume that the function $\tau_+^*(x,s)$ and $u_-^*(x,s)$ are exponentially bounded at infinity, which ensures the existence of their Fourier transform (24). In particular, it is shown by Noble [8] that if $|\tau_+^*(x,s)| < M_1 e^{\lambda_- x}$ as $x \to +\infty$ then $\Sigma_+(\omega)$ is analytic in $\mathrm{Re}(\omega) = \lambda > \lambda_-$, and if $|u_-^*(x,s)| < M_2 e^{\lambda_+ x}$ as $x \to -\infty$ then $U_-(\omega)$ is analytic in $\mathrm{Re}(\omega) = \lambda < \lambda_+$.

The function $R(\omega,s)$ is analytic everywhere in the complex plane except for at the branch cuts of γ_i between $\omega = \pm i s/c_s$ and $\omega = \pm i s/c_d$; it is single valued in the ω-plane cut as shown in Figure 2. It can be shown that the only zeros of $R(\omega,s)$ are of the

form $\pm i s/c_R$ where c_R is the Rayleigh wave speed. This can be seen by substituting $\omega = i s/v$ in $R(\omega, s)$, letting $R(\omega, s)=0$ and dividing by the non-zero factors, then $R(i s/v, s) = 0$ reduces to

$$\sqrt{\frac{c_{22}}{c_{11}}}\left(\frac{c_{22}c_{11} - c_{12}^{\,2}}{c_{22}} - \frac{v^2}{c_s^{\,2}}\right)\sqrt{1-\frac{v^2}{c_s^{\,2}}} - \frac{v^2}{c_s^{\,2}}\sqrt{1-\frac{v^2}{c_{11}c_s^{\,2}}} = 0\,, \tag{30}$$

which is the Rayleigh wave function for orthotropic materials [13]. The roots of this function are $v = \pm c_R$.

4 Wiener-Hopf technique

To solve the Weiner-Hopf equation, (25), we use the Weiner-Hopf technique as follows. The function $L(\omega)$ is defined and factored as

$$L(\omega) = L_+(\omega)L_-(\omega) = \mu_{12}C\frac{R(\omega, s)}{\sqrt{\omega^2 + s^2/c_s^{\,2}}}\,, \tag{31}$$

then the Weiner-Hopf equation becomes

$$L_-(\omega)U_-(\omega) = \frac{-q/s\,e^{i\omega x}}{L_+(\omega)} + \frac{\Sigma_+(\omega)}{L_+(\omega)}\,. \tag{32}$$

If the function $D(\omega)$ can be written and decomposed as

$$D(\omega) = -\frac{q/s\,e^{-i\omega x}}{L_+(\omega)} = D_+(\omega) + D_-(\omega)\,, \tag{33}$$

then the Weiner-Hopf equation, (32), is further reduced to

$$D_+(\omega) + \Sigma_+(\omega)/L_+(\omega) = L_-(\omega)U_-(\omega) - D_-(\omega) = W(\omega)\,. \tag{34}$$

The first expression for $W(\omega)$ in (34) is analytic in the right half plane, $\mathrm{Re}(\omega) > \lambda_-$, and the second expression is analytic in the left half plane, $\mathrm{Re}(\omega) < \lambda_+$. If $\lambda_- > \lambda_+$, the

regions of analyticity overlap and by invoking analytic continuation, it is concluded that $W(\omega)$ is analytic and single-valued in the whole ω-plane shown in Figure 2. Furthermore, invoking the extended Louisville theorem, it can be shown [8] that if $W(\omega)$ is bounded and entire and $W(\omega) \to 0$ *as* $\omega \to \infty$, then $W(\omega)$=0. Hence, we can solve for the transform of stress ahead of the crack tip, $\Sigma_+(\omega)$, and displacement, $U_-(\omega)$, behind,

$$\Sigma_+(\omega) = -D_+(\omega)L_+(\omega),$$
$$U_-(\omega) = \frac{D_-(\omega)}{L_-(\omega)}. \tag{35}$$

Following this outline, the first step is to factor $L(\omega)$, (31), by defining

$$F(\omega) = \frac{R(\omega, s)}{\omega^2 + s^2/{c_R}^2}. \tag{36}$$

Note that by making $\omega = is\varsigma$ in equation (36), then $F(\omega)$ is changed to a function only of ς,

$$\hat{F}(\varsigma) = \frac{R(is\varsigma, s)}{-s^2\varsigma^2 + s^2/{c_R}^2}. \tag{37}$$

It can be shown that $\hat{F}(\varsigma) \to 1$ as $\varsigma \to \infty$, (the constant C in (27) was chosen to make this possible). The function $\hat{F}(\varsigma)$ is regular and $\hat{F}(\varsigma) \neq 0$ in the ς-plane cut as shown in Figure 3. The only singularities of $\hat{F}(\varsigma)$ are the branch points shared with γ_i, $(i = 1, 2)$, i.e. $\varsigma = \pm 1/c_s$ and $\varsigma = \pm 1/c_d$. It is well-known that factorization of a function is accomplished most directly for functions which approach unity as $|\varsigma| \to \infty$ and which have neither zeros and nor poles in the finite plane. Indeed, $\hat{F}(\varsigma)$ is an example of such a function. Therefore, using Cauchy's integral formula, it can be shown that [10]

$$\hat{F}_{\pm}(\varsigma) = \exp\left\{\frac{1}{2\pi i}\int_{\Gamma_{\pm}} \frac{\log \hat{F}(\xi)}{\xi - \varsigma} d\xi\right\}, \tag{38}$$

where Γ_- is the closed counterclockwise contour enclosing the branch points $+1/c_d$ and $+1/c_s$, and also Γ_+ is the closed counterclockwise contour enclosing the branch points $-1/c_d$ and $-1/c_s$.

Using the fact that $\hat{F}(\bar{\varsigma}) = \overline{\hat{F}(\varsigma)}$, $H(-\eta) = -H(\eta)$, then

$$\hat{F}_{\pm}(\varsigma) = \exp\left\{-\frac{1}{\pi}\int_{1/c_d}^{1/c_s} H(\eta)\frac{d\eta}{\eta \pm \varsigma}\right\}, \tag{39}$$

where $H(\eta) = \tan^{-1}\left(\frac{\mathrm{Im}[\hat{F}(\eta)]}{\mathrm{Re}[\hat{F}(\eta)]}\right)$.

By making $\varsigma = \omega / is$ in equation (39), then $\hat{F}_{\pm}(\varsigma)$ is changed to $F_{\pm}(\omega)$.

Returning to the factorization of $L(\omega)$, we now have

$$L(\omega) = L_+(\omega)L_-(\omega) = \mu_{12} C \frac{F_+(\omega)F_-(\omega)(\omega + is/c_R)(\omega - is/c_R)}{\sqrt{\omega + is/c_s}\sqrt{\omega - is/c_s}}. \tag{40}$$

Therefore,

$$\begin{aligned} L_-(\omega) &= \mu_{12} C \frac{(\omega - is/c_R)}{\sqrt{\omega - is/c_s}} F_-(\omega), \\ L_+(\omega) &= \frac{(\omega + is/c_R)}{\sqrt{\omega + is/c_s}} F_+(\omega). \end{aligned} \tag{41}$$

Substituting equation (41) into equation (33) the function $D(\omega)$ can be obtained,

$$D(\omega) = \frac{-q/s\, e^{-i\omega\alpha}}{L_+(\omega)} = -\frac{\sqrt{\omega + is/c_s}}{(\omega + is/c_R)} \frac{q/s\, e^{-i\omega\alpha}}{F_+(\omega)}. \tag{42}$$

Through Cauchy's integral formula, we obtain

$$D_{\pm}(\omega)=\frac{1}{2\pi i}\int_{C_{\pm}}\frac{D(z)}{z-\omega}dz=-\frac{q}{s}\left\{\frac{1}{2\pi i}\int_{C_{\pm}}\frac{\sqrt{z+is/c_s}}{(z-\omega)(z+is/c_R)}\frac{e^{-iza}}{F_+(z)}dz\right\}, \quad (43)$$

where C_- is the closed counterclockwise contour enclosing the branch points $+is/c_d$ and $+is/c_s$, and C_+ is the closed counterclockwise contour enclosing the branch points $-is/c_d$ and $-is/c_s$.

Thus, we can show that $W(\omega)$=0, and using equation (35), we can readily obtain $\Sigma_+(\omega)$ and $U_-(\omega)$. We only give $\Sigma_+(\omega)$ here,

$$\Sigma_+(\omega)=-D_+(\omega)L_+(\omega)=\frac{q}{s}\frac{F_+(\omega)}{2\pi i}\frac{(\omega+is/c_R)}{\sqrt{\omega+is/c_s}}\int_{C_+}\frac{\sqrt{z+is/c_s}}{(z-\omega)(z+is/c_R)}\frac{e^{-iza}}{F_+(z)}dz. \quad (44)$$

5 Stress Intensity Factor

To find the stress intensity factor, an asymptotic expression for the shear stress near the crack tip is sought. A well-known result relating asymptotic expressions between a function and its Fourier transform (Abelian theorems) [8] is

$$\lim_{x\to 0_+}\sqrt{x}\tau_+^*(x,s)=\lim_{\omega\to+\infty}e^{-i\pi/4}\sqrt{\frac{\omega}{\pi}}\Sigma_+(\omega). \quad (45)$$

Thus, the usual definition of the stress intensity factor gives

$$K_{II}^*(s)=\lim_{x\to 0_+}\sqrt{2\pi x}\tau^*(x,s)=\lim_{\omega\to+\infty}e^{-i\pi/4}\sqrt{2\omega}\Sigma_+(\omega)=\lim_{\omega\to+\infty}\Phi(\omega),$$
$$\Phi(\omega)=e^{-i\pi/4}\sqrt{2\omega}\Sigma_+(\omega). \quad (46)$$

As $\omega\to+\infty$, $\Phi(\omega)$ becomes

$$\Phi(\omega)=-\frac{\sqrt{2}q}{s}\frac{e^{-i/4}}{2\pi i}\int_{C_+}\frac{\sqrt{z+is/c_s}}{(z+is/c_R)}\frac{e^{-iza}}{F_+(z)}dz. \quad (47)$$

and, by making $z=is\varsigma$, equation (47) becomes

$$\Phi(\omega) = -\frac{\sqrt{2}q}{s^{1/2}} \frac{1}{2\pi i} \int_{\Gamma_+} \frac{\sqrt{\varsigma + 1/c_s}}{(\varsigma + 1/c_R)} \frac{e^{s\varsigma a}}{\hat{F}_+(\varsigma)} d\varsigma, \qquad \text{as } \omega \to +\infty. \tag{48}$$

Thus,

$$K_{II}^*(s) = -\sqrt{2}q \left\{ \frac{1}{2\pi i} \int_{\Gamma_+} g(\varsigma) d\varsigma \right\}, \tag{49}$$

where

$$g(\varsigma) = \frac{\sqrt{\varsigma + 1/c_s}}{(\varsigma + 1/c_R)\hat{F}_+(\varsigma)} \frac{e^{s\varsigma a}}{s^{1/2}}.$$

Note that $g(\overline{\varsigma}) = \overline{g(\varsigma)}$, and $g(\varsigma) \to 0$ *as* $|\varsigma| \to \infty$ in the left half plane. Also, note that $\hat{F}_+(-\varsigma) = \hat{F}_-(\varsigma)$. Consequently, equation (49) can be written as the real integral

$$\begin{aligned} K_{II}^*(s) = & -\sqrt{2}q \left\{ \frac{1}{\pi} \int_{-1/c_d}^{-\eta^*} \mathrm{Im}[g(\eta)] d\eta \right\} \\ & = \frac{\sqrt{2}q}{\pi} \int_{1/c_d}^{\eta^*} \mathrm{Im} \left(\frac{\sqrt{1/c_s - \eta}}{(1/c_R - \eta)\hat{F}_-(\eta)} \frac{e^{-s\eta a}}{s^{1/2}} \right) d\eta, \end{aligned} \tag{50}$$

where η^* is a positive real number.

Applying the inverse Laplace transform to $K_{II}^*(s)$, using the convolution formula and letting $\eta^* a = t$, the stress intensity factor $K_{II}(t)$ can be written as follows

$$K_{II}(t) = -q\sqrt{2/\pi a} \left\{ -\frac{1}{\pi} \int_{1/c_d}^{t/a} \mathrm{Im} \left(\frac{\sqrt{1/c_s - \eta}}{(1/c_R - \eta)\sqrt{t/a - \eta}\hat{F}_-(\eta)} \right) d\eta \right\}, \tag{51}$$

The integrand of (51) has a first order singularity at $\varsigma = 1/c_R$ and branch points at $\varsigma = 1/c_d$, $\varsigma = 1/c_s$ *and* $\varsigma = \varsigma_0 = t/a$, which is shown in Figure 4. Here, pay attention to those points at $\varsigma = 1/c_d$, $\varsigma = 1/c_s$, $\varsigma = \varsigma_0 = t/a$ and $\varsigma = 1/c_R$, which are critical of the integrand of (51) as shown in the Figure 4.

For $t/a<1/c_d$, no waves generated by the applied loads have arrived at the crack tip, hence the stress intensity factor $K_{II}(t)$ is identically zero.

For $1/c_d<t/a<1/c_s$, a direct evaluation procedure for the stress intensity factor $K_{II}(t)$ can not be applied to the integral. It has to be obtained by numerical evaluation.

For $t/a>1/c_s$, the integrand of (51) is analytic in the entire ζ-plane cut along $1/c_d<\mathrm{Re}(\zeta)<t/a$, Im($\zeta$)=0, except for the pole point at $\varsigma=1/c_R$. In this case, the path of integration can be closed around the right side of the branch cut shown in Figure 4. The integral, (51), takes the form

$$K_{II}(t)=-\frac{q\sqrt{2}}{2\pi i\sqrt{\pi a}}\oint_{\Gamma(\varsigma_0)}\frac{\sqrt{1/c_s-\varsigma}}{(1/c_R-\varsigma)}\frac{1}{\sqrt{t/a-\varsigma}}\frac{1}{\hat{F}_-(\varsigma)}d\varsigma, \qquad (52)$$

where $\Gamma(\varsigma_0)$ denotes a closed counterclockwise contour embracing the branch cut of the integrand. Cauchy's integral formula can now be applied to show that value of the integral in (51) is equal to the value of the integral taken along a closed counterclockwise circular path of indefinitely large radius, (Ω), in ζ-plane shown in Figure 4. Therefore,

$$\frac{K_{II}(t)}{-q\sqrt{2/\pi a}}=1-\begin{cases}\dfrac{(1/c_R-1/c_s)^{1/2}}{(1/c_R-t/a)^{1/2}\hat{F}_-(1/c_R)} & \text{if } 1/c_s<t/a<1/c_R\\ 0 & \text{if } t/a>1/c_R\end{cases}. \qquad (53)$$

The first term on the right side of (53) is the contribution from the closed contour of the large radius and the second term is the residue contribution. In addition, The first term in (53) is the corresponding static solution for a semi-infinite crack under shear concentrated forces applied on it faces, $K_{II}(t)=-q\sqrt{2/\pi a}$.

6 Results and Discussion

Using equations (52) and (53), the stress intensity factor $K_{II}(t)$ can be calculated. The computed results are shown in Figure 5-8 for several materials, and the mechanical properties [14] used for the analysis are given in Table 1. The following tips should be taken into account when performing the numerical evaluation of the integral in (51).

(1) Theoretically, $R(\omega,s)$ in equation (26) can include either the factor $\sqrt{\omega^2+s^2/c_d^{\,2}}$ or $\sqrt{\omega^2+s^2/c_s^{\,2}}$, and we should have $\hat{F}(\varsigma)=1$ as $\varsigma\to\infty$. However, experience shows that if the factor $\sqrt{\omega^2+s^2/c_d^{\,2}}$ is selected in $R(\omega,s)$, it is difficult to numerically make $\hat{F}(\varsigma)=\hat{F}_+(\varsigma)\hat{F}_-(\varsigma)$ at points in the regions close to $[1/c_d, 1/c_s]$ and $[-1/c_s, -1/c_d]$, where $\hat{F}(\varsigma)$, $\hat{F}_-(\varsigma)$ and $\hat{F}_+(\varsigma)$ are respectively calculated using equations (37) and (38). This is true even though $\hat{F}(\varsigma)=1$ and $\hat{F}(\varsigma)=\hat{F}_+(\varsigma)\hat{F}_-(\varsigma)$ at points very far from $[1/c_d, 1/c_s]$ and $[-1/c_s, -1/c_d]$. For the problem with concentrated normal loads [3], the factor $\sqrt{\omega^2+s^2/c_d^{\,2}}$ should be selected in $R(\omega,s)$, while the factor $\sqrt{\omega^2+s^2/c_s^{\,2}}$ should be selected in $R(\omega,s)$ for the problem in this paper. Otherwise, there may be large errors in the calculations.

(2) It is best to adopt the formula $\hat{F}_-(\varsigma)=\hat{F}(\varsigma)/\hat{F}_+(\varsigma)$ to indirectly calculate the values of $\hat{F}_-(\varsigma)$ along $[1/c_d, 1/c_s]$ because $\hat{F}_-(\varsigma)$ is not analytic along $[1/c_d, 1/c_s]$. At $\varsigma=1/c_R$ the value of $\hat{F}_-(1/c_R)$ can be directly obtained by using the equation (39).

The numerical results presented correspond to isotropic and orthtropic materials. Properties of transversely isotropic materials with fibers parallel and perpendicular to the x-axis are considered in the orthtropic case.

For isotropic materials, as mentioned in [3], note that the mechanical parameters make $\gamma_1 = \gamma_2$ and further lead to $\beta = 1$ and $R(\omega, s)$ not defined. Consequently, in order to obtain the results for the isotropic case from the orthotropic formulation, we let $E_1 = E$, $E_2 = (1-\varepsilon)E$, $\nu_{12} = \nu_{23} = \nu$ and $\mu_{12} = E_2/2(1+\nu)$ where E and ν correspond to the isotropic properties and ε is a small quantity with $\varepsilon << 1$.

Figure 5 shows $K_{II}(t)$ for an isotropic material in the plane-strain case. The normalization factor is the long time limit $K_{II}(\infty) = -q\sqrt{2/\pi a}$ and the normalized time is $c_d\, t/a$. The behavior illustrated in Figure 5 is as expected from the surface displacements in the calculated solution of Lamb's problem where a concentrated shear load is applied on a half-space [15]. Horizontal displacements on the surface, generated by the point load, arrive at the crack tip with the arrival of the dilatational wave causing a rapid increase in the stress intensity factor. In addition, the results in Figure 5 are very similar to that of the problem in [2], before the arrival of the second dilatational wave, shear wave and Rayleigh wave, where a finite crack in infinite orthotropic body is impacted by two pairs of concentrated shear loads. After the arrival of the dilatational wave, a rapid increase in $K_{II}(t)$ is observed, and then the stress intensity factor gradually decreases until the shear wave front arrives at $t = a/c_s$. Thereafter, the stress intensity factor decreases rapidly to a negative square root singularity at $t = a/c_R$, which is the instant of the arrival of the Rayleigh wave traveling along the crack faces from the point of

application of load. For time $t > a/c_R$, the stress intensity factor takes on the constant value $-q\sqrt{2/\pi a}$, which is the equilibrium stress intensity factor for the specified loading. Obviously, the dilatational wave has an important effect on $K_{II}(t)$ under applied concentrated impact shear loads, unlike applied concentrated impact normal loads where the dilatational wave has a minimum effect on $K_I(t)$ [1, 3]. The stress intensity factor for an isotropic material in the plane-stress case is identical to the plane-strain case except for differences in the dilatational wave speed.

Figure 6(a) and 6(b) show the stress intensity factor history for a graphite-epoxy composite in the plane-strain state with fibers parallel to the x-axis and y-axis, respectively. Both figures are similar to the results for the isotropic material shown in Figure 5, except that there is a more uniform plateau from $t = a/c_d$ to $t = a/c_s$ and a steeper drop at $t = a/c_R$. In Figure 6(b) the plateau is lower than in Figure 6(a) and the duration of the plateau is longer due to the dramatic difference in c_d for these two cases. The Rayleigh wave speeds are approximately the same; the shear wave speeds are exactly the same.

As expected, the behavior illustrated in Figure 6(b) is the same as that for the corresponding case of Rubio-Gonzalez and Mason [2] before the second set of waves arrives crack tip. The behavior illustrated in Figure 6(a) can't be directly compared with that of the corresponding case of Rubio-Gonzalez and Mason [2] because in that work the second dilatational wave arrived at the crack tip before the arrival of the first shear wave and Rayleigh wave leading to very different loading conditions. To the knowledge of the

authors, this is the first presentation of results for this case that are not disturbed by reflected or secondary waves.

Figure 7 and 8(a) show the plane strain stress intensity factor history for the E-Glass Epoxy and Boron Epoxy composites, respectively. In both of cases the fibers are oriented along the x-axis. Figure 7 and 8(a) are very similar to Figure 6(a). Figure 8(b) shows the singularity at $t = a/c_R$ more clearly. The singularity can be quite difficult to capture using the method of Rubio-Gonzalez and Mason [2] because the shear and Rayleigh wave speeds are nearly equal. Here, equation (53) gives $K_{II}(t)$ explicitly.

7 Conclusions

(1) For impact concentrated shear loads on a semi-infinite crack in an orthotropic material, the arrival of the dilational wave at the crack tip makes an important contribution to the dynamic stress intensity factor $K_{II}(t)$, unlike in mode I loading where dilatational wave had a minimum effect on $K_I(t)$.

(2) The long time value, $K_{II}(\infty) = -q\sqrt{2/\pi a}$, is independent of the mechanical properties of the orthotropic material, however the curve shape and magnitude of $K_{II}(t)$ from $t = a/c_d$ to $t = a/c_R$ is very dependent on the mechanical properties of materials.

(3) From the results given here for an isotropic material and orthotropic materials, we can conclude that the normalized $K_{II}(t)$ from $t = a/c_d$ to $t = a/c_R$ is less than 1 except at a singularity at $t = a/c_R$. In addition, under similar conditions, when fibers are parallel to the crack direction $K_{II}(t)$ is generally greater than when the fibers are perpendicular to the crack direction.

(4) Finally, the method outlined here can easily be extended to solve the problem of a semi-infinite crack under more general impact shear loads on the faces of a semi-infinite crack. Alternatively, the solution presented here can be used as a Green's function to solve more general problems. Both methods should yield the same results.

Acknowledgment

Support of this work by the Office of Naval Research Young Investigator Program under grant N00014-96-1-0774 supervised by Dr. Y. Rajapakse and the Mexican Government through CONACYT (Consejo Nacional de Ciencia y Tecnologia) is gratefully acknowledged.

References

[1] Rubio-Gonzalez, C. and Mason, J. J. (1998) Fundamental solutions for the stress intensity factor evolution in finite cracks in orthotropic materials. Submitted to Int. J. of Fracture.

[2] Rubio-Gonzalez, C. and Mason, J. J. (1998) Response of finite cracks in orthotropic materials due to concentrated impact shear loads. Submitted to J. Appl. Mech.

[3] Rubio-Gonzalez, C. and Mason, J. J. (1998) Dynamic stress intensity factor for a semi-infinite crack in orthotropic materials due to concentrated normal impact loads. Submitted to J. of Composite Materials.

[4] Rubio-Gonzalez, C. and Mason, J. J. (1998) Closed form solutions for dynamic stress intensity factors at the tip of uniformly loaded semi-infinite cracks in orthotropic materials. Submitted to J. of Mechanics and Physics of Solids.

[5] Kassir, M. K., and Bandyopadhyay, K. K. (1983) Impact response of a cracked orthotropic medium, ASME, J. Appl. Mech., **50** , 630-636.

[6] Sneddon, I. N. (1946) The distribution of stress in the neighborhood of a crack in an elastic solid. Proceedings of the Royal Society (London) **A187**, 229-60.

[7] Sneddon, I. N. (1952) The stress produced by a pulse of pressure moving along the surface of a semi-infinite solid. Rendiconti del Circolo Matematico di Palermo **1**, 57-62.

[8] Noble B. (1958) Methods based on the Weiner-Hopf technique. Elmsford, New York, Pergamon.

[9] Freund, L. B. (1974) The stress intensity factor due to normal impact loading on the faces of a crack. Int. J. Engng. Sci., **12**, 179-189.

[10] Freund, L. B. (1990) Dynamic fracture mechanics, Cambridge University Press. New York.

[11] Kuo, M. K. and Chen T. Y. (1992) The Weiner-Hopf technique in elastodynamic crack problems with characteristic lengths in loading. Eng. Fracture Mech., **42,** 805-813.

[12] Nayfeh, A. H. (1995) Wave propagation in anisotropic media with applications to composites. North-Holland Publishing Company, Amsterdam.

[13] Ting, T.C.T. (1996) Anisotropic elasticity. Oxford University Press, New York.

[14] Schwartz, M. M. (1997) Properties, nondestructive testing and repair. Composite Material, **1**, Prentice-Hall, Upper Saddle River N. J.

[15] Chao C. C. (1960) Dynamic response of an elastic half-space to tangential surface loadings. ASME, J. Appl. Mech., **27**, 559-567.

Table 1 Mechanical properties used for the analysis

	Isotropic material	Graphite Epoxy	E-Glass Epoxy	Boron Epoxy
E_1 (Gpa)	200	156.75	45	207
E_2 (Gpa)	200	10.41	12	19
ν_{12}	0.3	0.31	0.19	0.21
ν_{23}	0.3	0.49	0.19	0.21
μ_{12} (Gpa)	76.92	7.07	5.5	6.4
$\rho(Kg/m^3)$	7840	1580	2100	1990

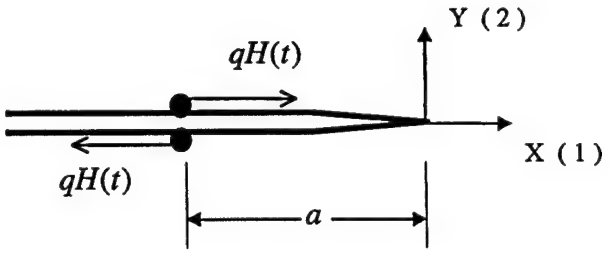

Figure 1 Schematic of the semi-infinite crack under concentrated shear impact loads

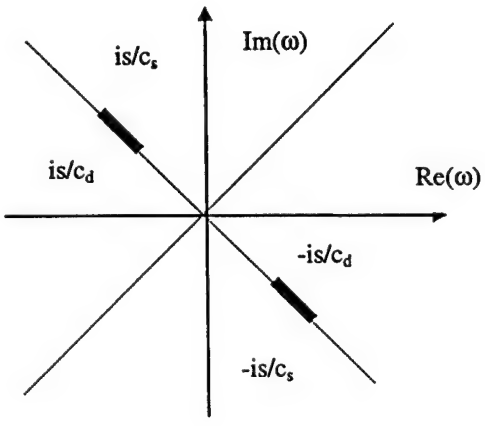

Figure 2 Branch cuts in the ω-plane

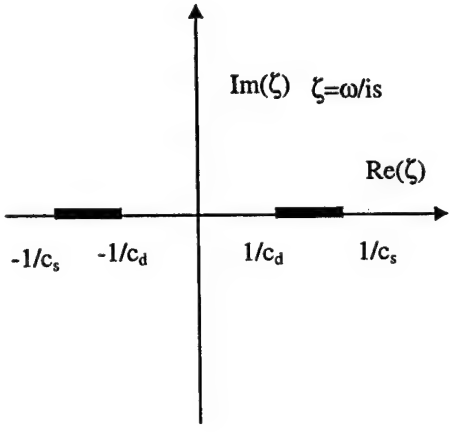

Figure 3 Branch cuts in the ζ-plane

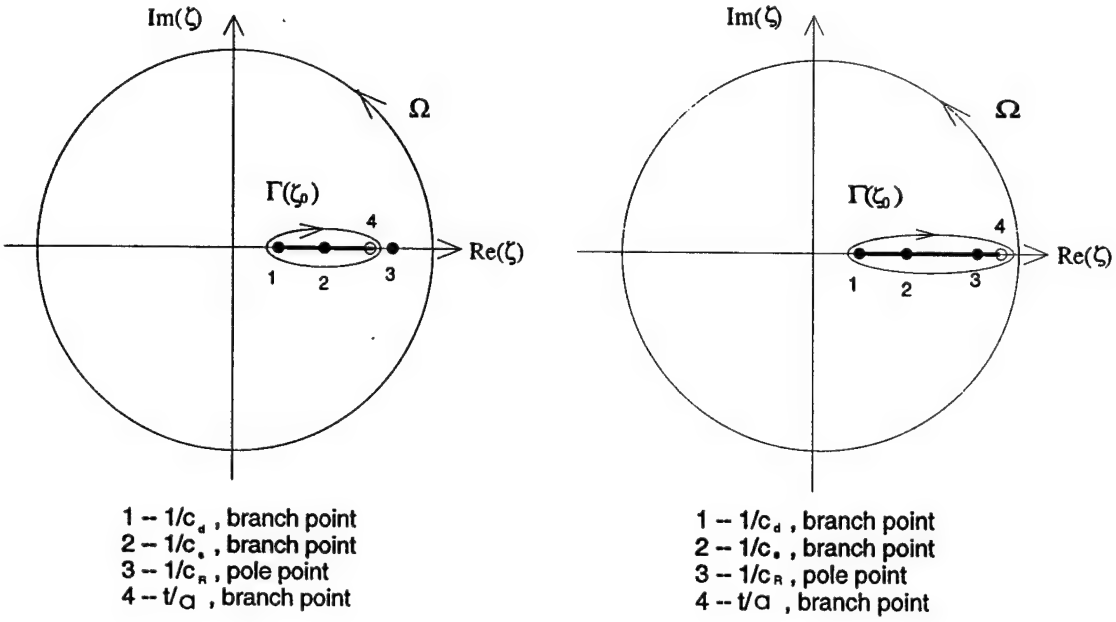

(a) For $1/c_s < t/a < 1/c_R$ (b) For $t/a > 1/c_R$

Figure 4 Branch cuts in the ζ-plane and Integral path

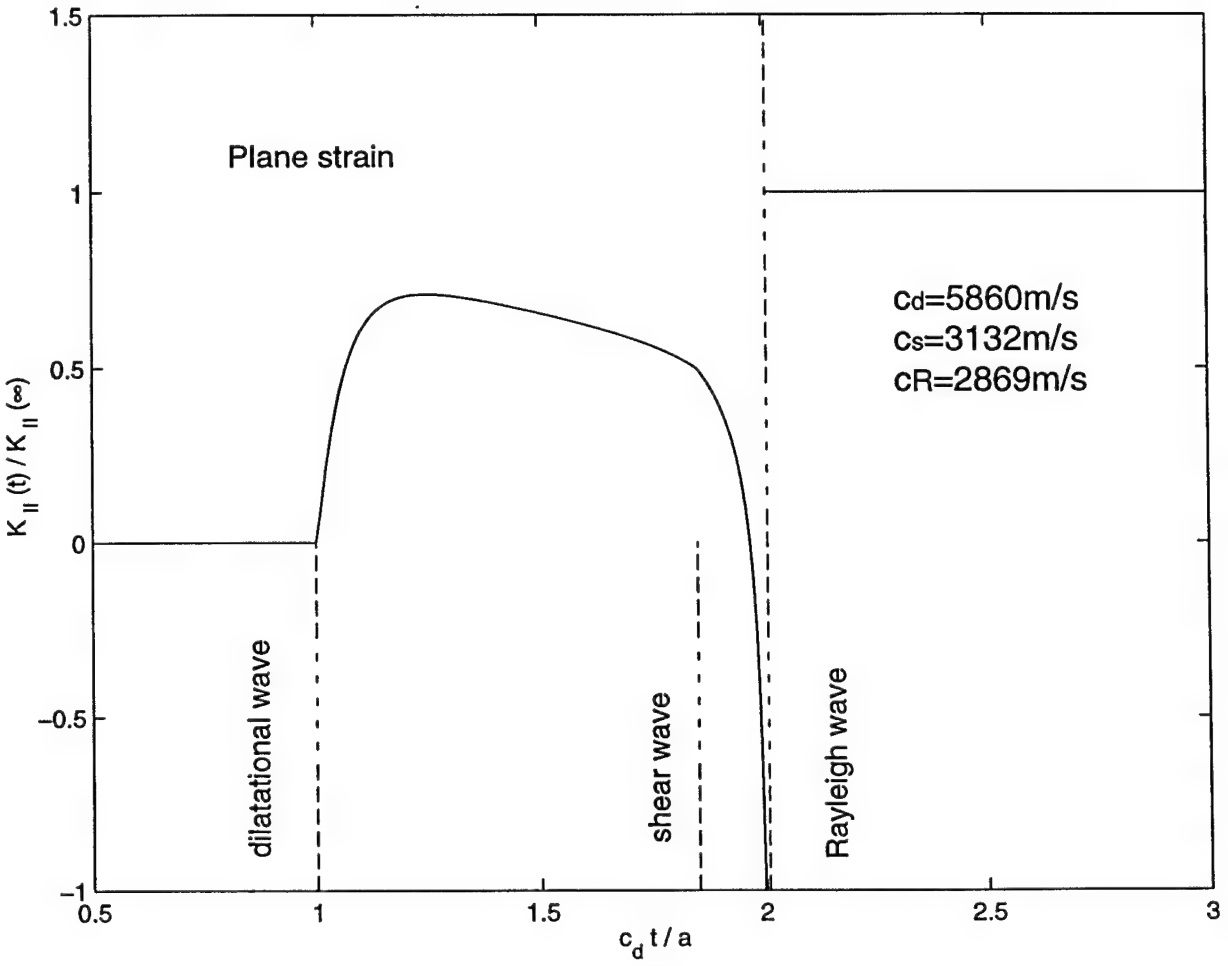

Figure 5 Stress intensity factor history in an isotropic material under concentrated shear loads

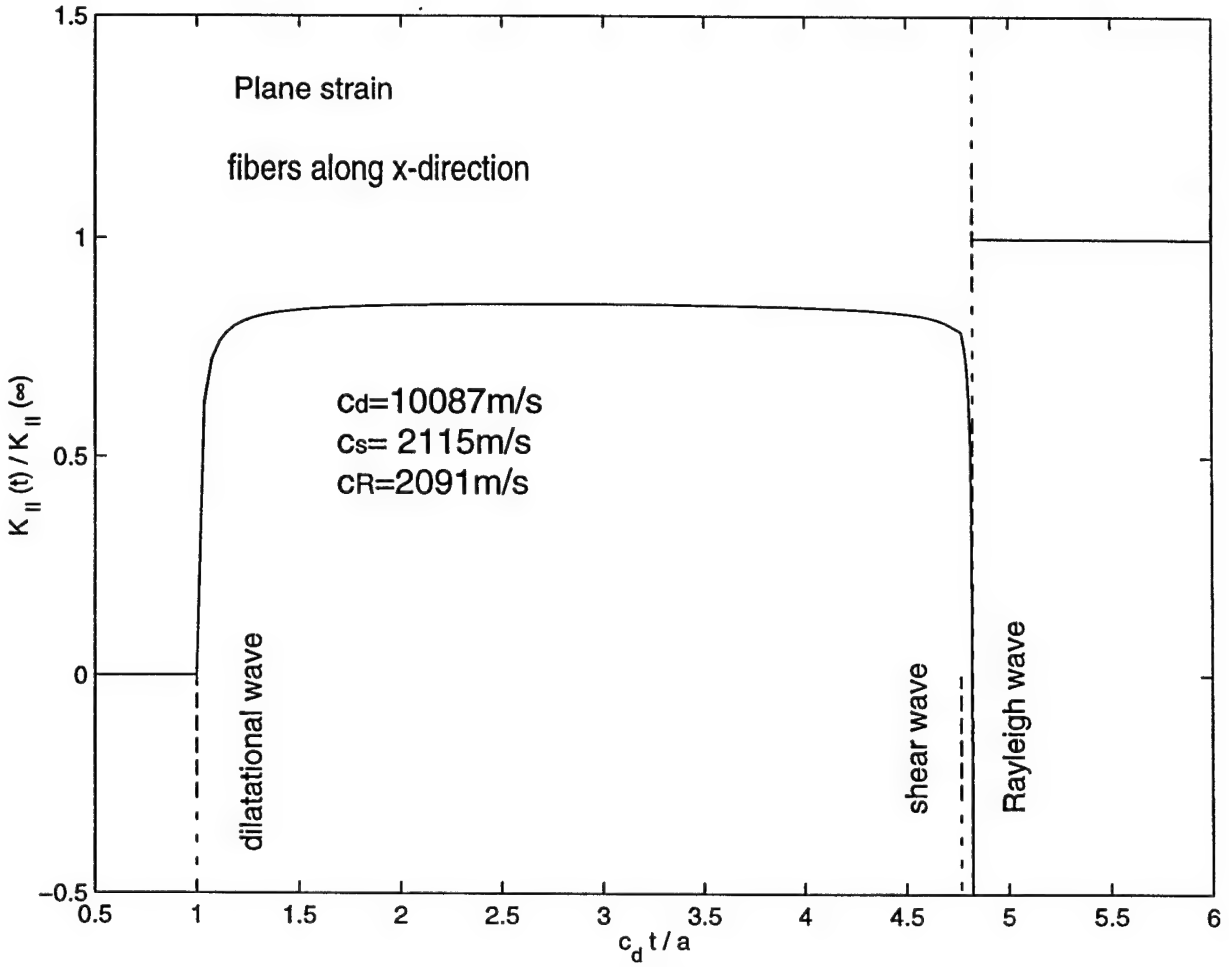

Figure 6(a) Stress intensity factor history in Graphite Epoxy under concentrated shear loads

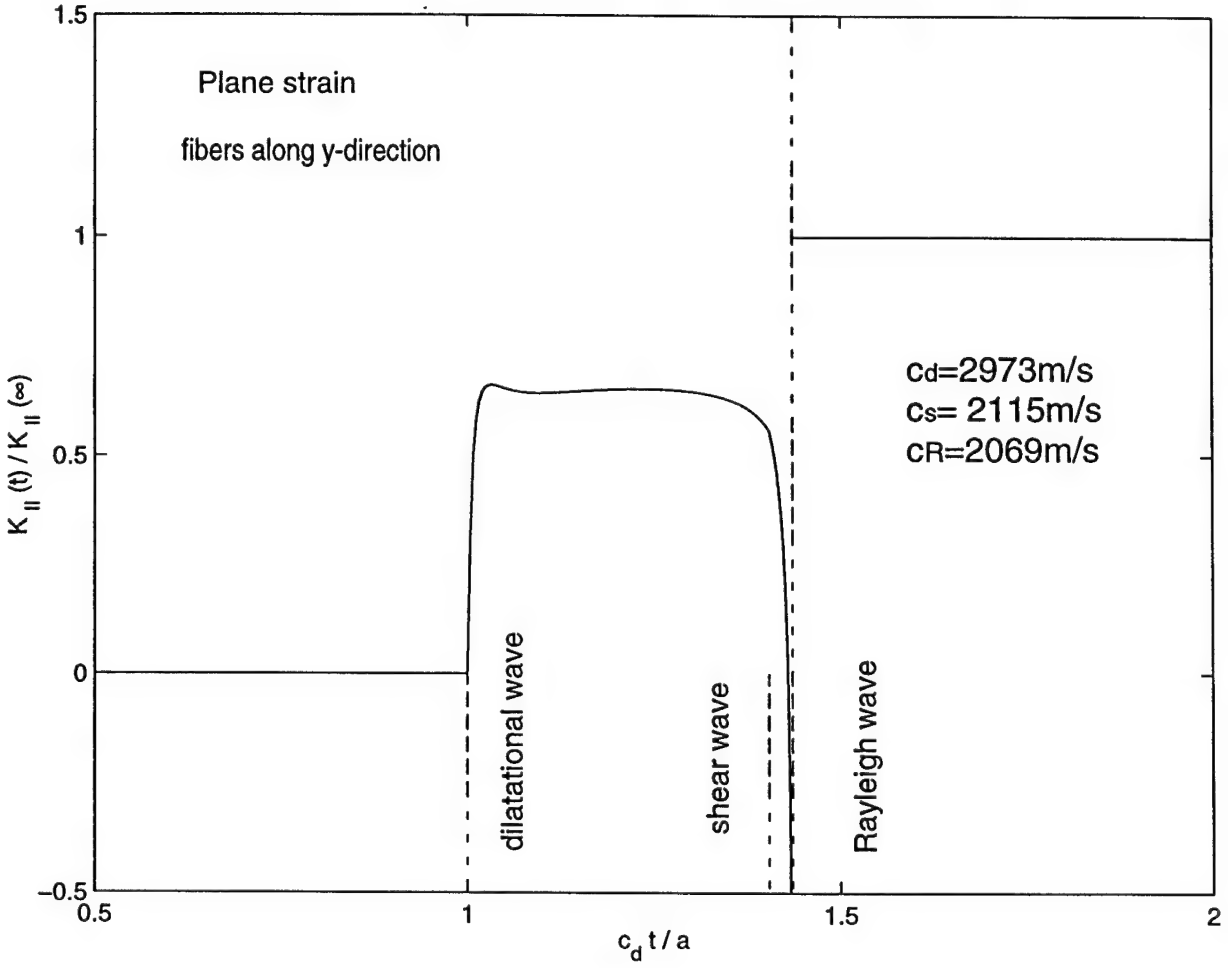

Figure 6(b) Stress intensity factor history in Graphite Epoxy under concentrated shear loads

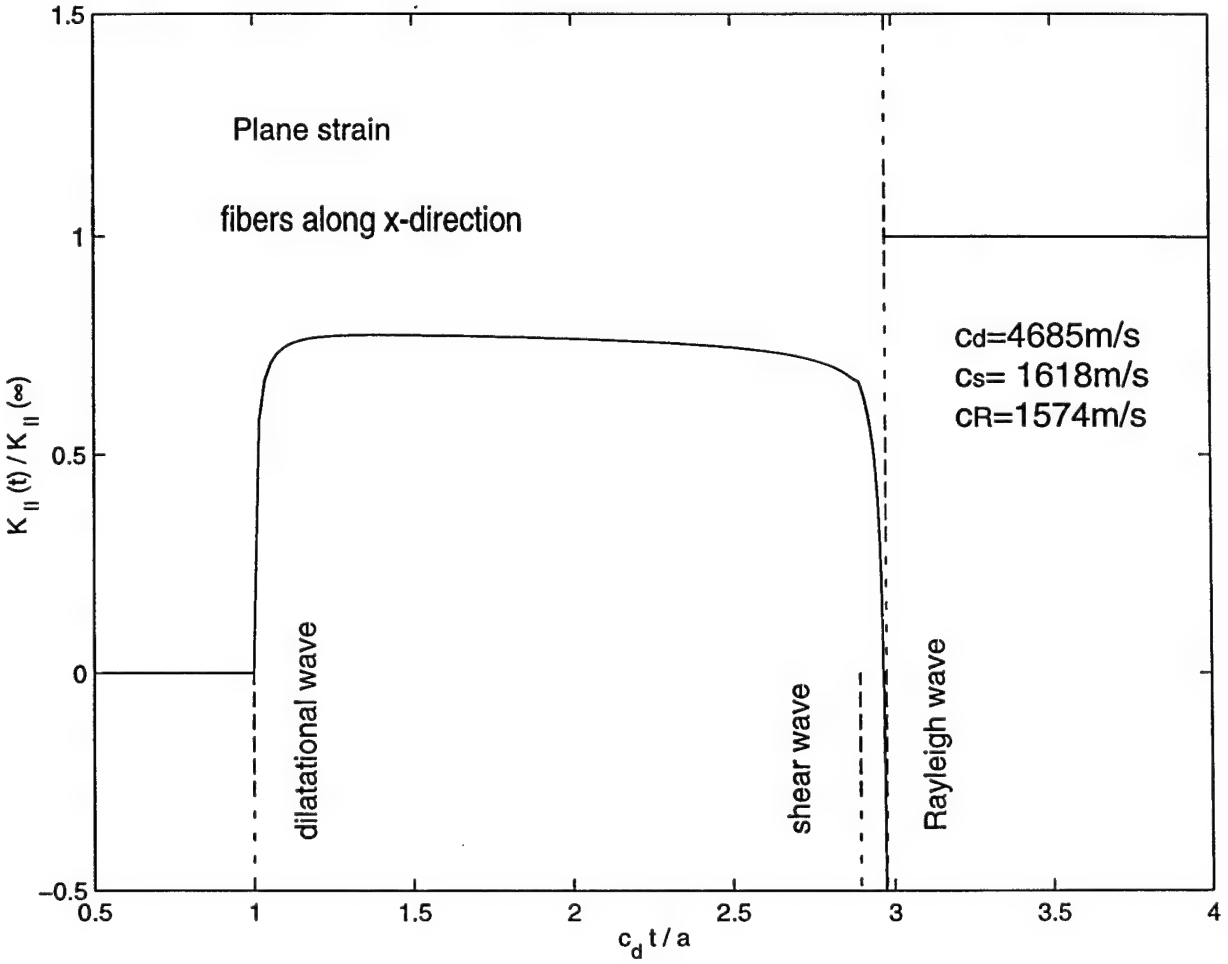

Figure 7 Stress intensity factor history in E-Glass Epoxy under concentrated shear loads

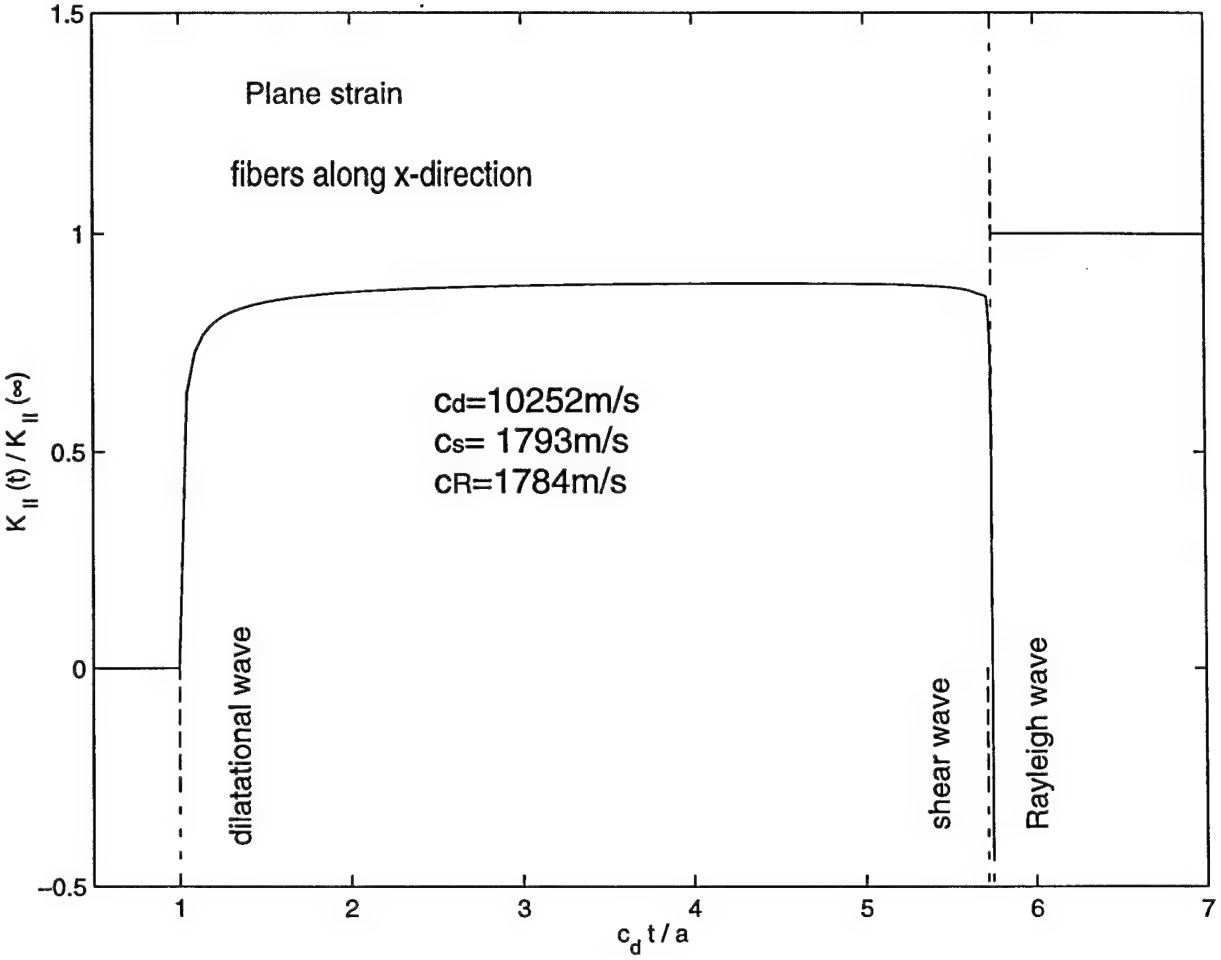

Figure 8(a) Stress intensity factor history in Boron Epoxy under concentrated shear loads

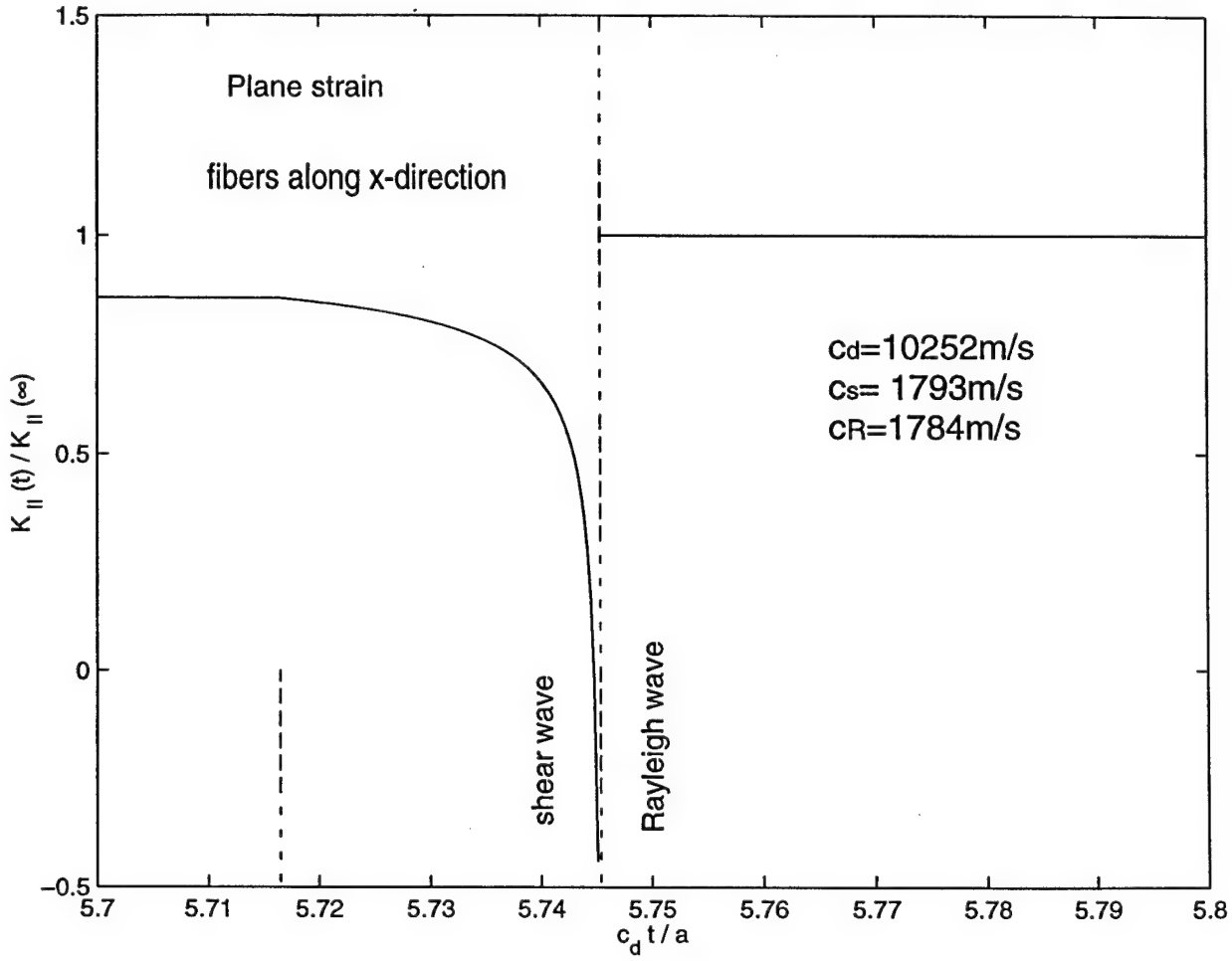

Figure 8(b) Stress intensity factor history in Boron Epoxy under concentrated shear loads

Chapter 5

The Dynamic Stress Intensity Factor and Strain Energy Release Rate for a Semi-infinite Crack in Rotated Transversely Isotropic Materials due to Uniform Impact Loading

co-authored with C.Y. Wang and submitted to International Journal of Fracture

The transient elastodynamic response of a rotated transversely isotropic material under uniform normal impact loading on the faces of a semi-infinite crack is examined. Three loading modes are considered, i.e., opening, in-plane shear and anti-plane shear. Their solutions for the stress intensity factor history around the crack tip are respectively found. Laplace and Fourier transforms together along with the Wiener-Hopf technique are employed to solve the equations of motion. The analyzed asymptotic expression of stress near the crack tip leads to a closed-form solution of the dynamic stress intensity factor for each loading mode. It is found that the stress intensity factors are proportional to the square root of time as in the isotropic case. Results for rotated transversely isotropic materials converge to known solutions for un-rotated orthotropic materials, un-rotated transversely isotropic materials and isotropic materials as special cases. For shear loading on a penny crack in a transversely isotropic material, the analysis is used to find approximate strain energy release rates.

1. Introduction

There are many closed-form solutions for stationary and propagating cracks in isotropic materials under dynamic loading [1, 2]. The stationary semi-infinite crack under uniform step loading in the crack faces was first considered by Maue [3]. The equivalent propagating case was studied by Baker [4]. Many solutions for various loadings of cracks in orthotropic materials have been found by applying transforms to the displacement formulation of the equations of motion. Previous researchers [5, 6] following this approach had solved the resulting dual integral equations using the method of Sneddon [7, 8]. For a semi-infinite crack under concentrated or uniform loads in orthotropic materials, Rubio-Gonzalez, Mason and Wang [9, 10 and 11] solve the same equations by converting the dual integral equations to a Wiener-Hopf equation. Solution of that equation requires only a straightforward application of the method of Noble [12]. The Wiener-Hopf technique was used to solve the equation, find the stress ahead of the crack tip and find the displacement on the crack faces. The asymptotic expression of stress near the crack tip leads to the stress intensity factor $K(t)$.

The growing use of composites in many engineering applications demands a fundamental understanding of the response of cracked orthotropic bodies to impact loading. In this paper, the problem of uniform normal impact loading on the faces of a semi-infinite crack in a rotated transversely isotropic material is analyzed using the same method as [9, 10, and 11]. While it has been thought that the Wiener-Hopf technique could not be applied to problems such as this [1, 13], the approach has recently been shown to be valid in such cases. Through Laplace and Fourier transforms combined with the Wiener-Hopf technique, a closed-form solution for the stress ahead of the crack tip is sought. The asymptotic expression of stress near the crack tip leads to the stress intensity factor $K(t)$.

The analysis is motivated by investigations of dynamically loaded penny shape cracks in orthotropic (or composite) materials. Because of the orientation of the composite fibers, or principle axes of the orthotropic material, the penny shaped crack problem is not axisymmetric and can not be solved using an axisymmetric approach. As an approximation, in this work, attention is focused on regions very near the crack front where a plane strain approach becomes an accurate approximation. There, the problem can be reduced to that of a semi-infinite crack in a rotated orthotropic material for short times. This is only approximate because the effects of waves generated at other points on the crack front are neglected. Thus the exact solutions presented here for semi-infinite cracks offer only an approximate solution for the penny shaped crack. The solution is useful, however, in developing intuition about the most probable location of crack initiation for the penny shaped crack and, consequently, can give qualitative predictions of the final shape of the crack after finite duration loading.

2 Equations of motion

The quasi-three-dimensional problem of an infinite transversely isotropic body with a semi-infinite crack is considered in Figure 1. The body is initially stress free and at rest. A Cartesian (x_1, x_2, x_3) coordinate system is chosen to coincide with the principle axes of material. The transversely isotropic material has a symmetry plane on $x_3 = 0$ and an axis of symmetry along x_3. Another right-handed rectangular (*x, y, z*) coordinate system is introduced in the body, oriented so that the *z*-axis coincides with the crack edge. The *y*-axis is identical with the x_2-axis, consequently, the coordinate system (*x, y, z*) is related to the (x_1, x_2, x_3) coordinate system by a rotation with θ around the x_2-axis. The crack faces are suddenly loaded by uniform traction, as

shown in Figure 1. Let E_i, G_{ij} *and* v_{ij} $(i, j = 1, 2, 3)$ be the engineering elastic constants of the material where in the indices (1, 2, and 3) respectively stands for the directions (x_1, x_2, x_3).

The problem is assumed to be two-dimensional and to include inertial effects. However, because of the constitutive law, the out of plane displacement (in the z-direction) can not be neglected and a coupling exists between in-plane and out-of-plane deformation. Hence, three components (*u, v and w*) of the displacement vector exist in the (*x, y, z*) coordinate system and are independent of *z*, that is,

$$\begin{aligned} u &= u(x, y), \\ v &= v(x, y), \\ w &= w(x, y). \end{aligned} \tag{2.1}$$

In the (x_1, x_2, x_3) coordinate system, the non-dimensional stiffness matrix for the a transversely isotropic material is

$$\mathbf{C} = \begin{bmatrix} c_{11} & c_{12} & c_{13} & 0 & 0 & 0 \\ c_{12} & c_{11} & c_{13} & 0 & 0 & 0 \\ c_{13} & c_{13} & c_{33} & 0 & 0 & 0 \\ 0 & 0 & 0 & c_{55} & 0 & 0 \\ 0 & 0 & 0 & 0 & c_{55} & 0 \\ 0 & 0 & 0 & 0 & 0 & \dfrac{c_{11} - c_{12}}{2} \end{bmatrix} \tag{2.2}$$

where **C** has only five independent constants. The non-dimensional parameters c_{ij} have the following relations with the engineering elastic constants for plane strain conditions

$$c_{11} = \frac{E_1(1 - \nu_{13}\nu_{31})}{G_{12}(1 + \nu_{12})\Delta},\ c_{33} = \frac{E_3(1 - \nu_{12})}{G_{12}\Delta},\ c_{12} = \frac{E_1(\nu_{12} + \nu_{13}\nu_{31})}{G_{12}(1 + \nu_{12})\Delta},\ c_{13} = \frac{E_1\nu_{13}}{G_{12}\Delta},$$

$$c_{55} = \frac{G_{13}}{G_{12}},\ \Delta = (1 - \nu_{12} - 2\nu_{13}\nu_{31}),\ G_{12} = \frac{E_1}{2(1 + \nu_{12})},\ \frac{\nu_{13}}{E_3} = \frac{\nu_{31}}{E_1},\ \frac{c_{11} - c_{12}}{2} = 1. \tag{2.3}$$

Next, by a coordinate transformation involving a rotation about x_2, the non-dimensional stiffness matrix **C** in the (x_1, x_2, x_3) coordinate system is changed to a new non-dimensional stiffness matrix **D** in the (x, y, z) coordinate system [14],

$$\mathbf{D}=\begin{bmatrix} d_{11} & d_{12} & d_{13} & 0 & d_{15} & 0 \\ d_{12} & d_{22} & d_{23} & 0 & d_{25} & 0 \\ d_{13} & d_{23} & d_{33} & 0 & d_{35} & 0 \\ 0 & 0 & 0 & d_{44} & 0 & d_{46} \\ d_{15} & d_{25} & d_{35} & 0 & d_{55} & 0 \\ 0 & 0 & 0 & d_{46} & 0 & d_{66} \end{bmatrix} \tag{2.4}$$

where the thirteen different constants in **D** are given as

$$d_{11} = c_{11}\cos^4\theta + 2(c_{13} + 2c_{55})\cos^2\theta\sin^2\theta + c_{33}\sin^4\theta,$$

$$d_{12} = c_{12}\cos^2\theta + c_{13}\sin^2\theta,$$

$$d_{13} = c_{13}\cos^4\theta + (c_{11} + c_{33} - 4c_{55})\cos^2\theta\sin^2\theta + c_{13}\sin^4\theta,$$

$$d_{15} = (c_{11} - c_{13} - 2c_{55})\cos^3\theta\sin\theta + (c_{13} - c_{33} + 2c_{55})\cos\theta\sin^3\theta,$$

$$d_{22} = c_{11},$$

$$d_{23} = c_{12}\sin^2\theta + c_{13}\cos^2\theta,$$

$$d_{25} = (c_{12} - c_{13})\sin\theta\cos\theta,$$

$$d_{33} = c_{11}\sin^4\theta + 2(c_{13} + 2c_{55})\cos^2\theta\sin^2\theta + c_{33}\cos^4\theta,$$

$$d_{35} = (c_{13} - c_{33} + 2c_{55})\cos^3\theta\sin\theta + (c_{11} - c_{13} - 2c_{55})\cos\theta\sin^3\theta,$$

$$d_{44} = \frac{1}{2}(c_{11} - c_{12})\sin^2\theta + c_{55}\cos^2\theta,$$

$$d_{46} = \frac{1}{2}(c_{11} - c_{12} - 2c_{55})\cos\theta\sin\theta,$$

$$d_{55} = c_{55}\cos^4\theta + (c_{11} - 2c_{13} + c_{33} - 2c_{55})\cos^2\theta\sin^2\theta + c_{55}\sin^4\theta,$$

$$d_{66} = \frac{1}{2}(c_{11} - c_{12})\cos^2\theta + c_{55}\sin^2\theta,$$

Note that for the case $\theta = 0$ the material is isotropic in the plane,

$$\begin{aligned} &d_{11} = c_{11}, d_{12} = c_{12}, d_{13} = c_{13}, d_{15} = 0, d_{22} = c_{11}, d_{23} = c_{13}, d_{25} = 0, \\ &d_{33} = c_{33}, d_{35} = 0, d_{44} = c_{55}, d_{46} = 0, d_{55} = c_{55}, d_{66} = (c_{11} - c_{12})/2. \end{aligned} \tag{2.5}$$

For $\theta = 90^\circ$ the material is orthotropic in the plane,

$$\begin{aligned} &d_{11} = c_{33}, d_{12} = c_{13}, d_{13} = c_{13}, d_{15} = 0, d_{22} = c_{11}, d_{23} = c_{12}, d_{25} = 0, \\ &d_{33} = c_{11}, d_{35} = 0, d_{44} = (c_{11} - c_{12})/2, d_{46} = 0, d_{55} = c_{55}, d_{66} = c_{55}. \end{aligned} \tag{2.6}$$

Due to the two-dimensional assumption, equation (2.1), all the derivatives with respect to z are zero. Thus, in the (*x, y, z*) coordinate system the equations of motion [16] become

$$\begin{aligned} &d_{11}\frac{\partial^2 u}{\partial x^2} + d_{66}\frac{\partial^2 u}{\partial y^2} + (d_{66} + d_{12})\frac{\partial^2 v}{\partial x \partial y} + d_{15}\frac{\partial^2 w}{\partial x^2} + d_{46}\frac{\partial^2 w}{\partial y^2} = \frac{\partial^2 u}{c_s{}^2 \partial t^2}, \\ &(d_{66} + d_{12})\frac{\partial^2 u}{\partial x \partial y} + d_{66}\frac{\partial^2 v}{\partial x^2} + d_{22}\frac{\partial^2 v}{\partial y^2} + (d_{46} + d_{25})\frac{\partial^2 w}{\partial x \partial y} = \frac{\partial^2 v}{c_s{}^2 \partial t^2}, \\ &d_{15}\frac{\partial^2 u}{\partial x^2} + d_{46}\frac{\partial^2 u}{\partial y^2} + (d_{46} + d_{25})\frac{\partial^2 v}{\partial x \partial y} + d_{55}\frac{\partial^2 w}{\partial x^2} + d_{44}\frac{\partial^2 w}{\partial y^2} = \frac{\partial^2 w}{c_s{}^2 \partial t^2}. \end{aligned} \tag{2.7}$$

where u, v and w are the *x, y and z* components of the displacement vector. In the rotated transversely isotropic solids shown in Figure 1, $c_s = \sqrt{G_{12}/\rho}$ represents the velocity of the shear wave propagating in x_1x_2-plane ($c_d = \sqrt{c_{11}}c_s$ is the velocity of the dilatational wave propagating along x_2-direction in x_1x_2-plane which will be used later) and ρ is the mass density. When $\theta = 0$ or $\theta = 90^\circ$, $d_{15} = d_{25} = d_{46} = 0$ and the third equation becomes uncoupled from the first two equations, when $0<\theta<90^\circ$, this coupled system is required.

Finally, the stresses are related to the displacements by the equations,

$$
\begin{aligned}
\frac{\tau_{xy}}{G_{12}} &= d_{46}\frac{\partial w}{\partial y} + d_{66}\left(\frac{\partial u}{\partial y} + \frac{\partial v}{\partial x}\right), \\
\frac{\tau_{yz}}{G_{12}} &= d_{44}\frac{\partial w}{\partial y} + d_{46}\left(\frac{\partial u}{\partial y} + \frac{\partial v}{\partial x}\right), \\
\frac{\sigma_{y}}{G_{12}} &= d_{12}\frac{\partial u}{\partial x} + d_{22}\frac{\partial v}{\partial y} + d_{25}\frac{\partial w}{\partial x}, \\
\frac{\sigma_{x}}{G_{12}} &= d_{11}\frac{\partial u}{\partial x} + d_{12}\frac{\partial v}{\partial y} + d_{15}\frac{\partial w}{\partial x}, \\
\frac{\sigma_{z}}{G_{12}} &= d_{13}\frac{\partial u}{\partial x} + d_{23}\frac{\partial v}{\partial y} + d_{35}\frac{\partial w}{\partial x}, \\
\frac{\tau_{xz}}{G_{12}} &= d_{15}\frac{\partial u}{\partial x} + d_{25}\frac{\partial v}{\partial y} + d_{55}\frac{\partial w}{\partial x}.
\end{aligned}
\qquad (2.8)
$$

3 Normal Impact

For the loading shown Figure 1, the spatially uniform normal traction with magnitude σ_0 is suddenly applied on the crack faces. Exploiting symmetry and limiting ourselves to upper half-plane, $y>0$, the corresponding boundary conditions are

$$
\begin{aligned}
&\sigma_y(x,0,t) = -\sigma_0 H(t), && -\infty < x < 0, \\
&\tau_{xy}(x,0,t) = 0 && -\infty < x < +\infty, \\
&\tau_{yz}(x,0,t) = 0 && -\infty < x < +\infty, \\
&v(x,0,t) = 0, && 0 < x < +\infty,
\end{aligned}
\qquad (3.1)
$$

where H(t) is the unit step function.

The displacement at infinity is zero, and the body is stress free and at rest everywhere for $t \le 0$.

3.1 Laplace transform

In equations (8), the time variable may be removed by application of the Laplace transform

$$f^*(s)=\int_0^\infty f(t)\,e^{-st}dt,\quad f(\mathrm{t})=\frac{1}{2\pi i}\int_{\mathrm{Br}} f^*(s)\,e^{st}ds=\frac{1}{2\pi i}\int_{\sigma-i\infty}^{\sigma+i\infty} f^*(s)\,e^{st}ds, \tag{3.1.1}$$

where Br denotes the Bromwich path of integration which is a line parallel to the imaginary axis in the s-plane. Thus, using the Laplace transform representation, the displacements have the form

$$\begin{aligned}
\mathrm{u}(x,\,y,\,t)&=\frac{1}{2\pi i}\int_{\mathrm{Br}}\mathrm{u}^*(x,\,y,\,s)\,e^{st}ds,\\
\mathrm{v}(x,\,y,\,t)&=\frac{1}{2\pi i}\int_{\mathrm{Br}}\mathrm{v}^*(x,\,y,\,s)\,e^{st}ds,\\
\mathrm{w}(x,\,y,\,t)&=\frac{1}{2\pi i}\int_{\mathrm{Br}}\mathrm{w}^*(x,\,y,\,s)\,e^{st}ds.
\end{aligned} \tag{3.1.2}$$

Applying the relations (3.1.2) to equations (2.7) and assuming zero initial condition, the transformed domain equations become

$$\begin{aligned}
&d_{11}\frac{\partial^2\mathrm{u}^*}{\partial x^2}+d_{66}\frac{\partial^2\mathrm{u}^*}{\partial\,y^2}+(d_{66}+d_{12})\frac{\partial^2\mathrm{v}^*}{\partial x\partial y}+d_{15}\frac{\partial^2\mathrm{w}^*}{\partial x^2}+d_{46}\frac{\partial^2\mathrm{w}^*}{\partial y^2}-\frac{s^2\mathrm{u}^*}{c_s{}^2}=0,\\
&(d_{66}+d_{12})\frac{\partial^2\mathrm{u}^*}{\partial x\partial y}+d_{66}\frac{\partial^2\mathrm{v}^*}{\partial\,\mathrm{x}^2}+d_{22}\frac{\partial^2\mathrm{v}^*}{\partial y^2}+(d_{46}+d_{25})\frac{\partial^2\mathrm{w}^*}{\partial x\partial y}-\frac{s^2\mathrm{v}^*}{c_s{}^2}=0,\\
&d_{15}\frac{\partial^2\mathrm{u}^*}{\partial x^2}+d_{46}\frac{\partial^2\mathrm{u}^*}{\partial\,\mathrm{y}^2}+(d_{46}+d_{25})\frac{\partial^2\mathrm{v}^*}{\partial x\partial y}+d_{55}\frac{\partial^2\mathrm{w}^*}{\partial x^2}+d_{44}\frac{\partial^2\mathrm{w}^*}{\partial y^2}-\frac{s^2\mathrm{w}^*}{c_s{}^2}=0.
\end{aligned} \tag{3.1.3}$$

Applying the relations (3.1.2) to equations (2.8), the transformed relations between stresses and displacements become

$$
\begin{aligned}
\frac{\tau_{xy}^{*}}{G_{12}} &= d_{46}\frac{\partial w^{*}}{\partial y} + d_{66}\left(\frac{\partial u^{*}}{\partial y} + \frac{\partial v^{*}}{\partial x}\right), \\
\frac{\tau_{yz}^{*}}{G_{12}} &= d_{44}\frac{\partial w^{*}}{\partial y} + d_{46}\left(\frac{\partial u^{*}}{\partial y} + \frac{\partial v^{*}}{\partial x}\right), \\
\frac{\sigma_{y}^{*}}{G_{12}} &= d_{12}\frac{\partial u^{*}}{\partial x} + d_{22}\frac{\partial v^{*}}{\partial y} + d_{25}\frac{\partial w^{*}}{\partial x}, \\
\frac{\sigma_{x}^{*}}{G_{12}} &= d_{11}\frac{\partial u^{*}}{\partial x} + d_{12}\frac{\partial v^{*}}{\partial y} + d_{15}\frac{\partial w^{*}}{\partial x}, \\
\frac{\sigma_{z}^{*}}{G_{12}} &= d_{13}\frac{\partial u^{*}}{\partial x} + d_{23}\frac{\partial v^{*}}{\partial y} + d_{35}\frac{\partial w^{*}}{\partial x}, \\
\frac{\tau_{xz}^{*}}{G_{12}} &= d_{15}\frac{\partial u^{*}}{\partial x} + d_{25}\frac{\partial v^{*}}{\partial y} + d_{55}\frac{\partial w^{*}}{\partial x}.
\end{aligned}
\qquad (3.1.4)
$$

The application of the Laplace transform to the boundary conditions (3.1) gives,

$$
\begin{aligned}
&\sigma_{y}^{*}(x, 0, t) = -\sigma_{0}/s, && -\infty<x<0, \\
&\tau_{xy}^{*}(x, 0, t) = 0, && -\infty<x<+\infty, \\
&\tau_{yz}^{*}(x, 0, t) = 0, && -\infty<x<+\infty, \\
&v^{*}(x, 0, t) = 0, && 0<x<+\infty.
\end{aligned}
\qquad (3.1.5)
$$

3.2 Fourier transform

To obtain a solution of the differential equations (3.1.3) subject to conditions (3.1.5), the Fourier transform is applied,

$$
\tilde{f}(\omega) = \int_{-\infty}^{\infty} f(x)\, e^{i\omega x} dx, \qquad f(x) = \frac{1}{2\pi}\int_{-\infty}^{\infty} \tilde{f}(\omega)\, e^{-i\omega x} d\omega \qquad (3.2.1)
$$

It is noted that the boundary conditions (3.1.5) are defined only on half of the range of x. Consequently, the Fourier transform can not be applied to these boundary conditions. To remedy this situation, the boundary conditions are extended to apply on the full range of x. Two-unknown functions $v_{-}^{*}(x,s)$ and $\sigma_{+}^{*}(x,s)$ are introduced. The function $v_{-}^{*}(x,s)$ is defined to

be the y-direction displacement of the crack face, y=0, for $-\infty < x < 0$ and $0 < t < \infty$, and to be identically zero for $0 < x < +\infty$ and $0 < t < \infty$. Likewise, the function $\sigma_+^*(x,s)$ is defined to be the shear stress in the x-direction on the plane, y=0, for $0 < x < \infty$ and $0 < t < \infty$, and to be identically zero for $-\infty < x < 0$ and $0 < t < \infty$. With these definitions, the boundary conditions (3.1.5) can be rewritten as

$$\begin{aligned}
&\sigma_y^*(x,\,0\,,\,s) = -\frac{\sigma_0}{s} H(-x) + \sigma_+^*(x,s)\,, && -\infty < x < +\infty,\\
&\tau_{xy}^*(x,\,0,\,s) = 0\,, && -\infty < x < +\infty\,,\\
&\tau_{yz}^*(x,\,0,\,s) = 0\,, && -\infty < x < +\infty\,,\\
&v^*(x,\,0,\,s) = v_-^*(x,s)\,, && -\infty < x < +\infty\,.
\end{aligned} \qquad (3.2.2)$$

Thus, the Laplace transformed displacements have the form

$$\begin{aligned}
u^*(x,\,y,\,s) &= \frac{1}{2\pi}\int_{-\infty}^{\infty} \tilde{u}^*(\omega,\,y,\,s)\, e^{-i\omega x} d\omega\,,\\
v^*(x,\,y,\,s) &= \frac{1}{2\pi}\int_{-\infty}^{\infty} \tilde{v}^*(\omega,\,y,\,s)\, e^{-i\omega x} d\omega\,,\\
w^*(x,\,y,\,s) &= \frac{1}{2\pi}\int_{-\infty}^{\infty} \tilde{w}^*(\omega,\,y,\,s)\, e^{-i\omega x} d\omega\,.
\end{aligned} \qquad (3.2.3)$$

Substituting these transforms into equations (3.1.3), the function $\tilde{u}^*$, $\tilde{v}^*$ and $\tilde{w}^*$ are found to satisfy the ordinary differential equations

$$\begin{aligned}
&-(d_{11}\omega^2 + s^2/c_s^{\,2})\tilde{u}^* + d_{66}\frac{\partial^2 \tilde{u}^*}{\partial y^2} - (d_{66}+d_{12})\omega i\frac{\partial \tilde{v}^*}{\partial y} - d_{15}\omega^2 \tilde{w}^* + d_{46}\frac{\partial^2 \tilde{w}^*}{\partial y^2} = 0\,,\\
&-(d_{66}+d_{12})\omega i\frac{\partial \tilde{u}^*}{\partial y} - (d_{66}\omega^2 + s^2/c_s^{\,2})\tilde{v}^* + d_{22}\frac{\partial^2 \tilde{v}^*}{\partial y^2} - (d_{46}+d_{25})\omega i\frac{\partial \tilde{w}^*}{\partial y} = 0\,,\\
&-d_{15}\omega^2 \tilde{u}^* + d_{46}\frac{\partial^2 \tilde{u}^*}{\partial y^2} - (d_{46}+d_{25})\omega i\frac{\partial \tilde{v}^*}{\partial y} - (d_{55}\omega^2 + s^2/c_s^{\,2})\tilde{w}^* + d_{44}\frac{\partial^2 \tilde{w}^*}{\partial y^2} = 0\,.
\end{aligned} \qquad (3.2.4)$$

This system of equations can be rewritten as

$$\begin{pmatrix} d_{66} & 0 & d_{46} \\ 0 & d_{22} & 0 \\ d_{46} & 0 & d_{44} \end{pmatrix} \frac{\partial^2 \tilde{\mathbf{U}}^*}{\partial y^2} + \begin{pmatrix} 0 & -(d_{66}+d_{12})\omega i & 0 \\ -(d_{66}+d_{12})\omega i & 0 & -(d_{46}+d_{25})\omega i \\ 0 & -(d_{46}+d_{25})\omega i & 0 \end{pmatrix} \frac{\partial \tilde{\mathbf{U}}^*}{\partial y} + \begin{pmatrix} -d_{11}\omega^2 - s^2/c_s^2 & 0 & -d_{15}\omega^2 \\ 0 & -d_{66}\omega^2 - s^2/c_s^2 & 0 \\ -d_{15}\omega^2 & 0 & -d_{55}\omega^2 - s^2/c_s^2 \end{pmatrix} \tilde{\mathbf{U}}^* = 0, \tag{3.2.5}$$

where $\tilde{\mathbf{U}}^* = (\tilde{u}^*, \tilde{v}^*, \tilde{w}^*)^T$. This is a second order system of ordinary differential equations with constant coefficients having solutions of the form

$$\tilde{\mathbf{U}}^* = \mathbf{A}(\omega, s)e^{-\gamma y}, \qquad \gamma > 0. \tag{3.2.6}$$

where $\mathbf{A}(\omega, s) = (A_1, A_2, A_3)^T$

The solution of equation (3.2.6) under the condition of zero displacement at infinity is

$$\begin{aligned} \tilde{\mathrm{u}}^*(\omega, y, s) &= \sum_{i=1}^{3} A_i(\omega, s)e^{-\gamma_i y}, \\ \tilde{\mathrm{v}}^*(\omega, y, s) &= \sum_{i=1}^{3} i\omega\gamma_i\alpha_i(\omega, s)A_i(\omega, s)e^{-\gamma_i y}, \\ \tilde{\mathrm{w}}^*(\omega, y, s) &= \sum_{i=1}^{3} \beta_i(\omega, s)A_i(\omega, s)e^{-\gamma_i y}. \end{aligned} \tag{3.2.7}$$

where $A_i(\omega, s)$ is arbitrary function, and $\alpha_i(\omega, s)$, $\beta_i(\omega, s)$ stand for the functions

$$\begin{aligned} \alpha_i(\omega, s) &= \frac{(d_{46}+d_{25})(d_{66}\gamma_i^2 - d_{11}\omega^2 - s^2/c_s^2) - (d_{66}+d_{12})(d_{46}\gamma_i^2 - d_{15}\omega^2)}{(d_{22}\gamma_i^2 - d_{66}\omega^2 - s^2/c_s^2)(d_{46}\gamma_i^2 - d_{15}\omega^2) + (d_{66}+d_{12})(d_{46}+d_{25})\omega^2\gamma_i^2}, \\ \beta_i(\omega, s) &= -\frac{(d_{66}+d_{12})^2\omega^2\gamma_i^2 + (d_{22}\gamma_i^2 - d_{66}\omega^2 - s^2/c_s^2)(d_{66}\gamma_i^2 - d_{11}\omega^2 - s^2/c_s^2)}{(d_{22}\gamma_i^2 - d_{66}\omega^2 - s^2/c_s^2)(d_{46}\gamma_i^2 - d_{15}\omega^2) + (d_{66}+d_{12})(d_{46}+d_{25})\omega^2\gamma_i^2}, \end{aligned} \tag{3.2.8}$$

with γ_1^2 , γ_2^2 and γ_3^2 being the eigenvalues of the sixth order equation

$$\det \begin{vmatrix} d_{66}\gamma^2 - d_{11}\omega^2 - s^2/c_s^2 & (d_{66}+d_{12})\omega i\gamma & d_{46}\gamma^2 - d_{15}\omega^2 \\ (d_{66}+d_{12})\omega i\gamma & d_{22}\gamma^2 - d_{66}\omega^2 - s^2/c_s^2 & (d_{46}+d_{25})\omega i\gamma \\ d_{46}\gamma^2 - d_{15}\omega^2 & (d_{46}+d_{25})\omega i\gamma & d_{44}\gamma^2 - d_{55}\omega^2 - s^2/c_s^2 \end{vmatrix} = 0. \tag{3.2.9}$$

This determinant is further expanded as

$$\gamma^6 + \frac{b}{a}\gamma^4 + \frac{c}{a}\gamma^2 + \frac{d}{a} = 0 \qquad (3.2.10)$$

where

$$a = d_{22}(d_{46}{}^2 - d_{66}d_{44}),$$

$$b = (d_{22}d_{44} - d_{46}{}^2 + d_{22}d_{66} + d_{44}d_{66})s^2/c_s{}^2 + (-d_{12}{}^2d_{44} + d_{11}d_{22}d_{44} - 2d_{15}d_{22}d_{46} + 2d_{12}d_{25}d_{46} + 2d_{12}d_{46}{}^2 - d_{25}{}^2d_{66} - 2d_{12}d_{44}d_{66} + d_{22}d_{55}d_{66})\omega^2,$$

$$c = -[(d_{22} + d_{44} + d_{66})s^4/c_s{}^4 + (-d_{12}{}^2 + d_{11}d_{22} - d_{25}{}^2 + d_{11}d_{44} - 2d_{15}d_{46} - 2d_{25}d_{46} - d_{46}{}^2 + d_{22}d_{55} - 2d_{12}d_{66} + d_{44}d_{66} + d_{55}d_{66})\omega^2 s^2/c_s{}^2 + (-d_{15}{}^2d_{22} + 2d_{12}d_{15}d_{25} - d_{11}d_{25}{}^2 + 2d_{12}d_{15}d_{46} - 2d_{11}d_{25}d_{46} - d_{11}d_{46}{}^2 - d_{12}{}^2d_{55} + d_{11}d_{22}d_{55} + 2d_{15}d_{25}d_{66} + d_{11}d_{44}d_{66} - 2d_{12}d_{55}d_{66})\omega^4],$$

$$d = (d_{66}\omega^2 + s^2/c_s{}^2)[s^4/c_s{}^4 + (d_{11} + d_{55})\omega^2 s^2/c_s{}^2 + (d_{11}d_{55} - d_{15}{}^2)\omega^4],$$

From (3.2.10), it is readily found that the functions $\gamma_1(\omega)$, $\gamma_2(\omega)$ and $\gamma_3(\omega)$ are multiple valued functions of ω in the complex ω-plane with branch point at $\omega = \pm is/\kappa_{s1}$, $\omega = \pm is/\kappa_{s2}$ and $\omega = \pm is/\kappa_d$, respectively, which are the roots of the equation given by $d=0$, i.e.

$$(d_{66}\omega^2 + s^2/c_s{}^2)[s^4/c_s{}^4 + (d_{11} + d_{55})\omega^2 s^2/c_s + (d_{11}d_{55} - d_{15}{}^2)\omega^4] = 0, \qquad (3.2.11)$$

so $\kappa_{s1} = \sqrt{d_1}c_{s1}$, $\kappa_{s2} = \sqrt{d_{66}}c_{s1}$, and $\kappa_d = \sqrt{d_2}c_{s1}$,

where

$$d_1 = \frac{2(d_{11}d_{55} - d_{15}{}^2)}{d_{11} + d_{55} + \sqrt{d_{11}{}^2 + 4d_{15}{}^2 - 2d_{11}d_{55} + d_{55}{}^2}},$$

$$d_2 = \frac{2(d_{11}d_{55} - d_{15}{}^2)}{d_{11} + d_{55} - \sqrt{d_{11}{}^2 + 4d_{15}{}^2 - 2d_{11}d_{55} + d_{55}{}^2}}.$$

Note that for the case $\theta = 0$, $\kappa_{s1}{}^0 = \sqrt{c_{55}}c_s$, $\kappa_{s2}{}^0 = \sqrt{\frac{c_{11} - c_{12}}{2}}c_s = c_s$ and $\kappa_d{}^0 = \sqrt{c_{11}}c_s$. The parameters, $\kappa_{s1}{}^0$, $\kappa_{s2}{}^0$ and $\kappa_d{}^0$, are the shear wave speed in x_2x_3-plane, the shear wave speed in

x_1x_2-plane and the dilatational wave speed along x_2-direction in x_1x_2-plane, respectively; for the case $\theta = 90^\circ$, $\kappa_{s1}^{90} = \sqrt{c_{55}}c_s$, $\kappa_{s2}^{90} = \sqrt{c_{55}}c_s$ and $\kappa_d^{90} = \sqrt{c_{33}}c_s$.

Later we will be interested in the behavior of these functions for $\omega \to \infty$. In this case, $\gamma_i^2 \to \omega^2 N_i^2$ $(i = 1, 2, 3)$, where N_i^2 are the roots of the following equation

$$N^6 + \frac{\hat{b}}{a}N^4 + \frac{\hat{c}}{a}N^2 + \frac{\hat{d}}{a} = 0 \tag{3.2.12}$$

where

$$a = d_{22}(d_{46}^2 - d_{66}d_{44}),$$

$$\hat{b} = -d_{12}^2 d_{44} + d_{11}d_{22}d_{44} - 2d_{15}d_{22}d_{46} + 2d_{12}d_{25}d_{46} + 2d_{12}d_{46}^2 - d_{25}^2 d_{66} - 2d_{12}d_{44}d_{66} + d_{22}d_{55}d_{66},$$

$$\hat{c} = -(-d_{15}^2 d_{22} + 2d_{12}d_{15}d_{25} - d_{11}d_{25}^2 + 2d_{12}d_{15}d_{46} - 2d_{11}d_{25}d_{46} - d_{11}d_{46}^2 - d_{12}^2 d_{55} + d_{11}d_{22}d_{55} + 2d_{15}d_{25}d_{66} + d_{11}d_{44}d_{66} - 2d_{12}d_{55}d_{66}),$$

$$\hat{d} = d_{66}(d_{11}d_{55} - d_{15}^2),$$

Similarly, as $\omega \to \infty$, $\alpha_i(\omega, s)$ and $\beta_i(\omega, s)$ become

$$\begin{aligned}
\alpha_i(\omega, s) \to \alpha_i^\infty &= \frac{(d_{46} + d_{25})(d_{66}N_i^2 - d_{11}) - (d_{66} + d_{12})(d_{46}N_i^2 - d_{15})}{(d_{22}N_i^2 - d_{66})(d_{46}N_i^2 - d_{15}) + (d_{66} + d_{12})(d_{46} + d_{25})N_i^2} \frac{1}{\omega^2}, \\
\beta_i(\omega, s) \to \beta_i^\infty &= -\frac{(d_{66} + d_{12})^2 N_i^2 + (d_{66}N_i^2 - d_{11})(d_{22}N_i^2 - d_{66})}{(d_{22}N_i^2 - d_{66})(d_{46}N_i^2 - d_{15}) + (d_{66} + d_{12})(d_{46} + d_{25})N_i^2}.
\end{aligned} \tag{3.2.13}$$

It can be shown that for many materials that the roots of (3.2.10), γ_1, γ_2 and γ_3, are real and positive and the expressions for the displacements in the Laplace transform domain become

$$u^* = \frac{1}{2\pi}\int_{-\infty}^{\infty}(A_1 e^{-\gamma_1 y} + A_2 e^{-\gamma_2 y} + A_3 e^{-\gamma_3 y})e^{-i\omega x}d\omega,$$

$$v^* = \frac{i\omega}{2\pi}\int_{-\infty}^{\infty}(\gamma_1\alpha_1 A_1 e^{-\gamma_1 y} + \gamma_2\alpha_2 A_2 e^{-\gamma_2 y} + \gamma_3\alpha_3 A_3 e^{-\gamma_3 y})e^{-i\omega x}d\omega, \qquad (3.2.14)$$

$$w^* = \frac{1}{2\pi}\int_{-\infty}^{\infty}(\beta_1 A_1 e^{-\gamma_1 y} + \beta_2 A_2 e^{-\gamma_2 y} + \beta_3 A_3 e^{-\gamma_3 y})e^{-i\omega x}d\omega.$$

Substituting these expressions for displacements, (3.2.14), into the constitutive law, (3.1.4), we have

$$\frac{\tau_{yz}^*}{G_{12}} = -\frac{1}{2\pi}\int_{-\infty}^{\infty}(m_1 A_1 e^{-\gamma_1 y} + m_2 A_2 e^{-\gamma_2 y} + m_3 A_3 e^{-\gamma_3 y})\, e^{-i\omega x}d\omega,$$

$$\frac{\tau_{xy}^*}{G_{12}} = -\frac{1}{2\pi}\int_{-\infty}^{\infty}(n_1 A_1 e^{-\gamma_1 y} + n_2 A_2 e^{-\gamma_2 y} + n_3 A_3 e^{-\gamma_3 y})\, e^{-i\omega x}d\omega, \qquad (3.2.15)$$

$$\frac{\sigma_y^*}{G_{12}} = -\frac{i\omega}{2\pi}\int_{-\infty}^{\infty}(k_1 A_1 e^{-\gamma_1 y} + k_2 A_2 e^{-\gamma_2 y} + k_3 A_3 e^{-\gamma_3 y})\, e^{-i\omega x}d\omega,$$

where

$$m_i = (d_{46} - d_{46}\omega^2\alpha_i + d_{44}\beta_i)\gamma_i,$$

$$n_i = (d_{66} - d_{66}\omega^2\alpha_i + d_{46}\beta_i)\gamma_i,$$

$$k_i = d_{12} + d_{22}\gamma_i^2\alpha_i + d_{25}\beta_i.$$

Substitution of expression for τ_{xy}^*, τ_{yz}^*, the first and second of equations (3.2.15), into the boundary condition for τ_{xy}^*, τ_{yz}^*, the second and third of equations (3.1.5), yields

$$\begin{aligned} &m_1 A_1 + m_2 A_2 + m_3 A_3 = 0, \\ &n_1 A_1 + n_2 A_2 + n_3 A_3 = 0. \end{aligned} \qquad (3.2.16)$$

These equations can be rewritten as

$$\begin{aligned} &A_2 = \lambda_1(\omega, s)A_1,\ A_3 = \lambda_2(\omega, s)A_1, \\ &\lambda_1(\omega, s) = \frac{m_1 n_3 - m_3 n_1}{m_3 n_2 - m_2 n_3},\ \lambda_2(\omega, s) = -\frac{m_1 n_2 - m_2 n_1}{m_3 n_2 - m_2 n_3}. \end{aligned} \qquad (3.2.17)$$

As $\omega \to \infty$, we have

$$\lambda_1(\omega,s)\to\lambda_1^{\infty}=\frac{m_1^{\infty}n_3^{\infty}-m_3^{\infty}n_1^{\infty}}{m_3^{\infty}n_2^{\infty}-m_2^{\infty}n_3^{\infty}},\quad \lambda_2(\omega,s)\to\lambda_2^{\infty}=-\frac{m_1^{\infty}n_2^{\infty}-m_2^{\infty}n_1^{\infty}}{m_3^{\infty}n_2^{\infty}-m_2^{\infty}n_3^{\infty}} \tag{3.2.18}$$

where $m_i(\omega,s)\to\omega m_i^{\infty}$ and $n_i(\omega,s)\to\omega n_i^{\infty}$ *as* $\omega\to\infty$.

Using this result in the expression for normal stress, the third of equation (3.2.15), the expression for vertical displacement, the second of equations (3.2.14), and the remaining boundary conditions, we obtain

$$\begin{aligned}
&-\frac{G_{12}}{2\pi}\int_{-\infty}^{\infty}(k_1+\lambda_1k_2+\lambda_2k_3)\omega A_1 i\,e^{-i\omega x}d\omega=-\sigma_0/s\,\mathrm{H}(-x)+\sigma_+^{*}(x,s),\\
&\frac{1}{2\pi}\int_{-\infty}^{\infty}(\alpha_1\gamma_1+\alpha_2\gamma_2\lambda_1+\alpha_3\gamma_3\lambda_2)\omega A_1 i e^{-i\omega x}d\omega=\mathrm{v}_-^{*}(x,s).
\end{aligned} \tag{3.2.19}$$

By Fourier transform inversion, these equations become

$$\begin{aligned}
&-\mathrm{G}_{12}(\mathrm{k}_1+\lambda_1\mathrm{k}_2+\lambda_2\mathrm{k}_3)\omega A_1 i=-\sigma_0/i\omega s+\Sigma_+(\omega,s),\\
&(\alpha_1\gamma_1+\alpha_2\gamma_2\lambda_1+\alpha_3\gamma_3\lambda_2)\omega A_1 i=\mathrm{V}_-(\omega,s).
\end{aligned} \tag{3.2.20}$$

where

$$\begin{aligned}
&\Sigma_+(\omega,s)=\int_0^{\infty}\sigma_+^{*}(x,s)e^{i\omega x}dx,\\
&V_-(\omega,s)=\int_{-\infty}^{0}\mathrm{v}_-^{*}(x,s)e^{i\omega x}dx.
\end{aligned} \tag{3.2.21}$$

Eliminating A_1 from equation, (3.2.20), we obtain a Wiener-Hopf equation,

$$G_{12}\chi_1\frac{\mathrm{F}(\omega,\mathrm{s})}{\sqrt{\omega^2+s^2/\kappa_d^{\,2}}}\mathrm{V}_-(\omega,s)=\sigma_0/i\omega s-\Sigma_+(\omega,s), \tag{3.2.22}$$

where the following functions are introduced

$$F(\omega,s)=\frac{\sqrt{\omega^2+s^2/\kappa_d^{\,2}}\,(k_1+\lambda_1k_2+\lambda_2k_3)}{\chi_1(\alpha_1\gamma_1+\alpha_2\gamma_2\lambda_1+\alpha_3\gamma_3\lambda_2)}, \tag{3.2.23}$$

$$\chi_1=\frac{k_1^{\infty}+\lambda_1^{\infty}k_2^{\infty}+\lambda_2^{\infty}k_3^{\infty}}{\alpha_1^{\infty}N_1+\alpha_2^{\infty}N_2\lambda_1^{\infty}+\alpha_3^{\infty}N_3\lambda_2^{\infty}}, \tag{3.2.24}$$

and χ_1 is dependent of θ and the material parameters. Its complete expression is given in the Appendix.

Here, note that the case of $\theta = 0$, $\chi_1^{\,0} = \dfrac{2(c_{11}-1)}{c_{11}}$ (it is a limit value), and $\theta = 90^\circ$,

$$\chi_1^{\,90} = \frac{(c_{11}c_{33} - c_{13}^{\,2})[c_{33} + c_{11}N_1N_2N_3(N_1+N_2+N_3)]}{c_{11}c_{33}(N_1+N_2)(N_3+N_2)(N_3+N_1)}, \tag{3.2.25}$$

where N_i are shown in equation A.5 of the Appendix. $\chi_1^{\,0}$ and $\chi_1^{\,90}$ are the limit values of χ_1 at $\theta = 0$ and $\theta = 90^\circ$, respectively.

For $\omega = 0$, after lengthy algebraic manipulation of equation (3.2.23), we have

$$F(0,s) = \frac{s^2}{\kappa_d \chi_1}\frac{\sqrt{c_{11}}}{c_s} = \frac{s^2}{\kappa_d \chi_1}\frac{c_{11}}{c_d}. \tag{3.2.26}$$

From the physics of the problem, it is reasonable to assume that the function $\sigma_+^{\,*}(x,s)$ and $\mathrm{v}_-^{\,*}(x,s)$ are exponentially bounded at infinity, which ensures the existence of their Fourier transform (3.2.1). In particular, it is shown by Noble [12] that if $\left|\sigma_+^{\,*}(x,s)\right| < M_1 e^{\xi_- x}$ as $x \to +\infty$ then $\Sigma_+(\omega)$ is analytic in $\mathrm{Re}(\omega) = \xi > \xi_-$, and if $\left|\mathrm{v}_-^{\,*}(x,s)\right| < M_2 e^{\xi_+ x}$ as $x \to -\infty$ then $\mathrm{V}_-(\omega)$ is analytic in $\mathrm{Re}(\omega) = \xi < \xi_+$.

This function, $F(\omega,s)$, is analytic everywhere in the complex plane except on at the branch cuts of γ_i at $\omega = \pm i s/\kappa_{s1}$, $\omega = \pm i s/\kappa_{s2}$ and $\omega = \pm i s/\kappa_d$. It is single valued in the ω-plane cut as shown in Figure 2. For general anisotropic materials, the Rayleigh wave equations are given by Nayfeh [15]. We found the algebraic equations, $F(\omega,s)$=0 (letting $\omega = is/v$) and equation (3.2.10) for γ are the same as the Rayleigh wave equations because $F(\omega,s)$=0 is equivalent to $\tau_{yz} = \tau_{xy} = \sigma_y = 0$ which are the necessary boundary conditions used when deriving the

Rayleigh wave equations. The system of Rayleigh wave equations is dependent on the "material properties" referring to the transformed properties through the rotation of the azimuthal angle θ. Therefore, the Rayleigh wave speed c_R is varying with the azimuthal angle θ. In general, finding the critical value of c_R requires numerical calculation because of the complexity of the system of Rayleigh wave equations for general anisotropic materials [16]. It is true, however, that the only zeros of $F(\omega,s)$ are of the form $\pm i\,s/c_R$.

3.3 Wiener-Hopf technique

The Wiener-Hopf technique can be outlined as follows, the function $L(\omega)$ is defined and factored as

$$L(\omega)=\frac{L_-(\omega)}{L_+(\omega)}=G_{12}\chi_1\frac{F(\omega,s)}{\sqrt{\omega^2+s^2/{\kappa_d}^2}}, \tag{3.3.1}$$

thus, the Wiener-Hopf equation, (3.3.1), becomes

$$L_-(\omega)\mathrm{V}_-(\omega)=\frac{\sigma_0}{i\omega s}L_+(\omega)-\Sigma_+(\omega,s)L_+(\omega)\,. \tag{3.3.2}$$

If the function $D(\omega)$ can be decomposed as

$$D(\omega)=\frac{\sigma_0}{i\omega s}L_+(\omega)=\frac{\sigma_0}{s}\left[\frac{L_+(\omega)-L_+(0)}{i\omega}+\frac{L_+(0)}{i\omega}\right]=D_+(\omega)+D_-(\omega)\,, \tag{3.3.3}$$

with

$$D_+(\omega)=\frac{\sigma_0}{s}\left[\frac{L_+(\omega)-L_+(0)}{i\omega}\right],\ D_-(\omega)=\frac{\sigma_0}{s}\left[\frac{L_+(0)}{i\omega}\right],$$

Then the Wiener-Hopf equation, (47), is further reduced to

$$D_+(\omega)-\Sigma_+(\omega)L_+(\omega)=L_-(\omega)\mathrm{V}_-(\omega)-D_-(\omega)=\Omega(\omega)\,. \tag{3.3.4}$$

The first member of (3.3.4) is analytic in the right half plane of $\mathrm{Re}(\omega) > \xi_-$ and the second member in the left half plane $\mathrm{Re}(\omega) < \xi_+$. If $\xi_- > \xi_+$, the regions of analyticity overlap and by invoking analytic continuation, it is concluded that $\Omega(\omega)$ is analytic and single-valued in the whole ω-plane shown in Figure 2. Furthermore, invoking the extended Liouville theorem, it can be shown [12] that if $\Omega(\omega)$ is bounded and entire and $\Omega(\omega) \to 0 \, as \, \omega \to \infty$, then $\Omega(\omega) = 0$. Hence, we can solve for the transform of stress ahead of the crack tip, $\Sigma_+(\omega)$, and displacement, $V_-(\omega)$, behind,

$$\Sigma_+(\omega) = \frac{D_+(\omega)}{L_+(\omega)} = \frac{\sigma_0}{si\omega}\left[1 - \frac{L_+(0)}{L_+(\omega)}\right],$$
$$V_-(\omega) = \frac{D_-(\omega)}{L_-(\omega)} = \frac{\sigma_0}{si\omega}\left[\frac{L_+(0)}{L_-(\omega)}\right]. \qquad (3.3.5)$$

Following this outline, the first step is to factor $L(\omega)$, (3.3.1), by defining

$$\hat{F}(\omega) = \frac{F(\omega, s)}{\omega^2 + s^2/c_R^{\,2}}. \qquad (3.3.6)$$

It can be shown that $\hat{F}(\omega) \to 1$ as $\omega \to \infty$, (the constant χ_1 in (3.2.24) was chosen to make this possible). The function $\hat{F}(\omega)$ is regular and $\hat{F}(\omega) \neq 0$ in the ω-plane cut as shown in Figure 2, the only singularities are the branch points shared with γ_i, $(i = 1, 2)$, i.e. $\omega = \pm is/\kappa_{s1}$, $\omega = \pm is/\kappa_{s2}$ and $\omega = \pm is/\kappa_d$. It is well known that factorization of a function is accomplished most directly for functions that approach unity as $\omega \to \infty$ and that have neither zeros and nor poles in the finite plane. Indeed, $\hat{F}(\omega)$ is an example of such a function. Therefore, using Cauchy integral formula, it can be shown that [1]

$$\hat{F}(\omega) = \hat{F}_+(\omega)\hat{F}_-(\omega)$$
$$\hat{F}_\pm(\omega) = \exp\left\{\frac{1}{2\pi i}\int_{R_\pm} \frac{\log \hat{F}(\omega)}{z-\omega} dz\right\}, \tag{3.3.7}$$

where R_- is the closed counterclockwise contour enclosing the branch points $+is/\kappa_{s1}$, $+is/\kappa_{s2}$ and $+is/\kappa_d$, and also R_+ is the closed counterclockwise contour enclosing the branch points $-is/\kappa_{s1}$, $-is/\kappa_{s2}$ and $-is/\kappa_d$.

Returning to the factorization of $L(\omega)$, we have now

$$L(\omega) = L_+(\omega)L_-(\omega) = G_{12}\chi_1 \frac{\hat{F}_+(\omega)\hat{F}_-(\omega)(\omega+is/c_R)(\omega-is/c_R)}{\sqrt{\omega+is/\kappa_d}\sqrt{\omega-is/\kappa_d}}. \tag{3.3.8}$$

Therefore,

$$L_-(\omega) = G_{12}\chi_1 \frac{(\omega-is/c_R)}{\sqrt{\omega-is/\kappa_d}}\hat{F}_-(\omega),$$
$$L_+(\omega) = \frac{\sqrt{\omega+is/\kappa_d}}{(\omega+is/c_R)\hat{F}_+(\omega)}. \tag{3.3.9}$$

Note that as $\omega \to \infty$, $\hat{F}_+(\omega) \to 1$, $\hat{F}_-(\omega) \to 1$, $L_+(\omega) = \frac{1}{\sqrt{\omega}}$, $L_-(\omega) = G_{12}\chi_1\sqrt{\omega}$ and $L_+(0) = \frac{c_R}{s^{1/2}\kappa_d^{1/2}\hat{F}_+(0)\sqrt{i}}$, and using equations (3.3.5), we can readily obtain $\Sigma_+(\omega)$ and $V_-(\omega)$ as $\omega \to \infty$, i.e.

$$\Sigma_+(\omega) \to -\frac{\sigma_0 c_R}{(si)^{3/2}\sqrt{\omega}\sqrt{\kappa_d}\hat{F}_+(0)}, \tag{3.3.10}$$

$$V_-(\omega) \to \frac{\sigma_0 c_R}{G_{12}\chi_1(si\omega)^{3/2}\kappa_d^{1/2}\hat{F}_+(0)}. \tag{3.3.11}$$

3.4 Stress Intensity Factor

To find the stress intensity factor, an asymptotic expression for the stress near the crack tip is sought. A well-known result relating asymptotic expressions between a function and its Fourier transform (Abelian theorems) [12, 17] is

$$\lim_{x\to 0}\sqrt{x}\sigma_+^*(x,s)=\lim_{\omega\to\infty}e^{-i\pi/4}\sqrt{\frac{\omega}{\pi}}\Sigma_+(\omega). \tag{3.4.1}$$

$$\lim_{x\to 0}\frac{v_-^*(x)}{\sqrt{x}}=\lim_{\omega\to\infty}e^{i\pi 3/4}\frac{2\omega^{3/2}}{\sqrt{\pi}}V_-(\omega) \tag{3.4.2}$$

Hence, the definition of the stress intensity factor gives

$$K_I^*(s)=\lim_{x\to 0_+}\sqrt{2\pi x}\sigma_+^*(x,s)=\lim_{\omega\to+\infty}e^{-i\pi/4}\sqrt{2\omega}\Sigma_+(\omega)=\frac{\sqrt{2}\sigma_0 c_R}{s^{3/2}\sqrt{\kappa_d}\hat{F}_+(0)}. \tag{3.4.3}$$

Note that $\hat{F}_+(0)=\hat{F}_-(0)=\sqrt{\hat{F}(0)}=\frac{c_R\sqrt{F(0,s)}}{s}$, consequently, equation (3.4.3) can be written as

$$K_I^*(s)=\frac{\sqrt{2}\sigma_0}{s^{1/2}\sqrt{\kappa_d}\sqrt{F(0,s)}}. \tag{3.4.5}$$

Using equation (3.2.26), $F(0,s)=\frac{s^2}{\kappa_d\chi_1}\frac{c_{11}}{c_d}$, it readily shown that

$$K_I^*(s)=\frac{\sqrt{2}\sigma_0}{s^{3/2}}\sqrt{\frac{c_d\chi_1}{c_{11}}}. \tag{3.4.6}$$

Applying the inverse Laplace transform to $K_I^*(s)$, the stress intensity factor $K_I(t)$ can be written as follows

$$\boxed{K_I(t)=2\sigma_0 C_I\sqrt{t}=2\sigma_0\sqrt{t}\sqrt{\frac{2}{\pi}\frac{c_d\chi_1}{c_{11}}},} \tag{3.4.7}$$

where

$$C_I = \sqrt{\frac{2c_d}{\pi}\frac{\chi_1}{c_{11}}}. \tag{3.4.8}$$

Thus, the stress $\sigma_y(x,0,t)$ can be expressed as

$$\sigma_y(x,0,t) = \frac{K_I(t)}{\sqrt{2\pi x}} \tag{3.4.9}$$

For $\theta = 0$, i.e. for the case of transversely isotropic material, C_I reduces to

$$C_I^{\,0} = \sqrt{\frac{2c_d}{\pi}\frac{2(c_{11}-1)}{c_{11}^{\,2}}}. \tag{3.4.10}$$

By using $c_{11} = \frac{2(1-\nu)}{(1-2\nu)}$, equation (3.4.10) further reduces to the well-known result for isotropic materials [13], i.e.

$$C_I^{\,0} = \frac{\sqrt{c_d(1-2\nu)/\pi}}{(1-\nu)}. \tag{3.4.11}$$

For $\theta = 90^\circ$, i.e. for the case of orthotropic materials, C_I reduces to

$$C_I^{\,90} = \sqrt{\frac{2}{\pi}\frac{c_d\chi_1^{\,90}}{c_{11}}}. \tag{3.4.12}$$

where $\chi_1^{\,90}$ is shown in (3.2.25). Tables 2 and 3 show that the numerical values of $C_I^{\,90}$ for orthotropic materials are same as those obtained by using formulation in [10], hence, equation (3.4.7) also reduces to the result for orthotropic materials as expected for $\theta = 90^\circ$. Thus, the value of $C_I^{\,0}$ and $C_I^{\,90}$ can be accurately calculated by using (3.4.10) and (3.4.12), or can be evaluated by using (3.4.8) and letting $\theta = \varepsilon$ and $\theta = 90^\circ - \varepsilon$, $\varepsilon << 0$. Satisfactory agreement of the present solution with known solutions is found.

From (3.4.2), we have

$$\lim_{x\to 0}\frac{\sqrt{2\pi}\,v_{-}^{*}(x)}{\sqrt{x}}=\lim_{\omega\to\infty}\sqrt{2\pi}e^{i\pi 3/4}\frac{2\omega^{3/2}}{\sqrt{\pi}}V_{-}(\omega)=\frac{2}{G_{12}\chi_1}K_I^{*}(s) \tag{3.4.13}$$

thus, the displacement $v(x,0,t)$ can be expressed as

$$v(x,0,t)=\frac{2}{G_{12}\chi_1}\sqrt{\frac{x}{2\pi}}K_I(t) \tag{3.4.14}$$

For a finite crack extension δ, the following Irwin's crack-closure integral (the definition of the strain energy release rate for single mode at once) can be evaluated [18, 19]

$$G_I(t)=\lim_{\delta\to 0}\int_0^{\delta}\frac{\sigma_y(x,0)v(\delta-x,0)}{\delta}dx=\frac{K_I^{\,2}}{2G_{12}\chi_1} \tag{3.4.15}$$

without ambiguity by using

$$\int_0^{\delta}\sqrt{\frac{\delta-x}{x}}dx=\frac{\sqrt{\pi}}{2}\frac{\Gamma(1/2)}{\Gamma(2)}=\frac{\pi}{2} \tag{3.4.16}$$

Equation (3.4.15) further reduces to the well-known result for isotropic materials [20], i.e.

$$G_I(t)=\frac{(1-\nu^2)K_I^{\,2}}{E} \tag{3.4.17}$$

4 In-plane Shear Impact

Consider the crack geometry illustrated in Figure 2. Figure 3 schematically shows the same crack with a spatially uniform shear traction of magnitude τ_0 applied suddenly on the crack faces. Exploiting symmetry and limiting ourselves to upper half-plane, $y>0$, the corresponding boundary conditions become

$$
\begin{aligned}
&\tau_{xy}(x,0,t) = -\tau_0 H(t), && -\infty<x<0,\\
&\sigma_y(x,0,t) = 0 && -\infty<x<+\infty,\\
&\tau_{yz}(x,0,t) = 0 && -\infty<x<+\infty,\\
&u(x,0,t) = 0, && 0<x<+\infty,
\end{aligned}
\tag{4.1}
$$

where H(t) is the unit step function. The displacement at infinity is assumed zero, and the body is stress free and at rest everywhere for $t \le 0$.

A method of solution similar to that that used for normal impact can be used. Applying the Laplace transform to boundary conditions (4.1) gives

$$
\begin{aligned}
&\tau_{xy}^{*}(x,0,t) = -\tau_0 / s, && -\infty < x < 0,\\
&\sigma_y^{*}(x,0,t) = 0, && -\infty < x < +\infty,\\
&\tau_{yz}^{*}(x,0,t) = 0, && -\infty < x < +\infty,\\
&u^{*}(x,0,t) = 0, && 0 < x < +\infty.
\end{aligned}
\tag{4.2}
$$

The displacement field given by (3.2.3) yields the same system of ordinary differential equations, (3.2.4), whose solution is given by equations (3.2.7) where $\alpha_i(\omega,s)$ and $\beta_i(\omega,s)$ are defined by (3.2.8) and γ_i are obtained from the solution of (3.2.10).

Substitution of the expressions for σ_y^*, τ_{yz}^*, the first and third of equations (3.2.15), into the boundary condition for σ_y^*, τ_{yz}^*, the second and third of equations (4.2), yields

$$
\begin{aligned}
&m_1 A_1 + m_2 A_2 + m_3 A_3 = 0,\\
&k_1 A_1 + k_2 A_2 + k_3 A_3 = 0.
\end{aligned}
\tag{4.3}
$$

These equations can be rewritten as

$$
\begin{aligned}
&A_2 = \lambda_1^{II}(\omega,s) A_1,\ A_3 = \lambda_2^{II}(\omega,s) A_1,\\
&\lambda_1^{II}(\omega,s) = \frac{m_1 k_3 - m_3 k_1}{m_3 k_2 - m_2 k_3},\ \lambda_2^{II}(\omega,s) = -\frac{m_1 k_2 - m_2 k_1}{m_3 k_2 - m_2 k_3}
\end{aligned}
\tag{4.4}
$$

As $\omega \to \infty$, we have

$$\lambda_1^{II}(\omega,s)\to\lambda_1^{II\infty}=\frac{m_1^{\infty}k_3^{\infty}-m_3^{\infty}k_1^{\infty}}{m_3^{\infty}k_2^{\infty}-m_2^{\infty}k_3^{\infty}},\quad \lambda_2^{II}(\omega,s)\to\lambda_2^{II\infty}=-\frac{m_1^{\infty}k_2^{\infty}-m_2^{\infty}k_1^{\infty}}{m_3^{\infty}k_2^{\infty}-m_2^{\infty}k_3^{\infty}} \tag{4.5}$$

where $m_i(\omega,s)\to\omega m_i^{\infty}$, $n_i(\omega,s)\to\omega n_i^{\infty}$ and $k_i(\omega,s)\to k_i^{\infty}$, $as\ \omega\to\infty$.

Using this result in the expression for shear stress, the second of equation (3.2.15), the expression for horizontal displacement, the first of equations (3.2.14), and the remaining boundary conditions, we obtain

$$\begin{aligned}&-\frac{G_{12}}{2\pi}\int_{-\infty}^{\infty}(\mathrm{n}_1+\lambda_1^{II}n_2+\lambda_2^{II}n_3)A_1\,e^{-i\omega x}d\omega=-\tau_0/\mathrm{s}\,\mathrm{H}(-\mathrm{x})+\tau_+^{*}(x,s),\\&\frac{1}{2\pi}\int_{-\infty}^{\infty}(1+\lambda_1^{II}+\lambda_2^{II})A_1e^{-i\omega x}d\omega=\mathrm{u}_-^{*}(x,s).\end{aligned} \tag{4.6}$$

By Fourier transform inversion, these equations become

$$\begin{aligned}&-G_{12}(n_1+\lambda_1^{II}n_2+\lambda_2^{II}n_3)A_1=-\tau_0/i\omega s+\mathrm{T}_+(\omega,s),\\&(1+\lambda_1^{II}+\lambda_2^{II})A_1=\mathrm{U}_-(\omega,s).\end{aligned} \tag{4.7}$$

where

$$\begin{aligned}&\mathrm{T}_+(\omega,s)=\int_0^{\infty}\tau_+^{*}(x,s)e^{i\omega x}dx,\\&U_-(\omega,s)=\int_{-\infty}^{0}\mathrm{u}_-^{*}(x,s)e^{i\omega x}dx.\end{aligned} \tag{4.8}$$

Eliminating A_1 from equation, (4.7), we obtain a Wiener-Hopf equation,

$$G_{12}\chi_2\frac{\mathrm{G}(\omega,\mathrm{s})}{\sqrt{\omega^2+s^2/\kappa_{s1}^{\,2}}}\mathrm{U}_-(\omega,s)=\frac{\tau_0}{i\omega s}-\mathrm{T}_+(\omega,s), \tag{4.9}$$

where the following functions are introduced

$$G(\omega,s)=\frac{\sqrt{\omega^2+s^2/\kappa_{s1}^{\,2}}\,(n_1+\lambda_1n_2+\lambda_2n_3)}{\chi_2(1+\lambda_1+\lambda_2)} \tag{4.10}$$

$$\chi_2=\frac{n_1^{\infty}+\lambda_1^{II\infty}n_2^{\infty}+\lambda_2^{II\infty}n_3^{\infty}}{1+\lambda_1^{II\infty}+\lambda_2^{II\infty}} \tag{4.11}$$

where χ_2 is dependent on θ and material parameters and its expression is shown in the Appendix. Here, note that for $\theta = 0$, $\chi_2^{\,0} = \dfrac{2(c_{11}-1)}{c_{11}}$, and for $\theta = 90^\circ$,

$$\chi_2^{\,90} = \frac{g}{h}, \tag{4.12}$$

where

$$g = (c_{11}c_{33} - c_{13}^{\,2})c_{55}[c_{33} + c_{11}N_1N_2N_3(N_1 + N_2 + N_3)],$$

$$h = c_{11}\{c_{33}[c_{11}N_1N_2N_3 + c_{55}(N_1 + N_2 + N_3)] + N_1N_2N_3[-c_{13}^{\,2} - 2c_{13}c_{55} + c_{11}c_{55}(N_1N_2 + N_3N_2 + N_3N_1)]\},$$

and N_i are shown in equation A.5 of the Appendix. $\chi_2^{\,0}$ and $\chi_2^{\,90}$ are the limit values of χ_2 at $\theta = 0$ and $\theta = 90^\circ$, respectively.

Also, for $\omega = 0$, after lengthy algebraic manipulation of equation (4.10), we have

$$G(0,s) = \frac{s^2 p}{\kappa_{s1}\chi_2 c_s} \tag{4.13}$$

where

$$p = \frac{2\sqrt{c_{55}}}{(1+\sqrt{c_{55}}) + (\sqrt{c_{55}} - 1)\cos 2\theta}$$

Equation (4.9) contains only the two unknown functions, $\mathrm{T}_+(\omega,s)$ and $\mathrm{U}_-(\omega,s)$, and can be solved using the Wiener-Hopf technique as in the normal impact analysis of section 3. The result is

$$D_+(\omega) - \Sigma_+(\omega)L_+(\omega) = L_-(\omega)\mathrm{U}_-(\omega) - D_-(\omega) = 0, \tag{4.14}$$

where

$$L_-(\omega) = G_{12}\chi_2 \frac{(\omega - is/c_R)}{\sqrt{\omega - is/\kappa_{s1}}}\hat{G}_-(\omega),$$

$$L_+(\omega) = \frac{\sqrt{\omega + is/\kappa_{s1}}}{(\omega + is/c_R)\hat{G}_+(\omega)}.$$

$$\hat{G}(\omega) = \frac{G(\omega, s)}{\omega^2 + s^2/{c_R}^2}.$$

and

$$D(\omega) = \frac{\tau_0}{i\omega s}L_+(\omega) = \frac{\tau_0}{s}\left[\frac{L_+(\omega) - L_+(0)}{i\omega} + \frac{L_+(0)}{i\omega}\right] = D_+(\omega) + D_-(\omega), \tag{4.15}$$

with

$$D_+(\omega) = \frac{\tau_0}{s}\left[\frac{L_+(\omega) - L_+(0)}{i\omega}\right],\ D_-(\omega) = \frac{\tau_0}{s}\left[\frac{L_+(0)}{i\omega}\right]. \tag{4.16}$$

Hence, we can solve for the transform of stress ahead of the crack tip, $\mathrm{T}_+(\omega)$, and displacement, $\mathrm{U}_-(\omega)$, behind,

$$\begin{aligned} \mathrm{T}_+(\omega) &= \frac{D_+(\omega)}{L_+(\omega)} = \frac{\tau_0}{si\omega}\left[1 - \frac{L_+(0)}{L_+(\omega)}\right], \\ \mathrm{U}_-(\omega) &= \frac{D_-(\omega)}{L_-(\omega)} = \frac{\tau_0}{si\omega}\left[\frac{L_+(0)}{L_-(\omega)}\right]. \end{aligned} \tag{4.17}$$

It can be shown that $\hat{G}(\omega) \to 1$ as $\omega \to \infty$ (the constant χ_2 in (4.11) was chosen to make this possible). Hence, $\hat{G}_\pm(\omega)$ is given by

$$\begin{aligned} &\hat{G}(\omega) = \hat{G}_+(\omega)\hat{G}_-(\omega) \\ &\hat{G}_\pm(\omega) = \exp\left\{\frac{1}{2\pi i}\int_{R_\pm}\frac{\log\hat{G}(\omega)}{z - \omega}dz\right\}, \end{aligned} \tag{4.18}$$

where R_- is the closed counterclockwise contour enclosing the branch points $+is/\kappa_{s1}$, $+is/\kappa_{s2}$ and $+is/\kappa_d$, and also R_+ is the closed counterclockwise contour enclosing the branch points $-is/\kappa_{s1}$, $-is/\kappa_{s2}$ and $-is/\kappa_d$.

Note that as $\omega \to \infty$, $\hat{G}_+(\omega) \to 1$, $\hat{G}_-(\omega) \to 1$, $L_+(\omega) = \frac{1}{\sqrt{\omega}}$, $L_-(\omega) = G_{12}\chi_2\sqrt{\omega}$ and $L_+(0) = \frac{c_R}{s^{1/2}\kappa_{s1}^{1/2}\hat{G}_+(0)\sqrt{i}}$, and using equation (4.17), we can readily obtain $\mathrm{T}_+(\omega)$ and $U_-(\omega)$ as $\omega \to \infty$

$$\mathrm{T}_+(\omega) \to -\frac{\tau_0 c_R}{(si)^{3/2}\sqrt{\omega}\sqrt{\kappa_{s1}}\hat{G}_+(0)}, \tag{4.19}$$

$$\mathrm{U}_-(\omega) \to \frac{\tau_0 c_R}{G_{12}\chi_2(si\omega)^{3/2}\kappa_{s1}^{1/2}\hat{G}_+(0)}. \tag{4.20}$$

From equations (4.7) and (4.4), the coefficients, A_1, A_2 and A_3, as $\omega \to \infty$ become

$$A_1 = f_1^{II}\mathrm{U}_-(\omega) \quad A_2 = f_2^{II}\mathrm{U}_-(\omega) \quad \text{and} \quad A_3 = f_3^{II}\mathrm{U}_-(\omega) \tag{4.21}$$

where $f_1^{II} = \frac{1}{1+\lambda_1^{II\infty}+\lambda_2^{II\infty}}$, $f_2^{II} = \frac{\lambda_1^{II\infty}}{1+\lambda_1^{II\infty}+\lambda_2^{II\infty}}$ and $f_3^{II} = \frac{\lambda_2^{II\infty}}{1+\lambda_1^{II\infty}+\lambda_2^{II\infty}}$.

Substituting (4.21) into (3.2.7), the dual transformed displacement, $\tilde{\mathrm{w}}_-^{II*}(\omega,0,s)$, as $\omega \to \infty$ becomes

$$\tilde{\mathrm{w}}_-^{II*}(\omega,0,s) \to W_-^{II}(\omega) = f_{II}\mathrm{U}_-(\omega) \tag{4.22}$$

where $f_{II} = \beta_1^{\infty} f_1^{II} + \beta_2^{\infty} f_2^{II} + \beta_3^{\infty} f_3^{II}$

From Abelian theorem [12, 17],

$$\lim_{x\to 0}\sqrt{x}\tau_+^*(x,s) = \lim_{\omega\to\infty} e^{-i\pi/4}\sqrt{\frac{\omega}{\pi}}T_+(\omega). \tag{4.23}$$

$$\lim_{x\to 0}\frac{u_-^*(x)}{\sqrt{x}} = \lim_{\omega\to\infty} e^{i\pi 3/4}\frac{2\omega^{3/2}}{\sqrt{\pi}}U_-(\omega) \tag{4.24}$$

$$\lim_{x\to 0}\frac{w_-^{II\,*}(x)}{\sqrt{x}} = \lim_{\omega\to\infty} e^{i\pi 3/4}\frac{2\omega^{3/2}}{\sqrt{\pi}}W_-^{II}(\omega) \tag{4.25}$$

Using (4.21) and the definition of the stress intensity factor gives

$$K_{II}^*(s) = \lim_{x\to 0_+}\sqrt{2\pi x}\tau_+^*(x,s) = \lim_{\omega\to+\infty} e^{-i\pi/4}\sqrt{2\omega}T_+(\omega) = \frac{\sqrt{2}\tau_0 c_R}{s^{3/2}\sqrt{\kappa_{s1}}\hat{G}_+(0)}. \tag{4.26}$$

Note that $\hat{G}_+(0) = \hat{G}_-(0) = \sqrt{\hat{G}(0)} = \dfrac{c_R\sqrt{G(0,s)}}{s}$, consequently, equation (4.26) can be rewritten as

$$K_{II}^*(s) = \frac{\sqrt{2}\sigma_0}{s^{1/2}\sqrt{\kappa_{s1}}\sqrt{G(0,s)}}. \tag{4.27}$$

Using equation (4.13), $G(0,s) = \dfrac{s^2 p}{\kappa_{s1}\chi_2 c_s}$, it readily shown that

$$K_{II}^*(s) = \frac{\sqrt{2}\sigma_0}{s^{3/2}}\sqrt{\frac{c_s\chi_2}{p}}. \tag{4.28}$$

Applying the inverse Laplace transform to $K_{II}^*(s)$, the stress intensity factor $K_{II}(t)$ can be written as follows

$$\boxed{K_{II}(t) = 2\tau_0 C_{II}\sqrt{t} = 2\tau_0\sqrt{t}\sqrt{\frac{2}{\pi}\frac{c_s\chi_2}{p}},} \tag{4.29}$$

where

$$C_{II} = \sqrt{\frac{2}{\pi}\frac{c_s\chi_2}{p}}. \tag{4.30}$$

Thus, the stress $\tau_{xy}(x,0,t)$ can be expressed as

$$\tau_{xy}(x,0,t)=\frac{K_{II}(t)}{\sqrt{2\pi x}} \tag{4.31}$$

For $\theta=0$, i.e. for the case of transversely isotropic material, C_{II} reduces to

$$C_{II}{}^{0}=\sqrt{\frac{2c_d}{\pi}\frac{2(c_{11}-1)}{c_{11}}}. \tag{4.32}$$

By using $c_{11}=\frac{2(1-\nu)}{(1-2\nu)}$, equation (4.32) further reduces to the well-known result for isotropic materials [13], i.e.

$$C_{II}{}^{0}=\sqrt{\frac{2c_s}{\pi(1-\nu)}} \quad . \tag{4.33}$$

For $\theta=90^{\circ}$, i.e. for the case of orthotropic materials, C_{II} reduces to

$$C_{II}{}^{90}=\sqrt{\frac{2c_s\chi_2{}^{90}}{\pi}}. \tag{4.34}$$

where $\chi_2{}^{90}$ is shown in (4.12). Tables 2 and 3 show that the numerical values of $C_{II}{}^{90}$ for orthotropic materials are same as those obtained by using formulation in [10], hence, equation (4.26) also reduces to the result for orthotropic materials as expected for $\theta=90^{\circ}$.

From (4.24), we have

$$\lim_{x\to 0}\frac{\sqrt{2\pi}\,u_{-}{}^{*}(x)}{\sqrt{x}}=\lim_{\omega\to\infty}\sqrt{2\pi}e^{i\pi 3/4}\frac{2\omega^{3/2}}{\sqrt{\pi}}U_{-}(\omega)=\frac{2}{G_{12}\chi_2}K_{II}{}^{*}(s) \tag{4.35}$$

thus, the displacement $u^{II}(x,0,t)$ can be expressed as

$$u^{II}(x,0,t)=\frac{2}{G_{12}\chi_2}\sqrt{\frac{x}{2\pi}}K_{II}(t) \tag{4.36}$$

Similarly, from equation (4.25) the displacement $w^{II}(x,0,t)$ can be expressed as

$$w^{II}(x,0,t) = \frac{2f_{II}}{G_{12}\chi_2}\sqrt{\frac{x}{2\pi}}K_{II}(t) \tag{4.37}$$

5 Anti-plane Shear Impact

Consider the crack geometry illustrated in Figure 1. Figure 4 schematically shows the same crack with a spatially uniform shear traction of magnitude τ_0 applied suddenly on the crack faces. Exploiting symmetry and limiting ourselves to upper half-plane, $y>0$, the corresponding boundary conditions become

$$\begin{aligned}
&\tau_{yz}(x,0,t) = -\tau_0 H(t), && -\infty < x < 0,\\
&\sigma_y(x,0,t) = 0 && -\infty < x < +\infty,\\
&\tau_{xy}(x,0,t) = 0 && -\infty < x < +\infty,\\
&w(x,0,t) = 0, && 0 < x < +\infty,
\end{aligned} \tag{5.1}$$

where H(t) is the unit step function.

The displacement at infinity is zero, and the body is stress free and at rest everywhere for $t \le 0$.

The method of solution is similar to that that used for normal impact. Applying the Laplace transform to boundary conditions (5.1) gives

$$\begin{aligned}
&\tau_{yz}^{*}(x,0,t) = -\tau_0 / s, && -\infty < x < 0,\\
&\sigma_y^{*}(x,0,t) = 0, && -\infty < x < +\infty,\\
&\tau_{xy}^{*}(x,0,t) = 0, && -\infty < x < +\infty,\\
&w^{*}(x,0,t) = 0, && 0 < x < +\infty.
\end{aligned} \tag{5.2}$$

Assuming the displacement field given by (3.2.3) yields the same system of ordinary differential equations, (3.2.4), whose solution is given by equations (3.2.7) where $\alpha_i(\omega,s)$ and $\beta_i(\omega,s)$ are defined by (3.2.8) and γ_i are obtained from the solution of (3.2.10).

Substitution of expression for σ_y^*, τ_{xy}^*, the second and third of equations (3.2.15), into the boundary condition for σ_y^*, τ_{xy}^*, the second and third of equations (5.2), yields

$$\begin{aligned} &n_1 A_1 + n_2 A_2 + n_3 A_3 = 0 \\ &k_1 A_1 + k_2 A_2 + k_3 A_3 = 0 \end{aligned} \tag{5.3}$$

These equations can be rewritten as

$$\begin{aligned} &A_2 = \lambda_1^{III}(\omega, s) A_1, \; A_3 = \lambda_2^{III}(\omega, s) A_1, \\ &\lambda_1^{III}(\omega, s) = \frac{n_1 k_3 - n_3 k_1}{n_3 k_2 - n_2 k_3}, \lambda_2^{III}(\omega, s) = -\frac{n_1 k_2 - n_2 k_1}{n_3 k_2 - n_2 k_3} \end{aligned} \tag{5.4}$$

As $\omega \to \infty$, we have

$$\lambda_1^{III}(\omega, s) \to \lambda_1^{III\infty} = \frac{n_1^{\infty} k_3^{\infty} - n_3^{\infty} k_1^{\infty}}{n_3^{\infty} k_2^{\infty} - n_2^{\infty} k_3^{\infty}}, \quad \lambda_2^{III}(\omega, s) \to \lambda_2^{III\infty} = -\frac{n_1^{\infty} k_2^{\infty} - n_2^{\infty} k_1^{\infty}}{n_3^{\infty} k_2^{\infty} - n_2^{\infty} k_3^{\infty}} \tag{5.5}$$

where $m_i(\omega, s) \to \omega m_i^{\infty}$, $n_i(\omega, s) \to \omega n_i^{\infty}$ as $\omega \to \infty$.

Using this result on the expression for normal stress, the secondary of equation (3.2.15), the expression for horizontal displacement, the first of equations (3.2.14), and the remaining boundary conditions, we obtain

$$\begin{aligned} &-\frac{G_{12}}{2\pi} \int_{-\infty}^{\infty} (m_1 + \lambda_1^{III} m_2 + \lambda_2^{III} m_3) A_1 \, e^{-i\omega x} d\omega = -\tau_0 / \mathrm{s}\,\mathrm{H}(-\mathrm{x}) + \tau_+^*(x, s), \\ &\frac{1}{2\pi} \int_{-\infty}^{\infty} (\beta_1 + \beta_2 \lambda_1^{III} + \beta_3 \lambda_2^{III}) A_1 e^{-i\omega x} d\omega = \mathrm{w}_-^*(x, s). \end{aligned} \tag{5.6}$$

By Fourier transform inversion, these equations become

$$\begin{aligned} &-G_{12}(m_1 + \lambda_1^{III} m_2 + \lambda_2^{III} m_3) A_1 = -\tau_0 / i\omega s + \Gamma_+(\omega, s), \\ &(\beta_1 + \beta_2 \lambda_1^{III} + \beta_3 \lambda_2^{III}) A_1 = \mathrm{W}_-(\omega, s), \end{aligned} \tag{5.7}$$

where

$$\begin{aligned} &\Gamma_+(\omega, s) = \int_0^{\infty} \tau_+^*(x, s) e^{i\omega x} dx, \\ &W_-(\omega, s) = \int_{-\infty}^{0} \mathrm{w}_-^*(x, s) e^{i\omega x} dx. \end{aligned}$$

Eliminating A_1 from equation, (99), we obtain a Wiener-Hopf equation,

$$G_{12}\chi_3 \frac{\mathrm{E}(\omega,\mathrm{s})}{\sqrt{\omega^2 + s^2/{\kappa_{s2}}^2}} \mathrm{W}_-(\omega,s) = \frac{\tau_0}{i\omega s} - \Gamma_+(\omega,s), \tag{5.8}$$

where the following functions are introduced

$$E(\omega,s) = \frac{\sqrt{\omega^2 + s^2/{\kappa_{s2}}^2}\,(m_1 + \lambda_1 m_2 + \lambda_2 m_3)}{\chi_2(\beta_1 + \beta_2\lambda_1 + \beta_3\lambda_2)} \tag{5.9}$$

$$\chi_3 = \frac{m_1^{\infty} + \lambda_1^{III\infty} m_2^{\infty} + \lambda_2^{III\infty} m_3^{\infty}}{1 + \lambda_1^{III\infty} + \lambda_2^{III\infty}} \tag{5.10}$$

where χ_3 is dependent on θ and material parameters and its expression is shown in the Appendix . Here, note that for $\theta = 0$, $\chi_3^{\,0} = \sqrt{c_{55}}$, and for $\theta = 90^\circ$, $\chi_3^{\,90} = \sqrt{c_{55}}$ when using N_i shown in equation A.5 of the Appendix. $\chi_3^{\,0}$ and $\chi_3^{\,90}$ are the limit values of χ_3 at $\theta = 0$ and $\theta = 90^\circ$, respectively.

For $\omega = 0$, after lengthy algebraic manipulation of equation (5.9), we have

$$E(0,s) = \frac{s^2}{\kappa_{s2}\chi_3}\frac{q}{c_s} \tag{5.11}$$

where

$$q = \frac{(\sqrt{c_{55}} + c_{55})}{\sqrt{c_{55}} + c_{55}\sin^2\theta + \cos^2\theta}.$$

Equation (5.8) contains only the two unknown functions, $\Gamma_+(\omega,s)$ and $\mathrm{W}_-(\omega,s)$, and can be solved using the Wiener-Hopf technique as in the normal impact analysis. The result is

$$D_+(\omega) - \Sigma_+(\omega)L_+(\omega) = L_-(\omega)W_-(\omega) - D_-(\omega) = 0. \tag{5.12}$$

where

$$L_-(\omega) = G_{12}\chi_3 \frac{(\omega - is/c_R)}{\sqrt{\omega - is/\kappa_{s2}}} \hat{E}_-(\omega),$$

$$L_+(\omega) = \frac{\sqrt{\omega + is/\kappa_{s2}}}{(\omega + is/c_R)\hat{E}_+(\omega)}.$$

$$\hat{E}(\omega) = \frac{E(\omega, s)}{\omega^2 + s^2/{c_R}^2}.$$

and

$$D(\omega) = \frac{\tau_0}{i\omega s} L_+(\omega) = \frac{\tau_0}{s}\left[\frac{L_+(\omega) - L_+(0)}{i\omega} + \frac{L_+(0)}{i\omega}\right] = D_+(\omega) + D_-(\omega), \qquad (5.13)$$

with

$$D_+(\omega) = \frac{\tau_0}{s}\left[\frac{L_+(\omega) - L_+(0)}{i\omega}\right],\ D_-(\omega) = \frac{\tau_0}{s}\left[\frac{L_+(0)}{i\omega}\right].$$

Hence, we can solve for the transform of stress ahead of the crack tip, $\Gamma_+(\omega)$, and displacement, $\mathrm{W}_-(\omega)$, behind,

$$\begin{aligned} \Gamma_+(\omega) &= \frac{D_+(\omega)}{L_+(\omega)} = \frac{\tau_0}{si\omega}\left[1 - \frac{L_+(0)}{L_+(\omega)}\right], \\ \mathrm{W}_-(\omega) &= \frac{D_-(\omega)}{L_-(\omega)} = \frac{\tau_0}{si\omega}\left[\frac{L_+(0)}{L_-(\omega)}\right]. \end{aligned} \qquad (5.14)$$

It can be shown that $\hat{E}(\omega) \to 1$ as $\omega \to \infty$ (the constant χ_3 in (5.10) was chosen to make this possible). Hence, $\hat{E}_\pm(\omega)$ can be given by

$$\begin{aligned} &\hat{E}(\omega) = \hat{E}_+(\omega)\hat{E}_-(\omega) \\ &\hat{E}_\pm(\omega) = \exp\left\{\frac{1}{2\pi i}\int_{R_\pm} \frac{\log \hat{E}(\omega)}{z - \omega} dz\right\}, \end{aligned} \qquad (5.15)$$

where R_- is the closed counterclockwise contour enclosing the branch points $+is/\kappa_{s1}$, $+is/\kappa_{s2}$ and $+is/\kappa_d$, and also R_+ is the closed counterclockwise contour enclosing the branch points $-is/\kappa_{s1}$, $-is/\kappa_{s2}$ and $-is/\kappa_d$.

Note that as $\omega \to \infty$, $\hat{E}_+(\omega) \to 1$, $\hat{E}_-(\omega) \to 1$, $L_+(\omega) = \frac{1}{\sqrt{\omega}}$, $L_-(\omega) = G_{12}\chi_3\sqrt{\omega}$ and $L_+(0) = \frac{c_R}{s^{1/2}\kappa_{s1}^{1/2}\hat{E}_+(0)\sqrt{i}}$, and using equation (108), we can readily obtain $\Gamma_+(\omega)$ as $\omega \to \infty$

$$\Gamma_+(\omega) \to -\frac{\tau_0 c_R}{(si)^{3/2}\sqrt{\omega}\sqrt{\kappa_{s2}}\hat{E}_+(0)}. \tag{5.16}$$

$$\mathrm{W}_-(\omega) \to \frac{\tau_0 c_R}{G_{12}\chi_3(si\omega)^{3/2}\kappa_{s2}^{1/2}\hat{E}_+(0)}. \tag{5.17}$$

From equations (5.7) and (5.4), the coefficients, A_1, A_2 and A_3, as $\omega \to \infty$ become

$$A_1 = \mathrm{g}_1^{III}\mathrm{W}_-(\omega) \quad A_2 = \mathrm{g}_2^{III}\mathrm{W}_-(\omega) \quad \text{and} \quad A_3 = \mathrm{g}_3^{III}\mathrm{W}_-(\omega) \tag{5.18}$$

where

$$g_1^{III} = \frac{1}{\beta_1^{--} + \beta_2^{--}\lambda_1^{III--} + \beta_2^{--}\lambda_2^{III--}}, \quad g_2^{III} = \frac{\lambda_1^{III--}}{\beta_1^{--} + \beta_2^{--}\lambda_1^{III--} + \beta_2^{--}\lambda_2^{III--}} \quad \text{and} \quad g_3^{III} = \frac{\lambda_2^{III--}}{\beta_1^{--} + \beta_2^{--}\lambda_1^{III--} + \beta_2^{--}\lambda_2^{III--}}.$$

Substituting (5.18) into (3.2.7), the dual transformed displacement, $\tilde{\mathrm{u}}_-^{III*}(\omega,0,s)$, as $\omega \to \infty$ becomes

$$\tilde{\mathrm{u}}_-^{III*}(\omega,0,s) \to U_-^{III}(\omega) = g_{III}\mathrm{W}_-(\omega) \tag{5.19}$$

where $g_{III} = g_1^{III} + g_2^{III} + g_3^{III}$

From Abelian theorem [12, 17],

$$\lim_{x\to 0}\sqrt{x}\tau_+^*(x,s) = \lim_{\omega\to\infty} e^{-i\pi/4}\sqrt{\frac{\omega}{\pi}}\Gamma_+(\omega). \tag{5.20}$$

$$\lim_{x\to 0}\frac{w_-^*(x)}{\sqrt{x}} = \lim_{\omega\to\infty} e^{i\pi 3/4}\frac{2\omega^{3/2}}{\sqrt{\pi}}W_-(\omega) \tag{5.21}$$

$$\lim_{x\to 0}\frac{u_-^{III*}(x)}{\sqrt{x}} = \lim_{\omega\to\infty} e^{i\pi 3/4}\frac{2\omega^{3/2}}{\sqrt{\pi}}U_-^{III}(\omega) \tag{5.22}$$

Using (5.18) and the definition of the stress intensity factor gives

$$K_{III}^*(s) = \lim_{x\to 0_+}\sqrt{2\pi x}\tau_+^*(x,s) = \lim_{\omega\to+\infty} e^{-i\pi/4}\sqrt{2\omega}\Gamma_+(\omega) = \frac{\sqrt{2}\tau_0 c_R}{s^{3/2}\sqrt{\kappa_{s2}}\hat{E}_+(0)}. \tag{5.23}$$

Note that $\hat{E}_+(0) = \hat{E}_-(0) = \sqrt{\hat{E}(0)} = \frac{c_R\sqrt{E(0,s)}}{s}$, consequently, equation (5.20) can be rewritten as

$$K_{III}^*(s) = \frac{\sqrt{2}\tau_0}{s^{1/2}\sqrt{\kappa_{s2}}\sqrt{E(0,s)}}. \tag{5.24}$$

Using equation (5.11), $E(0,s) = \frac{s^2}{\kappa_{s2}\chi_3}\frac{q}{c_s}$, it readily shown that

$$K_{III}^*(s) = \frac{\sqrt{2}\tau_0}{s^{3/2}}\sqrt{\frac{c_s\chi_3}{q}}. \tag{5.25}$$

Applying the inverse Laplace transform to $K_{III}^*(s)$, the stress intensity factor $K_{III}(t)$ can be written as follows

$$\boxed{K_{III}(t) = 2\tau_0 C_{III}\sqrt{t} = 2\tau_0\sqrt{t}\sqrt{\frac{2}{\pi}\frac{c_s\chi_3}{q}}} \tag{5.26}$$

where

$$C_{III} = \sqrt{\frac{2}{\pi}\frac{c_s\chi_3}{q}}. \tag{5.27}$$

Thus, the stress $\tau_{yz}(x,0,t)$ can be expressed as

$$\tau_{yz}(x,0,t)=\frac{K_{III}(t)}{\sqrt{2\pi x}} \tag{5.28}$$

For $\theta=0$, i.e. for the case of transversely isotropic material, C_{III} reduces to

$$C_{III}{}^{0}=\sqrt{\frac{2\sqrt{c_{55}}c_s}{\pi}}. \tag{5.29}$$

By using $c_{55}=1$, equation (5.29) further reduces to the well-known result for isotropic materials [13], i.e.

$$C_{III}{}^{0}=\sqrt{\frac{2c_s}{\pi}}. \tag{5.30}$$

For $\theta=90^{\circ}$, i.e. for the case of orthotropic materials, C_{III} reduces to

$$C_{III}{}^{90}=\sqrt{\frac{2c_s\sqrt{c_{55}}}{\pi}} \tag{5.31}$$

Tables 2 and 3 show that the numerical values of $C_{III}{}^{90}$ for orthotropic materials are same as those obtained by using formulation in [10], hence, equation (5.26) also reduces to the result for orthotropic materials as expected for $\theta=90^{\circ}$. From (5.29) and (5.31), $C_{III}{}^{0}$ is same as $C_{III}{}^{90}$, which is because $d_{55}(0^{\circ})=d_{55}(90^{0})$.

From (5.21), we have

$$\lim_{x\to 0}\frac{\sqrt{2\pi}\,w_{-}{}^{*}(x)}{\sqrt{x}}=\lim_{\omega\to\infty}\sqrt{2\pi}e^{i\pi 3/4}\frac{2\omega^{3/2}}{\sqrt{\pi}}W_{-}(\omega)=\frac{2}{G_{12}\chi_3}K_{III}{}^{*}(s) \tag{5.32}$$

thus, the displacement $w^{III}(x,0,t)$ can be expressed as

$$w^{III}(x,0,t)=\frac{2}{G_{12}\chi_3}\sqrt{\frac{x}{2\pi}}K_{III}(t) \tag{5.33}$$

Similarly, from equation (5.22) the displacement $u^{III}(x,0,t)$ can be expressed as

$$u^{III}(x,0,t) = \frac{2g_{III}}{G_{12}\chi_3}\sqrt{\frac{x}{2\pi}}K_{III}(t) \tag{5.34}$$

6 Results and Conclusion

Closed form expressions of the dynamic stress intensity factors $K_I(t)$, $K_{II}(t)$ and $K_{III}(t)$ have been determined for semi-infinite cracks in rotated transversely isotropic materials under the three loading modes, i.e. opening, in-plane shear and anti-plane shear loadings, respectively. The stress intensity factors for the three modes are proportional to the square root of time; there is no equivalent quasi-static problem for semi-infinite crack under uniform loadings and there is no long-time equilibrium value. The method of solution in this paper differs from that typically used in the isotropic case. The displacement formulation of the equations of motion is solved without the use of Helmholtz potentials. This allows solutions to be found. As $\theta = 0^\circ$ and $\theta = 90^\circ$, we can use the formulae in [10] for the coefficient of stress intensity factor for the three modes to check our result. The results of the comparison are shown in Tables 2 and 3. The results found here are completely the same as those in Table 2, as expected. Thus, it has been shown that the rotated transversely isotropic formulation includes the case of the crack located in the transversely isotropic plane, the case of the fiber along the crack, and the case of isotropic materials as special cases. That is, for each loading mode, the dynamic stress intensity factor for these special materials is recovered from the rotated transversely isotropic expressions with the proper substitution of elastic constants.

The calculated results for $C_I(\theta)$, $C_{II}(\theta)$ and $C_{III}(\theta)$, where $K_i(t,\theta) = 2\sigma_i C_i(\theta)\sqrt{t}$, are shown in Figure 5-8 for several materials, and the mechanical properties [16] used for the analysis are given in Table 1. In these figures, it can be seen that the fiber reinforcement of

epoxy leads to an increase of the stress intensity factor for all three modes, i.e., the stress intensity factors $K(t)$ for Graphite-Epoxy, Eglass-Epoxy, and Boron-Epoxy composites are greater than the corresponding $K(t)$ for epoxy at all rotation angles. For mode-I and mode-II, the coefficient of stress intensity factor increases as the rotation angle θ increases, and at $\theta = 0^\circ$ and $\theta = 90^\circ$ the coefficient of stress intensity factor reaches its minimum value and maximum value, respectively.

Figure 7 shows the coefficient of stress intensity factor for mode-III with rotation angle θ. The shape of the curve is different from those for mode-I and mode-II. Surprisingly, at $\theta = 0^\circ$ and $\theta = 90^\circ$ the coefficients of stress intensity factor are same, which can be obtained by proper substitution of elastic constants. This is because $d_{55}(0^\circ) = d_{55}(90^\circ)$, i.e. shear on the principle axis is independent of rigid body rotation through 90°. Also at $\theta = 0^\circ$ and $\theta = 90^\circ$ the coefficient of the stress intensity factor has its minimum value. The point of the maximum value for coefficient of stress intensity factor is between $\theta = 0^\circ$ and $\theta = 90^\circ$. The maximum value and its corresponding rotation angle are clearly dependent on the material properties.

Figure 8 shows the coefficient of the stress intensity factors $K_I(t)$, $K_{II}(t)$ and $K_{III}(t)$ for isotropic (epoxy) and orthotropic (graphite-epoxy) materials, note that with same load amplitude the coefficient of stress intensity factor $K_{II}(t)$ and $K_{III}(t)$ are greater than $K_I(t)$. By comparison of both cases, it can be seen that the introduction of fibers results in an increase in the stress intensity factor. This effect is more dramatic in the shear modes than in the normal mode.

In terms of the penny shaped crack problem, these results offer some intuitive insights. If the crack is loaded in mode I, Figure 5 leads us to expect the crack front to advance in the direction

of the fibers, provided the toughness is constant in all directions. If, however, the crack is loaded in shear, the problem is more complex because the crack front sees mixed shear mode loading. There are components of both mode II and mode III loading along the crack front. Letting the shear loading with magnitude, τ_0, be applied on the surface of the penny crack, and letting φ be the angle of that shear loading relative to the principle axis of the material (fiber-orientation) as shown in Figure 9. The shear loading at a point θ on the crack front is given by a *mode II* and *mode III* component,

$$\begin{aligned} \tau_{II} &= \tau_0 \cos(\varphi - \theta) \\ \tau_{III} &= \tau_0 \sin(\varphi - \theta) \end{aligned} \tag{6.1}$$

In this case, due to the presence of both modes at once, hence there are cross-influences.

For a finite collinear crack extension, δ, the following Irwin's crack-closure integral (the definition of the strain energy release rate for both modes at once) can be evaluated [18, 19]

$$G_{II}(t) = \lim_{\delta \to 0} \int_0^{\delta} \frac{\tau_{xy}(x,0)[\mathrm{u}^{\mathrm{II}}(\delta - \mathrm{x},0) + \mathrm{u}^{\mathrm{III}}(\delta - \mathrm{x},0)]}{\delta} dx \tag{6.2}$$

$$G_{III}(t) = \lim_{\delta \to 0} \int_0^{\delta} \frac{\tau_{yz}(x,0)[\mathrm{w}^{\mathrm{III}}(\delta - \mathrm{x},0) + \mathrm{w}^{\mathrm{II}}(\delta - \mathrm{x},0)]}{\delta} dx \tag{6.3}$$

Using (3.4.16), and the $\tau_{xy}(x,0)$, $\tau_{yz}(x,0)$, $\mathrm{u}^{\mathrm{II}}(x,0)$, $\mathrm{u}^{\mathrm{III}}(x,0)$, $\mathrm{w}^{\mathrm{II}}(x,0)$ and $\mathrm{w}^{\mathrm{III}}(x,0)$ derived above, $G_{II}(t)$ *and* $G_{III}(t)$ are expressed as

$$G_{II}(t) = \frac{1}{2G_{12}\chi_2} K_{II}^{\,2} + \frac{g_{III}}{2G_{12}\chi_3} K_{II} K_{III} \tag{6.4}$$

$$G_{III}(t) = \frac{1}{2G_{12}\chi_3} K_{III}^{\,2} + \frac{f_{II}}{2G_{12}\chi_2} K_{II} K_{III} \tag{6.5}$$

where equations (6.4) and (6.5) further reduce to the known result for isotropic materials [20], i.e.

$$G_{II}(t)=\frac{(1-\nu^2)K_{II}^{\ 2}}{E} \tag{6.6}$$

$$G_{III}(t)=\frac{(1+\nu)K_{III}^{\ 2}}{E} \tag{6.7}$$

Substituting the expression for $K_{II}(t)$ and $K_{III}(t)$ derived here, (4.29) and (5.26), the strain energy release rates, $G_{II}(t)$ *and* $G_{III}(t)$, become

$$G_{II}(t)=\frac{4c_s t}{G_{12}\pi}\frac{\tau_{II}^{\ 2}}{p}+\frac{4c_s t}{G_{12}\pi}g_{III}\tau_{II}\tau_{III}\sqrt{\frac{\chi_2}{\chi_3 pq}}\ , \tag{6.8}$$

$$G_{III}(t)=\frac{4c_s t}{G_{12}\pi}\frac{\tau_{III}^{\ 2}}{q}+\frac{4c_s t}{G_{12}\pi}f_{II}\tau_{II}\tau_{III}\sqrt{\frac{\chi_3}{\chi_2 pq}}\ . \tag{6.9}$$

The total energy release rate is given by

$$G_{total}(t)=G_{II}(t)+G_{III}(t), \tag{6.10}$$

thus,

$$\frac{G_{12}\pi}{4c_s\tau_0^{\ 2}t}G_{total}(t)=\frac{\cos^2(\varphi-\theta)}{p}+\frac{\sin^2(\varphi-\theta)}{q}+\cos(\varphi-\theta)\sin(\varphi-\theta)\left[g_{III}\sqrt{\frac{\chi_2}{\chi_3 pq}}+f_{II}\sqrt{\frac{\chi_3}{\chi_2 pq}}\right] \tag{6.11}$$

For a given shear loading angle, φ, $\frac{G_{12}\pi}{4c_s\tau_0^{\ 2}t}G_{total}(t)$ is a function of only θ. Thus, the maximum energy release rate, $max\left[\frac{G_{12}\pi}{4c_s\tau_0^{\ 2}t}G_{total}(t)\right]$, occurs at $\theta=\theta_c$ $(0\le\theta_c<\pi)$ and θ_c is a function of φ. The functions are periodic in φ and θ with a period of π.

Figure 10, 11 and 12 show the normalized strain energy release rates for $0<\theta<180^\circ$ and $0<\varphi<180^\circ$ in Graphite-Epoxy, Eglass-Epoxy and Boron-Epoxy, respectively. There are two

different peaks for given φ in each of these figures, where the loading is most severe. Meanwhile we also find valleys in these figures where the loading is least severe. The most probable direction of propagation for each case and the corresponding value of the normalized strain energy release rate are shown in Figures 13 and Figure 14. It is seen that $\theta_c \approx \frac{\pi}{2} + \varphi$ for each material, that is, the crack will most likely propagate in the direction perpendicular to shear loading.

Acknowledgment

Support of this work by the Office of Naval Research Young Investigator Program under grant N00014-96-1-0774 supervised by Dr. Y. Rajapakse who is gratefully acknowledged.

References

[1] Freund, L. B., Dynamic fracture mechanics. Cambridge University Press, 1990, New York.

[2] Chen, E. P. and Sih, G. C., Transient response of cracks to impact laods in elastodynamic crack problems, ed. Sih, G. C., Norordhoff International Publishing, 1977, Leyden.

[3] Maue A. W., Die entspannungswellle bei plotzlichem einschnitt eines gespannten elastischen korpes, ZAMM, 1954, **34**, n1/2, 1-10

[4] Baker B. R., Dynamic stress created by a moving crack, ASME, J. Appl. Mech., 1962, **29**, 449-458

[5] Kassir, M. K., and Bandyopadhyay, K. K., Impact response of a cracked orthotropic medium, ASME, J. Appl. Mech., 1983, **50**, 630-636

[6] Shindo, Y. and Nozaki, H., Impact response of a finite crack in an orthotropic strip, Acta Mechanica, 1991, **62**, 87-104

[7] Sneddon, I. N., The distribution of stress in the neighborhood of a crack in an elastic solid, Proceedings of the Royal Society (London), 1946, **A187**, 229-60

[8] Sneddon, I. N., The stress produced by a pulse of pressure moving along the surface of a semi-infinite solid, Rendiconti del Circolo Matematico di Palermo, 1952, **1**, 57-62.

[9] Rubio-Gonzalez, C. and Mason, J. J., Dynamic stress intensity factor for a semi-infinite crack in orthotropic materials due to concentrated normal impact loads, Submitted to J. of Composite Materials, 1998.

[10] Rubio-Gonzalez, C. and Mason, J. J., Closed form solutions for dynamic stress intensity factors at the tip of uniformly loaded semi-infinite cracks in orthotropic materials, Submitted to J. of Mechanics and Physics of Solids, 1998.

[11] Wang, C.Y., Rubio-Gonzalez, C. and Mason, J. J., Dynamic stress intensity of factor on a semi-infinite crack in orthotropic materials due to concentrated shear impact load. Submitted to Int. J. of Solids and Structures, 1998.

[12] Noble B., Methods based on the Weiner-Hopf technique. Elmsford, New York, Pergamon, 1958.

[13] Freund, L. B., The stress intensity factor due to normal impact loading on the faces of a crack. Int. J. Engng. Sci., 1974, **12**, 179-189

[14] Ting, T.C.T., Anisotropic elasticity. Oxford University Press, New York, 1996.

[15] Nayfeh, A. H., Wave propagation in anisotropic media with applications to composites, North-Holland Publishing Company, Amsterdam, 1995.

[16] Schwartz, M. M., Properties, nondestructive testing and repair, Composite Material, 1997, **1**, Prentice-Hall, Upper Saddle River N. J.

[17] Erdelyi A., Asymptotic expansions, Dover, 1956.

[18] Sih, G. C., Paris, P.C. and Irwin, G. R., On cracks in rectilinearly anisotropic bodies, International Journal of Fracture Mechanics, 1965, **1**, 189-203

[19] Qian, W. and Sun, C. T., Calculation of stress intensity factors for interlaminar cracks in composite laminates, Composites Science and Technology, 1997, **57**, 637-650

[20] Ying, S. Z, Fracture and damage theories and their application, Qing Hua University Press, P. R. China, 1992.

Appendix

(1) Roots of the characteristic equation, (3.2.10)

The solutions of the cubic equation (3.2.10) of γ^2, ${\gamma_1}^2$, ${\gamma_2}^2$ and ${\gamma_3}^2$, are related to *a, b, c* and *d* by the following relations,

$$ {\gamma_1}^2+{\gamma_2}^2+{\gamma_3}^2=-\frac{b}{a},\ {\gamma_1}^2{\gamma_2}^2{\gamma_3}^2=-\frac{d}{a},\ \gamma_1^2\gamma_2^2+\gamma_2^2\gamma_3^2+\gamma_1^2\gamma_3^2=\frac{c}{a}. \qquad \text{(A.1)} $$

where these expressions, ${\gamma_i}^2$, can be given as

$$ {\gamma_1}^2=\frac{2s^2/{c_s}^2+(1+c_{55})\omega^2+(1-c_{55})\omega^2\cos 2\theta}{2} $$

$$ {\gamma_2}^2=\frac{(2c_{55}-2c_{11})s^2/{c_s}^2+(B_1+B_2\cos 2\theta)\omega^2-\sqrt{B_3}}{4c_{11}c_{55}} $$

$$ {\gamma_3}^2=\frac{(2c_{55}-2c_{11})s^2/{c_s}^2+(B_1+B_2\cos 2\theta)\omega^2+\sqrt{B_3}}{4c_{11}c_{55}} $$

and,

$$ B_1=-{c_{13}}^2-2c_{13}c_{55}+c_{11}c_{33}+2c_{11}c_{55}, $$

$$ B_2={c_{13}}^2-c_{11}c_{33}+2c_{11}c_{55}+2c_{13}c_{55}, $$

$$ \begin{aligned} B_3=&[2c_{55}\,s^2/{c_s}^2-c_{13}\,\omega^2-2c_{13}c_{55}+c_{11}(2s^2/{c_s}^2+c_{33}\omega^2+2c_{55}\omega^2)+B_2\omega^2\cos^2 2\theta]^2-2c_{11}c_{55}\\ &[8s^4/{c_s}^4+4(c_{11}+c_{33}+2c_{55})\omega^2s^2/{c_s}^2+(-{c_{13}}^2+c_{11}c_{33}+3c_{11}c_{55}-2c_{13}c_{55}+3c_{33}c_{55}+\\ &4(c_{11}-c_{33})\omega^2(s^2/{c_s}^2+c_{55}\omega^2)\cos 2\theta+({c_{13}}^2-c_{11}c_{33}+c_{11}c_{55}+2c_{13}c_{55}+c_{33}c_{55})\omega^4\cos 4\theta \end{aligned} $$

As $\omega=0$, equation (3.2.10) becomes

$$ \gamma^{0^6}+\frac{b_0}{a}\gamma^{0^4}+\frac{c_0}{a}\gamma^{0^2}+\frac{d_0}{a}=0 \qquad \text{(A.2)} $$

where

$$ a=d_{22}({d_{46}}^2-d_{44}d_{66})=\frac{-c_{11}(c_{11}-c_{12})}{2}, $$

$$b_0 = (d_{22}d_{44} - d_{46}^{\ 2} + d_{22}d_{66} + d_{44}d_{66})\frac{s^2}{c_s^{\ 2}} = \frac{(c_{11}^{\ 2} - c_{11}c_{12} + 3c_{11}c_{55} - c_{12}c_{55})}{2}\frac{s^2}{c_s^{\ 2}}$$

$$c_0 = -(d_{22} + d_{44} + d_{66})\frac{s^4}{c_s^{\ 4}} = \frac{(-3c_{11} + c_{12} - 2c_{55})}{2}\frac{s^4}{c_s^{\ 4}},$$

$$d_0 = \frac{s^6}{c_s^{\ 6}},$$

Three roots of equation (A.2) are given as,

$$\gamma_1^{\ 0} = \frac{s}{\sqrt{c_{55}}c_s},$$

$$\gamma_2^{\ 0} = \sqrt{\frac{2}{(c_{11} - c_{12})}}\frac{s}{c_s} = \frac{s}{c_s}$$

$$\gamma_3^{\ 0} = \frac{s}{\sqrt{c_{11}}c_s} = \frac{s}{c_d}$$

We note that the three roots are independent of θ.

(2) Solution of the characteristic equation for $\omega \to \infty$ (3.2.12)

For any θ, we have

$$N_1^{\ 2} = \frac{1 + c_{55} + (1 - c_{55})\cos 2\theta}{2},$$

$$N_2^{\ 2} = \frac{B_1 + B_2\cos 2\theta - 2\sqrt{B_4}\sin^2\theta}{4c_{11}c_{55}}, \qquad \text{(A.3)}$$

$$N_3^{\ 2} = \frac{B_1 + B_2\cos 2\theta + 2\sqrt{B_4}\sin^2\theta}{4c_{11}c_{55}},$$

where B_1 and B_2 are given above

$$B_4 = (c_{13}^{\ 2} - c_{11}c_{33})(c_{13}^{\ 2} - c_{11}c_{33} + 4c_{13}c_{55} + 4c_{55}^{\ 2}).$$

Note that for the case $\theta = 0$,

$$N_1^2 = N_2^2 = N_3^2 = 1, \tag{A.4}$$

and for the case $\theta = 90^0$,

$$\begin{aligned} N_1^2 &= c_{55}, \\ N_2^2 &= \frac{-c_{13}^2 + c_{11}c_{33} - 2c_{13}c_{55} - \sqrt{(c_{13}^2 - c_{11}c_{33})((c_{13}^2 - c_{11}c_{33} + 4c_{13}c_{55} + 4c_{55}^2)}}{2c_{11}c_{55}}, \\ N_3^2 &= \frac{-c_{13}^2 + c_{11}c_{33} - 2c_{13}c_{55} + \sqrt{(c_{13}^2 - c_{11}c_{33})((c_{13}^2 - c_{11}c_{33} + 4c_{13}c_{55} + 4c_{55}^2)}}{2c_{11}c_{55}}, \end{aligned} \tag{A.5}$$

which are same as those in [10].

(3) Expression for χ_1

After much algebraic manipulation of equation (3.2.24), it is found that χ_1 can be written as

$$\chi_1 = \frac{\chi_{1n}}{\chi_{1d}} \tag{A.6}$$

where

$$\begin{aligned} \chi_{1n} = {} & (K_2^{\infty}K_3^{\infty} - K_1^{\infty}K_4^{\infty})[-K_6^{\infty}N_1N_2N_3 + K_5^{\infty}(N_1 + N_2 + N_3)] + \\ & a_1\{-K_4^{\infty}[-K_6^{\infty}N_1N_2N_3(N_1^2 + N_2^2 + N_3^2 + N_1N_2 + N_1N_3 + N_2N_3) + \\ & K_5^{\infty}(N_1^3 + N_2^3 + N_3^3 + N_1N_2N_3 + N_1N_2(N_1 + N_2) + N_1N_3(N_1 + N_3) + N_3N_2(N_3 + N_2))] \\ & + K_3^{\infty}[K_6^{\infty}N_1^2N_2^2N_3^2(N_1 + N_2 + N_3) + K_5^{\infty}(N_1N_2N_3(N_1 + N_2 + N_3) + 2N_1N_2N_3(N_1N_2 + \\ & N_1N_3 + N_2N_3) + N_1^2N_2^2(N_1 + N_2) + N_1^2N_3^2(N_1 + N_3) + N_3^2N_2^2(N_3 + N_2))]\}, \end{aligned}$$

$$\chi_{1d} = a_1\left(a_2K_4^{\infty} + K_3^{\infty}K_7^{\infty}\right)(N_1N_2N_3(N_1 + N_2)(N_2 + N_3)(N_1 + N_3)),$$

and,

$$a_1 = d_{22}(d_{46}^2 - d_{44}d_{66}),$$

$$a_2 = d_{12}d_{46} - d_{25}d_{66},$$

$$K_1^{\infty} = -d_{12}^2d_{44} + d_{11}d_{22}d_{44} - d_{15}d_{22}d_{46} + d_{12}d_{25}d_{46} + 2d_{12}d_{46}^2 - 2d_{12}d_{44}d_{66},$$

$$K_2^{\infty} = d_{12}d_{15}d_{46} - d_{11}d_{25}d_{46} - d_{11}d_{46}^{\ 2} + d_{11}d_{44}d_{66},$$

$$K_3^{\infty} = -d_{12}^{\ 2}d_{46} + d_{11}d_{22}d_{46} - d_{15}d_{22}d_{66} + d_{12}d_{25}d_{66},$$

$$K_4^{\infty} = d_{12}d_{15}d_{66} - d_{11}d_{25}d_{66},$$

$$K_5^{\infty} = d_{66}(d_{11}d_{25} - d_{12}d_{15}),$$

$$K_6^{\infty} = -d_{12}^{\ 2}d_{46} + d_{11}d_{22}d_{46} - d_{15}d_{22}d_{66} + d_{12}d_{25}d_{66},$$

$$K_7^{\infty} = -d_{12}d_{15} + d_{11}d_{25} + d_{11}d_{46} - d_{15}d_{66},$$

the expressions for N_i are shown in equation (A.3) in the Appendix.

(4) Expression of χ_2

After tediously long algebraic manipulation of equation (4.11), it is found that χ_2 can be written as

$$\chi_2 = \frac{\chi_{2n}}{\chi_{2d}} \tag{A.7}$$

where

$$\begin{aligned}\chi_{2n} = {} & (L_1^{\infty}L_3^{\infty} + L_2^{\infty}L_4^{\infty})[-L_4^{\infty}N_1N_2N_3 + L_5^{\infty}(N_1 + N_2 + N_3)] + \\ & b_1[(L_4^{\infty})^2N_1^{\ 2}N_2^{\ 2}N_3^{\ 2}(N_1 + N_2 + N_3) + (L_3^{\infty})^2[N_1^{\ 3} + N_2^{\ 3} + N_3^{\ 3} + \\ & N_1N_2N_3 + N_1N_2(N_1 + N_2) + N_1N_3(N_1 + N_3) + N_3N_2(N_3 + N_2)] + \\ & L_3^{\infty}L_4^{\infty}[N_1N_2N_3(N_1N_2 + N_1N_3 + N_2N_3) + \\ & N_1^{\ 2}N_2^{\ 2}(N_1 + N_2) + N_1^{\ 2}N_3^{\ 2}(N_1 + N_3) + N_3^{\ 2}N_2^{\ 2}(N_3 + N_2)]],\end{aligned}$$

$$\chi_{2d} = -L_1^{\infty}[L_4^{\infty}[b_2 N_1^{\,2} N_2^{\,2} N_3^{\,2} + L_6^{\infty}(N_1N_2 + N_1N_3 + N_2N_3)] +$$
$$L_3^{\infty}[L_5^{\infty}(N_1N_2 + N_1N_3 + N_2N_3) + b_2[N_1N_2N_3(N_1 + N_2 + N_3) +$$
$$N_1^{\,2}N_2^{\,2} + N_1^{\,2}N_3^{\,2} + N_3^{\,2}N_2^{\,2}]]] - b_1[L_4^{\infty}[-a_2 N_1^{\,2}N_2^{\,2}N_3^{\,2}(N_1N_2 + N_1N_3 + N_2N_3) +$$
$$L_6^{\infty}[N_1N_2N_3(N_1 + N_2 + N_3) + 2N_1N_2N_3(N_1N_2 + N_1N_3 + N_2N_3) +$$
$$N_1^{\,2}N_2^{\,2}(N_1 + N_2) + N_1^{\,2}N_3^{\,2}(N_1 + N_3) + N_3^{\,2}N_2^{\,2}(N_3 + N_2)] + L_3^{\infty}[L_5^{\infty}$$
$$[N_1^{\,2}N_2^{\,2} + N_1^{\,2}N_3^{\,2} + N_3^{\,2}N_2^{\,2} + (N_1^{\,2} + N_2^{\,2})N_1N_2 + (N_1^{\,2} + N_3^{\,2})N_1N_3 +$$
$$(N_3^{\,2} + N_2^{\,2})N_3N_2 + 2N_1N_2N_3(N_1 + N_2 + N_3)] - b_2[N_1^{\,3}N_2^{\,3} + N_1^{\,3}N_3^{\,3} + N_2^{\,3}N_3^{\,3}$$
$$+ N_1^{\,2}N_2^{\,2}N_3(N_1 + N_2) + N_1N_2^{\,2}N_3^{\,2}(N_3 + N_2) + N_1^{\,2}N_2N_3^{\,2}(N_1 + N_3)]] +$$
$$L_2^{\infty}[-L_4^{\infty}[L_6^{\infty} + b_2 N_1N_2N_3(N_1 + N_2 + N_3)] + L_3^{\infty}[L_5^{\infty} + b_2(N_1^{\,2} + N_2^{\,2} + N_3^{\,2} +$$
$$N_1N_2 + N_1N_3 + N_2N_3)]],$$

and,

$$b_1 = d_{22}(d_{46}^{\,2} - d_{44}d_{66}),$$

$$b_2 = d_{22}d_{46},$$

$$L_1^{\infty} = -(d_{12}^{\,2}d_{44} - d_{11}d_{22}d_{44} + d_{15}d_{22}d_{46} - d_{12}d_{25}d_{46} - 2d_{12}d_{46}^{\,2} + 2d_{12}d_{44}d_{66}),$$

$$L_2^{\infty} = d_{12}d_{15}d_{46} - d_{11}d_{25}d_{46} - d_{11}d_{46}^{\,2} + d_{11}d_{44}d_{66},$$

$$L_3^{\infty} = d_{66}(d_{11}d_{25} - d_{12}d_{15}),$$

$$L_4^{\infty} = -d_{12}^{\,2}d_{46} + d_{11}d_{22}d_{46} - d_{15}d_{22}d_{66} + d_{12}d_{25}d_{66},$$

$$L_5^{\infty} = d_{15}d_{22} - d_{12}d_{25} - d_{12}d_{46} - d_{25}d_{66},$$

$$L_6^{\infty} = d_{15}d_{66},$$

the expressions for N_i are shown in equation (A.3) in the Appendix.

(5) Expression for χ_3

Finally, the expression for χ_3 can be written as

$$\chi_3 = \frac{\chi_{3n}}{\chi_{3d}} \qquad \text{(A.8)}$$

where

$$\chi_{3n} = -(M_1^{\infty})^2 N_1 N_2 N_3[-M_4^{\infty} + c_1 N_1 N_2 N_3 (N_1 + N_2 + N_3)] + M_1^{\infty} M_2^{\infty}[-M_3^{\infty} N_1 N_2 N_3 + M_4^{\infty}(N_1 + N_2 + N_3) + c_1[N_1^2 N_2^2 (N_1 + N_2) + N_1^2 N_3^2 (N_1 + N_3) + N_3^2 N_2^2 (N_3 + N_2) + N_1 N_2 N_3 (N_1 N_2 + N_1 N_3 + N_2 N_3)]] - (M_2^{\infty})^2[M_3^{\infty}(N_1 + N_2 + N_3) + c_1(N_1^3 + N_2^3 + N_3^3 + N_1 N_2 N_3 + N_1 N_2 (N_1 + N_2) + N_1 N_3 (N_1 + N_3) + N_3 N_2 (N_3 + N_2))],$$

$$\chi_{3d} = -M_1^{\infty} M_2^{\infty}[M_5^{\infty} - M_6^{\infty}(N_1 N_2 + N_1 N_3 + N_2 N_3) - c_2(N_1^2 N_2^2 + N_1^2 N_3^2 + N_3^2 N_2^2)] + (M_1^{\infty})^2[c_2 N_1^2 N_2^2 N_3^2 + M_5^{\infty}(N_1 N_2 + N_1 N_3 + N_2 N_3)] + (M_2^{\infty})^2[-M_6^{\infty} + c_2(N_1^2 + N_2^2 + N_3^2 + N_1 N_2 + N_1 N_3 + N_2 N_3] + N_1 N_2 N_3 + N_1 N_2 (N_1 + N_2) + N_1 N_3 (N_1 + N_3) + N_3 N_2 (N_3 + N_2))],$$

and,

$$c_1 = d_{22}(d_{46}^2 - d_{44} d_{66}),$$

$$c_2 = d_{22} d_{66},$$

$$M_1^{\infty} = -d_{12}^2 d_{46} + d_{11} d_{22} d_{46} - d_{15} d_{22} d_{66} + d_{12} d_{25} d_{66},$$

$$M_2^{\infty} = d_{66}(d_{12} d_{15} - d_{11} d_{25}),$$

$$M_3^{\infty} = -(d_{12}^2 d_{44} - d_{11} d_{22} d_{44} + d_{15} d_{22} d_{46} - d_{12} d_{25} d_{46} - 2 d_{12} d_{46}^2 + 2 d_{12} d_{44} d_{66}),$$

$$M_4^{\infty} = d_{12} d_{15} d_{46} - d_{11} d_{25} d_{46} - d_{11} d_{46}^2 + d_{11} d_{44} d_{66},$$

$$M_5^{\infty} = d_{11} d_{66},$$

$$M_6^{\infty} = -(d_{12}^2 - d_{11} d_{22} + 2 d_{12} d_{66}),$$

the expressions for N_i are shown in equation (A.3) in the Appendix.

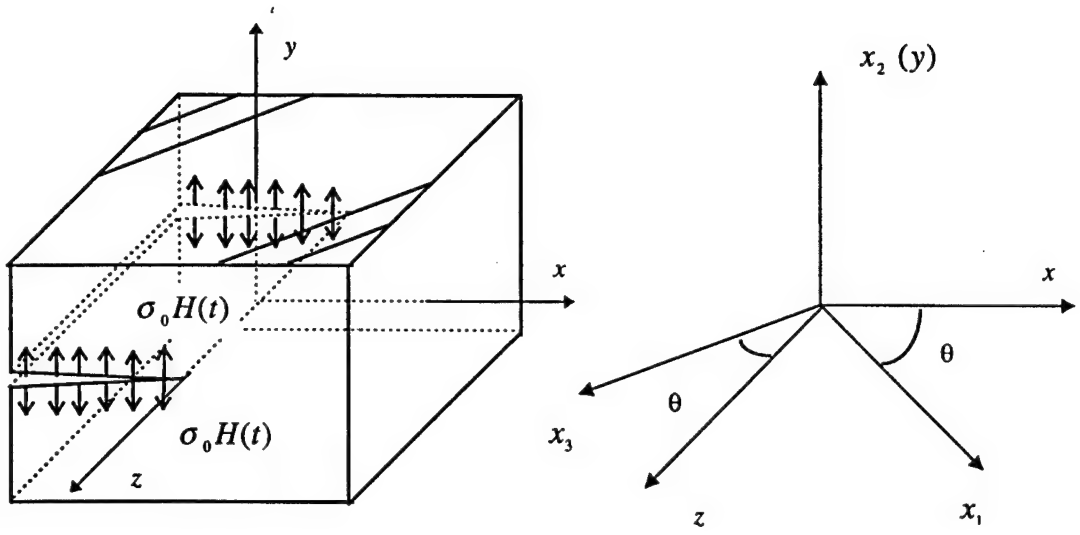

Figure 1 The semi-infinite crack in rotated transversely isotropic materials under uniform normal impact loading

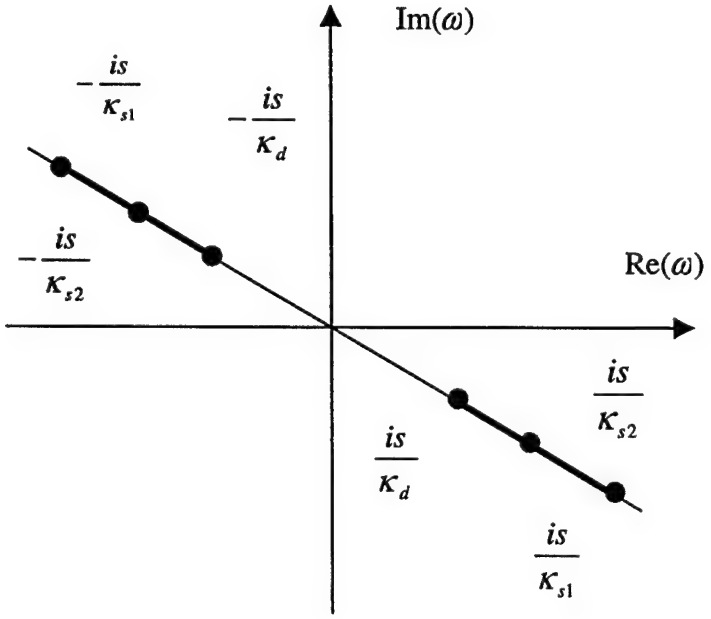

Figure 2 ω -plane and branch cut

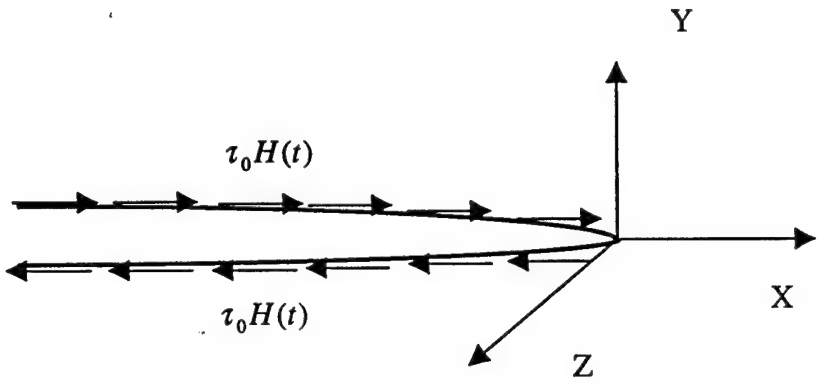

Figure 3 In-plane shear loading

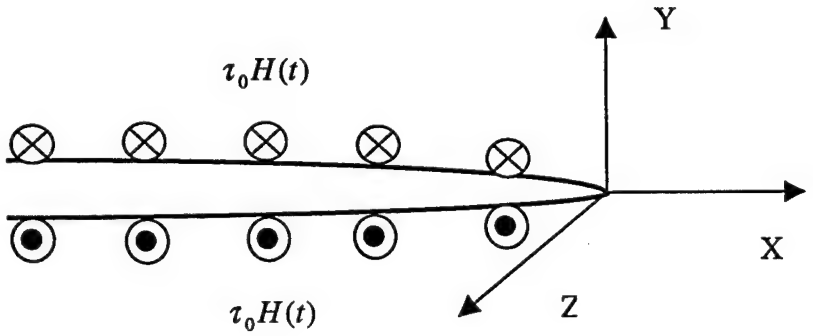

Figure 4 Anti-plane shear loading

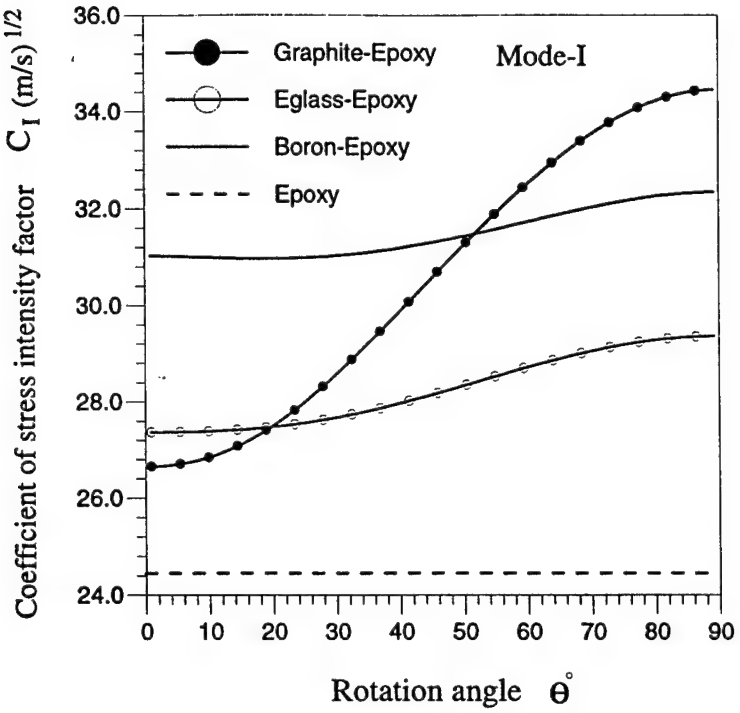

Figure 5 Coefficient of stress intensity factor for Mode-I for a semi-infinite crack in different materials

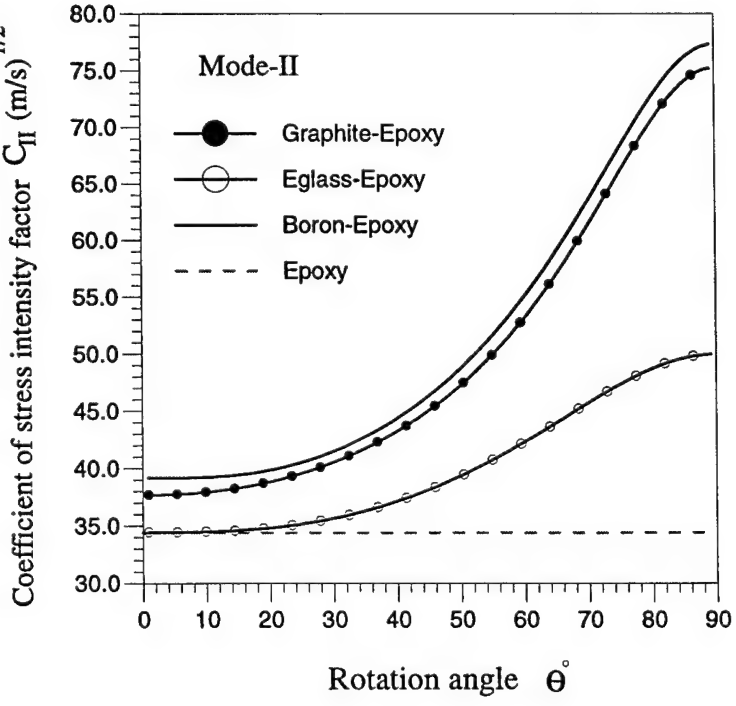

Figure 6 Coefficient of stress intensity factor for Mode-II for a semi-infinite crack in different materials

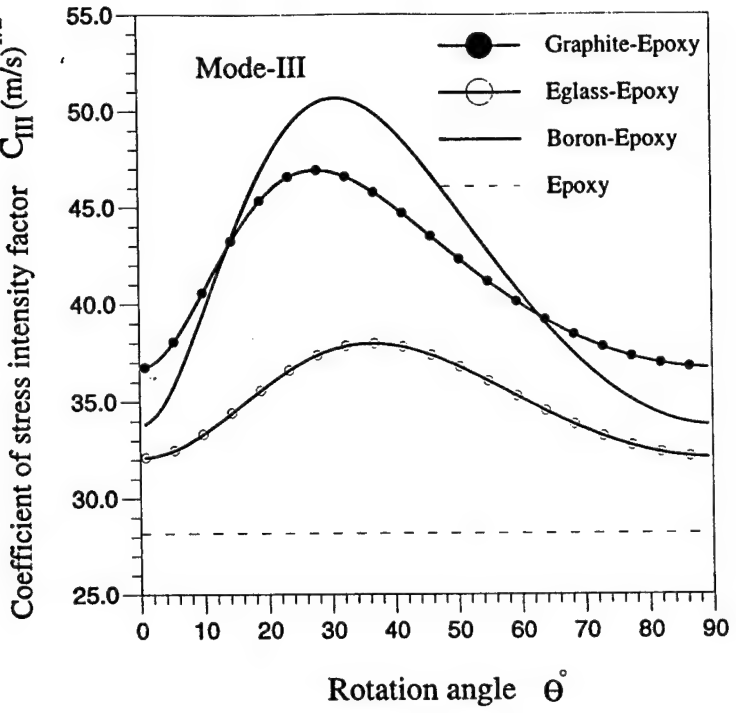

Figure 7 Coefficient of stress intensity factor for Mode-III
for a semi-infinite crack in different materials

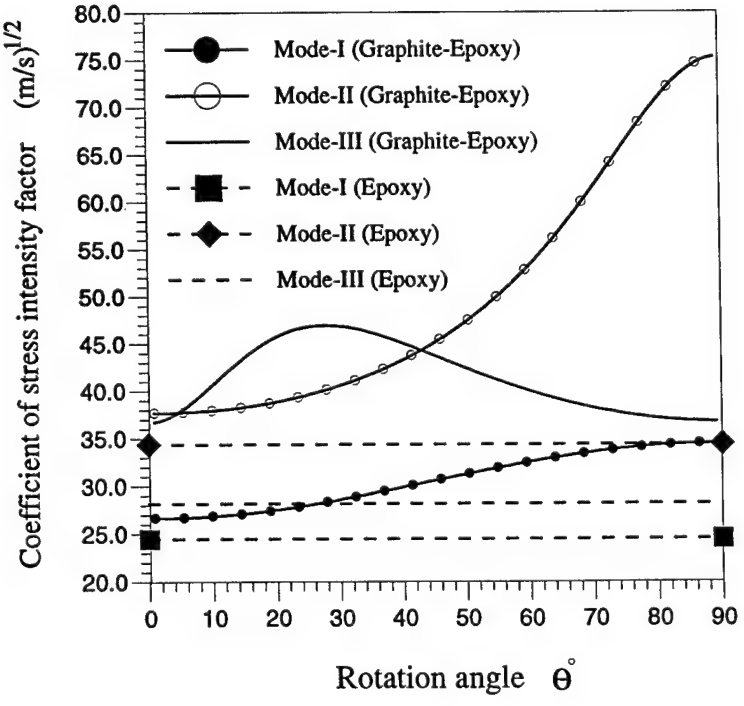

Figure 8 Coefficient of stress intensity factor for three modes
for a semi-infinite crack in different materials
The isotropic corresponds to Epoxy and the orthotropic to Graphite-epoxy

Table 1 Material parameters

	Graphite-Epoxy	Eglass-Epoxy	Boron-Epoxy	Epoxy
E_1 (Gpa)	10.41	12.	19.	5.21
E_2 (Gpa)	156.75	45.	207.	5.21
ν_{12}	0.49	0.19	0.21	0.328
ν_{31}	0.31	0.19	0.21	0.328
G_{12} (Gpa)	3.49	5.04	7.85	1.96
G_{13} (Gpa)	7.07	5.5	6.4	1.96
$\rho(Kg/m^3)$	1580	2100	1990	1260

Table 2 Coefficient of stress intensity factor for three modes at $\theta=0^0$ and $\theta=90^\circ$ in different materials by using of the formulation in [10] (with proper substitution of elastic constants)

		Graphite-Epoxy	Eglass-Epoxy	Boron-Epoxy	Epoxy
$\theta=0^0$	I	26.65	27.37	31.02	24.45
	II	37.68	34.43	39.20	34.38
	III	36.70	32.10	33.79	28.18
$\theta=90^\circ$	I	34.56	29.36	32.35	24.45
	II	75.24	49.96	77.33	34.38
	III	36.70	32.10	33.79	28.18

Table 3 Coefficient of stress intensity factor for three modes at $\theta=0^0$ and $\theta=90^\circ$ for several materials by using of the formulation in the paper with $\theta=0^0$ and $\theta=90^\circ$

		Graphite-Epoxy	Eglass-Epoxy	Boron-Epoxy	Epoxy
$\theta=0^0$	I	26.65	27.37	31.02	24.45
	II	37.68	34.43	39.20	34.38
	III	36.70	32.10	33.79	28.18
$\theta=90^\circ$	I	34.56	29.36	32.35	24.45
	II	75.24	49.96	77.33	34.38
	III	36.70	32.10	33.79	28.18

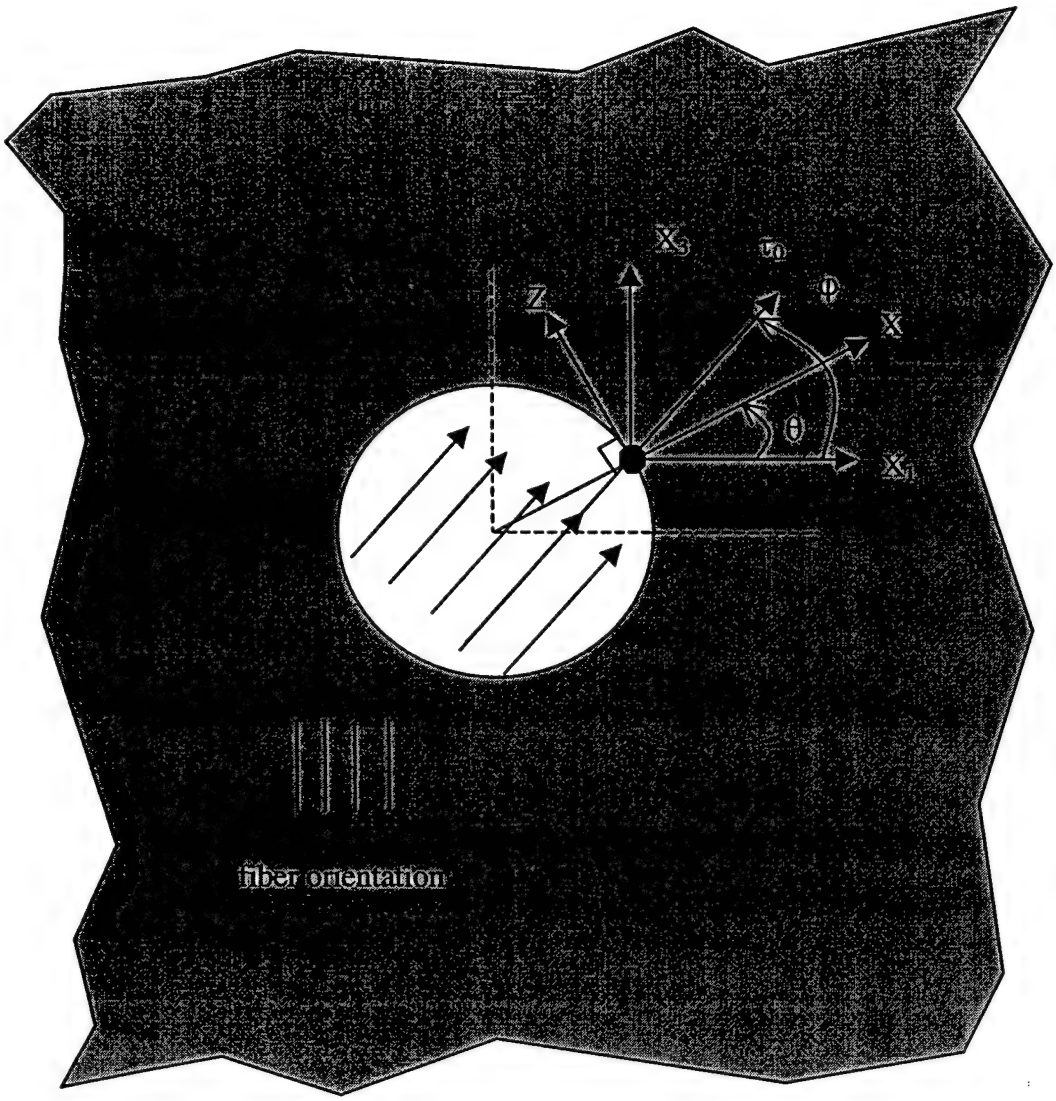

Figure 9 Penny shape crack in orthotropic (or composite) materials

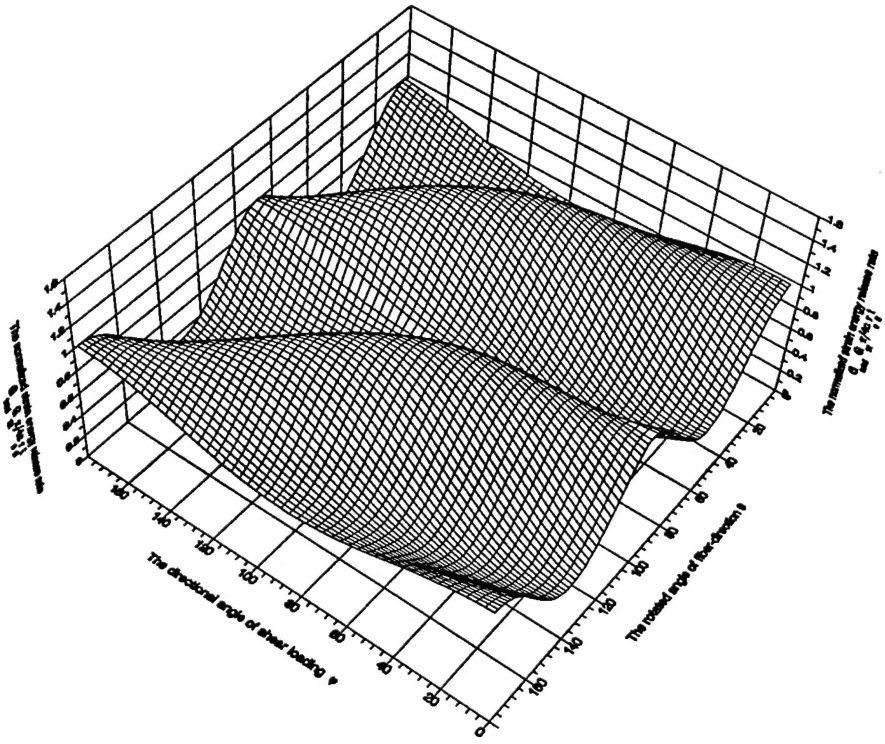

Figure 10 Normalized strain energy release rate for Graphite-Epoxy

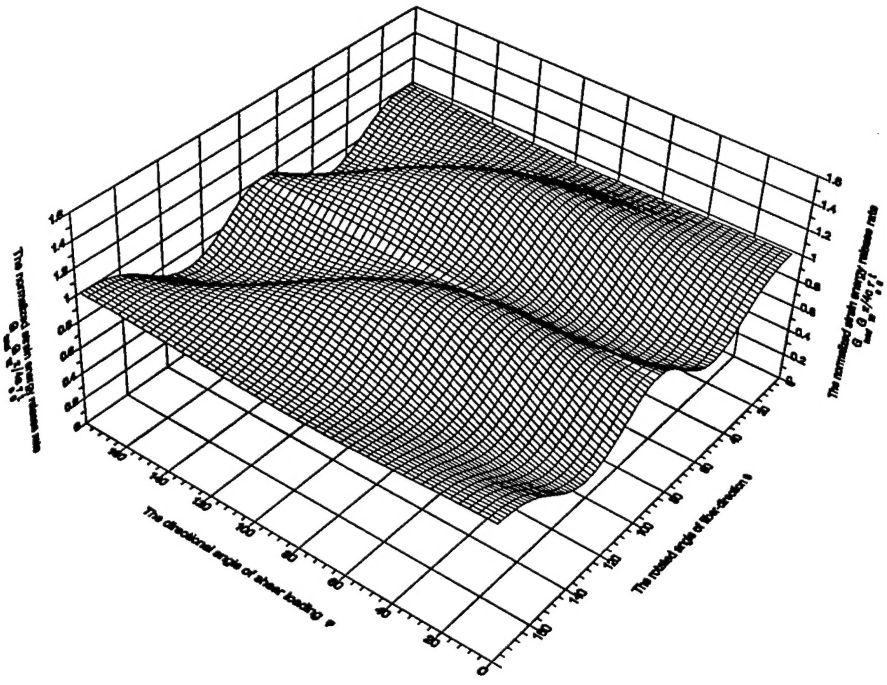

Figure 11 Normalized strain energy release rate for Eglass- Epoxy

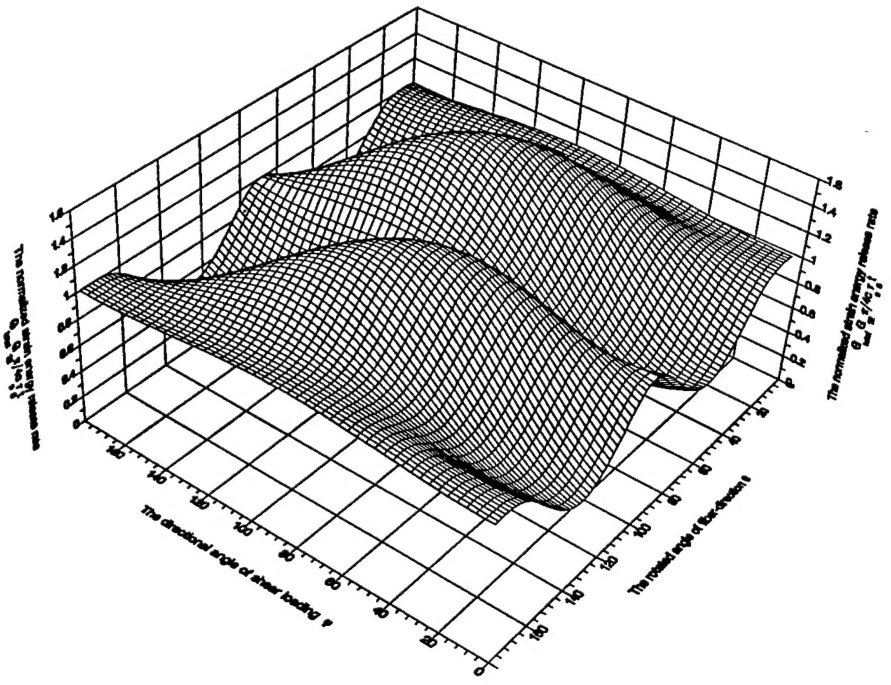

Figure 12 Normalized strain energy release rate for Boron- Epoxy

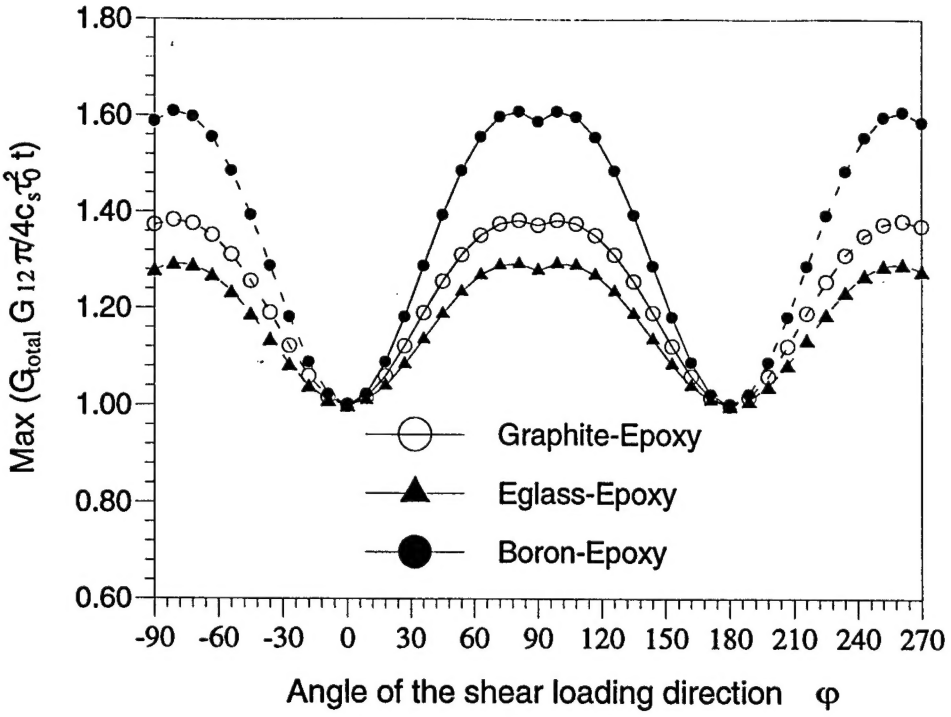

Figure 13 Maximum strain energy release rate as a function of shear loading angle, φ

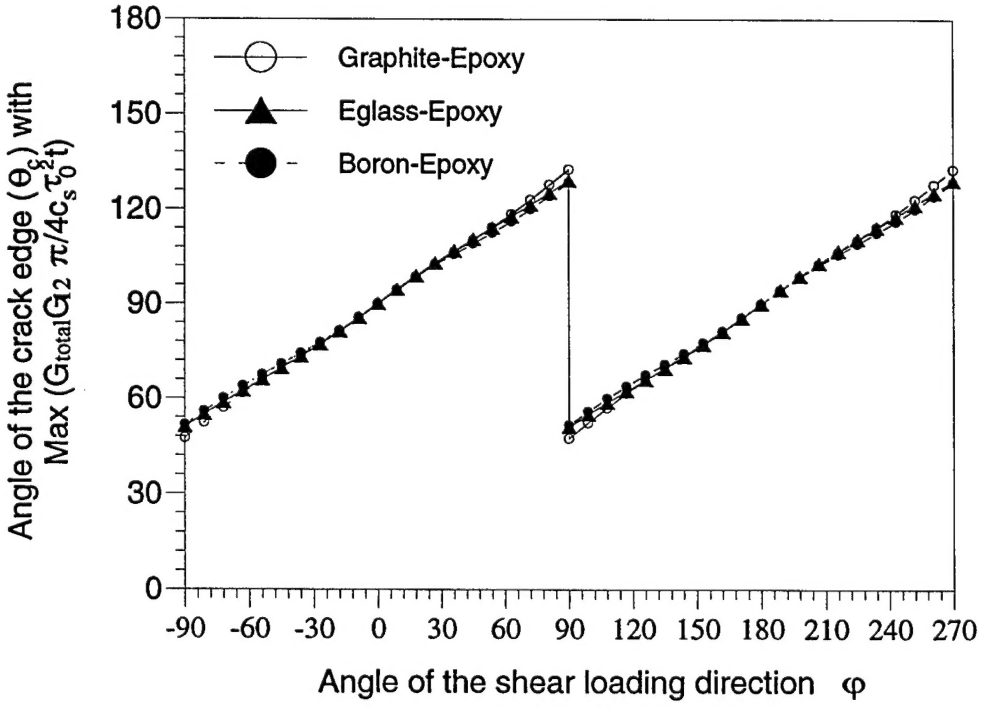

Figure 14 Direction of maximum strain energy release rate, θ_c, measured relative to the X_1 axis